Technical Report Documentation Page

1. Report No.	2. Government Accession No.	3. Recipient's Catalog No.
FHWA/TX-94+1264-2		

4. Title and Subtitle	5. Report Date
REDUCING FRICTION LOSSES IN MONOLITHIC AND SEGMENTAL BRIDGE TENDONS	*October 1993*
	6. Performing Organization Code

7. Author(s)	8. Performing Organization Report No.
R. T. Davis, T. T. Tran, J. E. Breen, and K. H. Frank	*Research Report 1264-2*

9. Performing Organization Name and Address	10. Work Unit No. (TRAIS)
Center for Transportation Research *The University of Texas at Austin* *3208 Red River, Suite 200* *Austin, Texas 78705-2650*	11. Contract or Grant No. *Research Study 0-1264*
	13. Type of Report and Period Covered *Interim*
12. Sponsoring Agency Name and Address *Texas Department of Transportation* *Research and Technology Transfer Office* *P. O. Box 5051* *Austin, Texas 78763-5051*	14. Sponsoring Agency Code

15. Supplementary Notes

Study conducted in cooperation with the U.S. Department of Transportation, Federal Highway Administration
Research Study Title: "Corrosion Protection for Post-Tension Tendons and Cable Stay Systems"

16. Abstract

In the construction of post-tensioned bridges, the increased use of precast technology has resulted in somewhat tighter radii of curvature and greater total angle changes. Both factors make friction losses during stressing higher and somewhat less predictable. Various design recommendations have suggested different values. There have not been any reported tests of actual friction losses in segmentally cast girders.

Historically, the solution to the friction reduction problem has been use of a lubricant, often an emulsifiable oil applied to the surface of the tendon or stay. The agent is usually flushed immediately before grouting. Particularly in bonded post-tensioned girders, it is essential that any residues of these agents not diminish the bond between the strand and the grout. The tests showed flushing was ineffective and emulsifiable oils are potentially harmful in bonded tendon applications.

In a preliminary study, thirteen agents were identified as practical candidates for tendon lubrication and/or temporary corrosion protection. Ten were emulsifiable oils, one was a sodium silicate solution, one was a soap and one was powdered graphite. The powdered graphite was the best lubricating agent but is not a corrosion inhibitor.

17. Key Words	18. Distribution Statement
post-tensioned, bridges, precast technology, radii of curvature, angle changes, friction losses, monolithic girders, segmentally cast girders, tendon sheaths, joints, agent, emulsifiable oil, grout, strand, friction reduction, corrosion protection, tendon lubrication	*No restrictions. This document is available to the public through the National Technical Information Service, Springfield, Virginia 22161.*

19. Security Classif. (of this report)	20. Security Classif. (of this page)	21. No. of Pages	22. Price
Unclassified	*Unclassified*	*134*	

REDUCING FRICTION LOSSES IN MONOLITHIC AND SEGMENTAL BRIDGE TENDONS

by

R. T. Davis, T. T. Tran, J. E. Breen, and K. H. Frank

Research Report Number 1264-2

Research Project 0-1264

CORROSION PROTECTION FOR POST-TENSION TENDONS AND CABLE STAY SYSTEMS

conducted for the

Texas Department of Transportation

in cooperation with the

U. S. Department of Transportation
Federal Highway Administration

by the

CENTER FOR TRANSPORTATION RESEARCH
BUREAU OF ENGINEERING RESEARCH
THE UNIVERSITY OF TEXAS AT AUSTIN

OCTOBER 1993

IMPLEMENTATION

This report provides a detailed description of an experimental program to determine the actual performance of several agents which have been indicated as good candidates for friction reduction in post tensioned girders. These agents have typically been recommended when tight or extensive curvatures exist in a medium- or long-span bridge girders when checks during stressing indicate high friction losses and/or insufficient elongations of the tendons, or when there will be a time delay between installation of the tendons in ducts and subsequent cement grouting. While such agents have been used under such special circumstances and are generally permitted or encouraged under existing design and construction guidelines, there has not been any systematic study of their effects or side effects.

In previous studies, reported in CTR Report 1264-1, several agents are identified as having very good temporary corrosion protection ability. Use of such agents would greatly enhance long-term life of post-tensioned bridges when there is need for delay between tendon installation and grouting. Several agents were also identified as having good, but not great, lubrication properties. Use of such agents could substantially reduce (20-30%) friction losses and in this way contribute 5-6% to increased efficiency of the post-tensioning strand. This could result in some cost savings. Unfortunately, the comparative bond tests indicated that all of the emulsifiable oils had a serious side effect. Even when thoroughly flushed with substantially amounts of water, enough residue of the oil was present to practically destroy bond between the strand and the grout. Thus the study showed it would be dangerous to use these agents whenever a bonded design was being used. In such cases, the development of the strand could be substantially reduced which could reduce the ultimate capacity of the girder. Fortunately the study identified two agents which provide acceptable lubrication and do not significantly harm the bond between strand and grout after they are flushed. Unfortunately, neither of these agents is designed for corrosion protection.

The results reported herein utilized the most promising agents in a series of friction tests in full scale girders to evaluate their efficiency in friction reduction. As an extra benefit, half of the tests were run in a segmentally cast specimen. No previous friction tests have been reported for internal tendons in segmental construction. The results showed that the best temporary lubricant was powdered graphite. They further showed that the wobble friction coefficient needs to be increased for segmental girders and that the current tolerances for duct offsets at joints are acceptable. If the recommendations for AASHTO revisions are accepted, they should result in more efficient use of post-tensioning as well as safer structures under overload conditions.

Prepared in cooperation with the Texas Department of Transportation and the U.S. Department of Transportation, Federal Highway Administration.

J.E. Breen, P.E. #18479
K.H. Frank, P.E. #48953

Research Supervisor

TABLE OF CONTENTS

LIST OF FIGURES

LIST OF TABLES

SUMMARY

In the construction of post-tensioned bridges, the increased use of precast technology has resulted in somewhat tighter radii of curvature and greater total angle changes. Both factors make friction losses during stressing higher and somewhat less predictable. In both cast-in-situ and precast post-tensioned bridges, friction loss estimation is difficult and various design recommendations have suggested different values. While there has been a number of previous studies of friction losses in monolithic girders, there have not been any reported tests of actual friction losses in segmentally cast girders. The extra discontinuities in the tendon sheaths at the joints between segments have been suspected to have caused extra friction losses.

Historically, the solution to the friction reduction problem has been use of a single agent, often an emulsifiable oil applied to the surface of the tendon or stay. The agent is usually flushed immediately before grouting. Particularly in bonded post-tensioned girders, it is essential that any residues of these agents not diminish the bond between the strand and the grout.

There are numerous oils available, as well as several other agents often used in these applications. There is very little prior data indicating the amount of friction reduction that can be expected from different oils or agents. In a preliminary study thirteen agents were identified as practical candidate for tendon lubrication and/or temporary corrosion protection. Ten were emulsifiable oils, one was a sodium silicate solution, one was a soap and one was powdered graphite.

The top candidates from a preliminary series of tests were evaluated in the current full size girder tests. A series of identical straight ducts and of identical curved ducts were cast in two girders. One girder was built monolithically with continuous tendon ducts. The other girder was built segmentally with discrete tendon ducts in each segment. Carefully controlled offsets ranging from zero to twice the current allowed tolerances were provided between the matching ducts at each segmental joint. Carefully conducted stressing tests were run to measure tendon curvature friction and wobble friction. The most promising lubricants were used to attempt to reduce friction losses. After use, the lubricants were flushed and some of the tendons removed and subjected to grout pull out tests to evaluate the efficacy of the flushing technique.

Based on the program measurements as well as other reported tests, curvature friction coefficients were recommended for ducts. The coefficients vary with duct radii of curvature. The wobble friction coefficient was found to be greater for segmental construction when compared to monolithic construction.

Most of the lubricants tested in the full-size specimens gave marginal improvements in friction characteristics and the water soluble oils were found to destroy strand to grout bond, even after a thorough flushing with water. The best agent was powdered graphite which reduced friction about 15% and could be effectively neutralized by flushing as evaluated from subsequent bond tests. Some water soluble oils had higher friction reduction (22%) but could not be effectively removed by flushing even though no visible traces remained to examination by eye.

A series of recommendations for changes in both the main *AASHTO Standard Specifications for Highway Bridges* and the *AASHTO Guide Specifications for Design and Construction of Segmental Concrete Bridges* are made.

CHAPTER ONE
INTRODUCTION

1.1 Background

In the mid 1970's prestressed concrete became the most commonly used structural material for new bridges in the United States [1]. For short to medium spans, pretensioned I girders and adjoining box beams have become the most economical structural element. These structural members are easy to design, construct, and erect. They have been readily accepted for use by most state transportation agencies.

For medium to medium-long spans, post-tensioned concrete box girders have also been gaining in popularity as an economical alternative to steel plate girders. Design of a post-tensioned box girder is more involved than design of simple span pretensioned girders, and all aspects of behavior are not as well known. The size and cost of this type structure naturally limits the number of bridges built. The less frequent use has limited large scale research on the subject. Cast-in-place concrete box girders are commonplace in states like California, but acceptance nationwide has generally lagged behind that of the pretensioned girders and box beams.

As a result of the emergence of post-tensioning, and as its advantages were seen, the use of post-tensioning increased nation-wide more than 500 percent in the period 1965 - 1985. This rapid growth of post-tensioning can be credited to the following:

1) The recognition of the economic and structural advantages of post-tensioning, which include reduced structural depth; watertight, virtually crack-free slabs; durability; low maintenance cost; and control of deflection;

2) The aesthetic advantages and environmental protection;

3) The construction time-saving advantages; and

4) The development of the capabilities of post-tensioning material [1, 3, 24].

1.1.1 Development of the Segmental Bridge Industry. Cast-in-place post-tensioned concrete box girders have been commonly constructed in the United States since the 1960s. Cast-in-place non-segmental construction requires massive falsework and formwork to be erected and maintained for long periods of time. Final geometry and duct alignment can be checked before concrete is placed. The resulting monolithic structure has inherently fewer design uncertainties than a continuous structure which is precast and assembled piece by piece. Since post-tensioning is safe, fast and economical, this method has been a standard in Texas in the construction of elevated highways and medium-to-moderately long span bridges. In these bridges and elevated highways, the individual segmental box girders are assembled together longitudinally or transversely by post-tensioning. The box girders can be either cast-in-place or precast, or a combination of cast-in-place and precast. Texas has taken advantage of both of these methods.

The concrete box girder structure type can be modified for use at sites where cast-in-place construction would prove difficult. Harsh weather, traffic maintenance, extreme structure height, and over-water construction are a few of the reasons segmentally constructed box girders came into being. In precast segmental construction, the segments are mass produced in a nearby plant or in a factory under well controlled quality, geometry, and match casting conditions. After casting, the segments are transported to the construction site for final positioning and assembly. The match casting technique is almost universally used today. Using this technique, one segment is match cast against another in the same order in which they are required to be assembled. The major advantages of precast segments are as follows:

1) Segments can be cast well before the time of assembly;

2) Segments have the capability of attaining substantial strength before post-tensioning occurs;

3) The rapid construction.

The John F. Kennedy Memorial Causeway in Corpus Christi was the first bridge constructed in the United States using the concept of precast segmental box girders and erected in a cantilever fashion. Designed by the Bridge Division of the Texas Highway Department (now the Texas Department of Transportation), this bridge demonstrated a reserve strength capacity that is substantially in excess of the specification requirements set by early test results. These criteria were developed from the extensive testing of a model done at the University of Texas at Austin [1, 2].

The Texas Department of Transportation has just completed constructing several miles of elevated highways in the San Antonio area. Known as the "Y" projects, this construction uses precast segmental box girders. These projects are examples of the low cost bid alternate and of the remarkable construction time-saving characteristic of precast segmental applications. Off-site fabrication of segments complicates construction engineering, yet provides a work environment likely to improve craftsmanship in the girder. Quality control must be monitored in the casting yard (see Figure 1.1) to ensure that ducts are placed within tolerance. Out of tolerance or poorly secured ducts can cause significant increases in friction loss during post-tensioning.

In cast-in-place segmental construction, the segments are cast one after another. Special equipment is required for cast-in-place construction: a form traveller for cantilever construction or a mobile formwork that is moved along a supporting gantry for span-by-span construction. While the assembly of segments in the longitudinal direction is done by post-tensioning, each segment when constructed is reinforced with conventional steel and sometimes by transverse and/or longitudinal prestressing strands.

The Houston Ship Channel Bridge is an example of the cast-in-place segmental application. The total length of this bridge is 1,500 feet (457 m). It consists of a main span of 750 feet (229 m) and two side spans of 375 feet (114 m) each. The 750-foot (229 m) main span is the longest in the United States for a segmental box-girder bridge constructed by the cantilever method [1].

Figure 1.1 Segment fabrication yard.

The success of such bridges as the Corpus Christi bridge, the Houston Ship Channel bridge, the elevated San Antonio "Y" projects and others similar to these only reaffirm that in Texas post-tensioning has become a major factor in the construction of long-span bridges and elevated highways.

1.1.2 Problems Encountered During Construction. Cross sections of segments generally are also the cross section for the entire bridge superstructure, or major portions thereof. This differs greatly from pretensioned girder systems in which the girders are placed in simple spans with a cast-in-place deck. In these latter systems, the deck elevation is controlled by the elevations of the bearing pads on the pier caps. Beams are statically determinant when placed, and therefore, unless joined longitudinally by special connections, have no potential for secondary moments and automatically follow the approximate deck elevation along the beam's longitudinal axis.

Cast in situ and segmental box girders, on the other hand, often have secondary moments from multi-span continuous construction. The deck elevations are not automatically controlled by the bearing pad elevations. Each segment must be custom cast. Fabrication may be simple, as for a straight bridge or for the somewhat more complex case of bridges with constant curvature and super elevation. Geometry control may also be very complex, as for the Linn Cove Viaduct. No two segments on this structure have the same dimension, and horizontal and vertical curvature are changed many times [3].

Overall concrete dimension geometry errors may effect the structure's alignment and hence appearance and ride quality. More importantly, major or minor internal and external post-tensioning duct placement errors may greatly influence the amount of prestress force and thus effect durability and safety.

1.1.3 Research Needs. In order for segmental construction to continue increasing in popularity, both field and laboratory research need to be conducted to refine design and construction. Wide acceptance of a structure type usually occurs after accurate design methods have been established, and construction methods have been refined to reduce costs and eliminate delays.

Accurate prediction of prestress losses due to friction during post-tensioning has been a problem on many segmental and monolithic box girder bridges. The structural design relies on achieving a desired prestress force which is specified within reasonably tight limits for the construction to attain. Actual friction losses, checked by elongation measurements, are known only after the bridge has been erected. Therefore, accurately predicting prestress losses is of utmost importance to both the designer and constructor.

Duct placement in segmental girders is inherently more difficult than in monolithic girders because many short pieces of duct are used for internal tendons. The differences in friction loss between the two methods of construction need to be quantified, and the current duct placement tolerances checked for their impact on friction loss. Methods also need to be studied for reducing friction losses in general, such as the use of lubricants.

This report studies friction losses in internal ducts only. Segments with a combination of internal and external tendons (see Figure 1.2), or only external tendons are also quite common. Friction losses in the deviators of external tendons have been recently measured by Roberts [4].

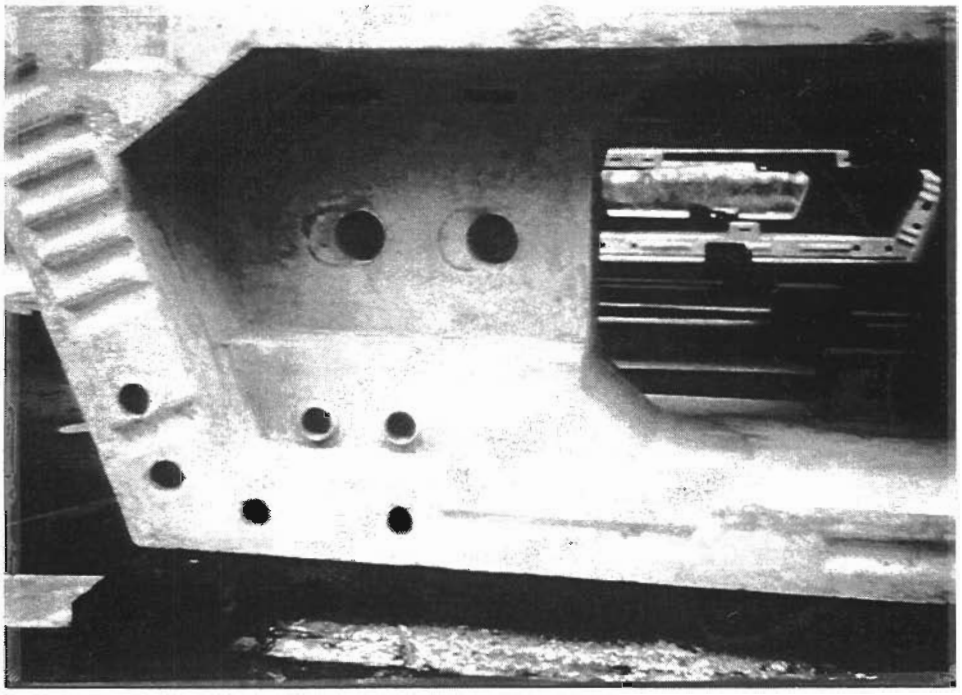

Figure 1.2 Segment with internal and external tendon openings.

1.2 Friction Losses During Post-Tensioning.

Friction losses during post-tensioning are produced as the tendon tries to move along a curved duct surface. As the tendon goes into tension, a normal force is generated between duct and tendon. As the tendon elongates under stress, the surface condition of the duct and prestressing strand interface result in a friction force developing. Tendon force is lost to friction as is shown for the simple span beam in Figure 1.3.

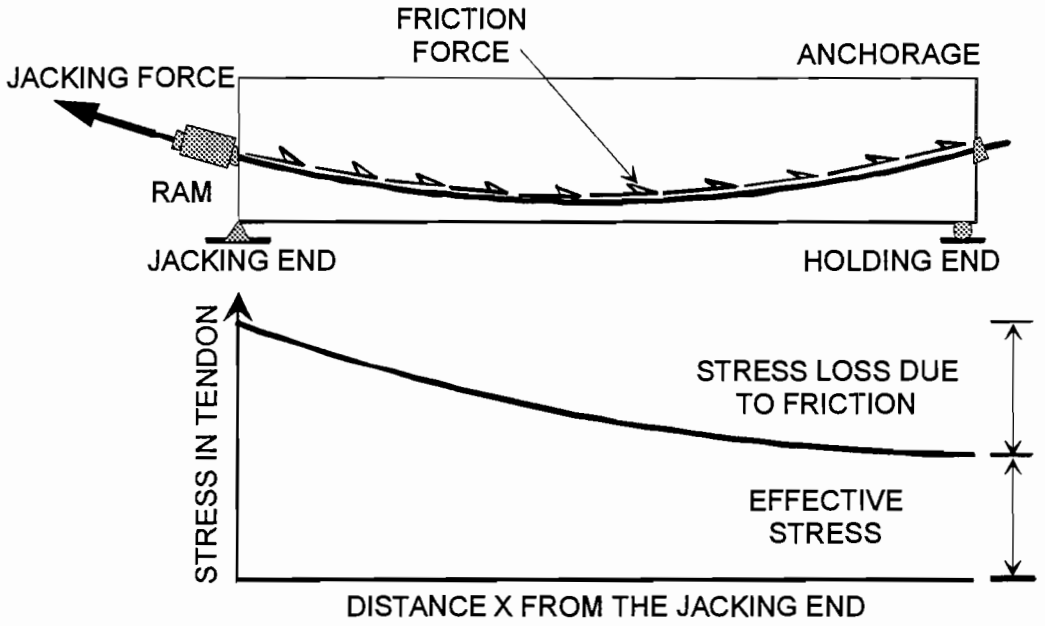

Figure 1.3 Variation of stress along tendon due to frictional loss.

Additional tendon force can be lost in a segmentally constructed girder because of duct mismatch at the segment joints, and the general difficulty in setting and maintaining duct profiles using many short pieces. Possible differences in tendon force between a monolithically constructed girder and segmentally constructed girder are shown in Figure 1.4. These two specimens are described in detail in Chapters 2 and 3.

In the design process, it is important to have an accurate estimation of the prestress forces in continuous post-tensioning structures. Both serviceability and the ultimate moment capacity of the structures heavily rely on the final effective prestress forces. Continuous post-tensioned structures often have several design control points; that is, points along the structure at which forces are critical. The final effective prestress forces at these points are dependent on several factors: the applied force, the losses due to friction and to creep, the shrinkage of the concrete, and the prestressing steel relaxation. During post-tensioning, in a long girder with large curvature along the path, the total losses may be as great as 50% of the applied force. Friction resistance along the tendon accounts for a major fraction of this loss; friction loss may be as much as 35% of the applied force. Other types of loss account for lesser amount of the whole, but may be as much as 15% of the applied force; they are usually nearly uniform along the entire length of the tendon.

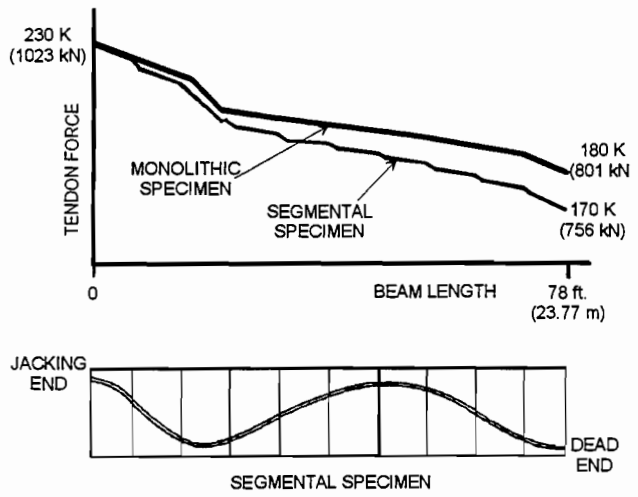

Figure 1.4 Possible effect of duct offsets in a segmental girder in comparison to a monolithic girder.

Because friction accounts for so much of the loss of the applied force, a great deal of work has gone into reducing this loss. In particular, water-soluble oils have frequently been used in the field to lubricate tendons during the stressing process.

1.2.1 Construction Procedures. Duct geometry is nearly impossible to check once concrete has been placed for all but straight duct profiles. In-place friction tests and elongation measurements during post-tensioning will reveal the level of craftsmanship only after the tendon has been installed, stressed, and possibly permanently anchored.

Tendons may be pulled through or pushed through the duct as an entire tendon or one strand at a time. Pulling or pushing entire tendons into a duct simplifies the application of a lubricant to the strands. Lubricant must otherwise be applied to strands one at a time, or be pumped into the duct after the tendon has been installed. Water soluble oil was sprayed on to the tendons on the JFK Memorial Bridge because very high friction losses were encountered during post-tensioning, as was the case on many early post-tensioned structures. Today, prestressing contractors generally feel the friction coefficients used by designers are too conservative, yet realize there is an increase in friction associated with segmental construction over monolithic construction.

Friction losses may be considerable for long tendons. Figure 1.5a shows a 455-ft. (138.7 m) tendon in a three-span continuous girder. Figure 1.5b gives a plot of calculated tendon force versus length for this girder, using realistic friction coefficients ($\mu = 0.16$, K = 0.0005/ft (= 0.00164/m)). Thirty-nine percent of the prestressing force is lost to friction at the dead end. This can be partially remedied by

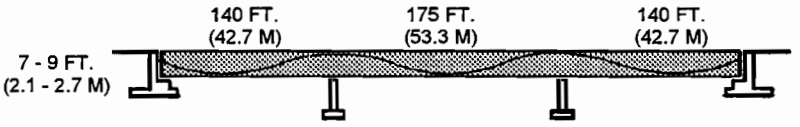

(a) Typical three-span continuous tendon

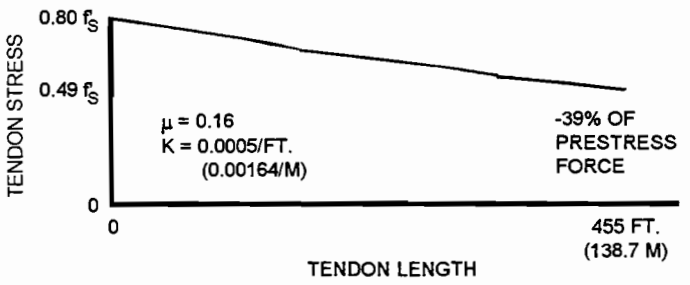

(b) Tendon stress vs. length for three-span continuous tendon

Figure 1.5 Stress loss in long continuous tendon.

jacking at both ends. This example shows that prestress friction loss can be very large, and that accurate prediction of the loss is essential.

1.2.2 Theoretical Friction Losses. The static and dynamic coefficients of friction between smooth surfaces in close contact are easily determined by performing tests similar to the small scale friction test described in Chapter 2 of this document. Unfortunately, the mating of multi-strand tendons and curved metallic duct produces behavior characteristic of contact between very rough surfaces. As described in Reference [5], the three basic elements that are involved in the friction of unlubricated solids are:

1) the true area of contact between mating rough surfaces;

2) the type and strength of bond formed at the interface where contact occurs; and,

3) the way in which material in and around the contacting regions is sheared and ruptured during sliding.

Through inspection it can be seen that post-tensioning duct surfaces are damaged during stressing. Damage was noted on the ducts used in the test programs for this report. Ducts were examined during destruction of the test girders. Also, the area of contact between duct and tendon is not easily calculated, and will vary with the number of strands, the duct diameter, and the duct rib pattern. In addition, as duct curvature in a member changes from positive to negative, the tendon must bear on the opposite sides of the duct. This transition occurs over some length, and complicates the prediction of friction loss in this region. During stressing of a tendon, a combination of static and dynamic friction forces are acting, depending on the rate of load. Static friction maintains the force gradient in the tendon after stressing. Based on all these factors, it is not evident which coefficient of friction, static or dynamic, to use when developing a model for friction loss along a curved duct profile.

In general, the coefficient of friction realized for a curved duct profile is substantially less than the coefficient of friction, either static or dynamic, as determined from a simple planar friction test. The friction loss model developed should use this lower, more representative, coefficient of friction, and must also be able to account for length dependent losses along the duct, such as minor construction error in duct placement. The normal force on the strand is generated along the curved surface of the duct. Duct misalignment will introduce additional curvature and friction loss, and must be accounted for in the "wobble loss" term.

To develop a model, consider a differential length element of mated duct and tendon shown in Figure 1.6. Normal force is a function of curvature. Friction loss is a function of curvature and length (two components acting along the tendon). Stressing force P is changed along the element due to friction loss.

Codes allow the use of an approximation of the exponential equation for small values of length and curvature change. Figure 1.7 shows how the equations compare for the example girder from Figure 1.5.

While there is theoretically no friction loss in a straight duct, experience has shown that accidental deviations from the straight line and other imperfections result in accidental friction losses termed "wobble loss". This loss is usually calculated by adding to the exponential $\mu\alpha$ coefficient, a "wobble coefficient" K (in reality a friction factor times the length of the tendon).

CURVATURE FRICTION MODEL WITH WOBBLE

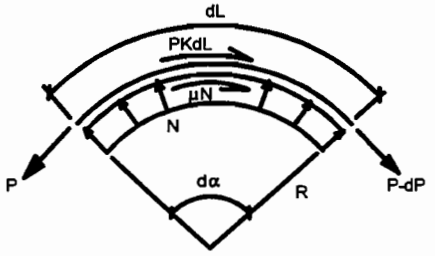

Equilibrating the forces along the tendon about the right end of the element gives

$$P + \mu N + P K dL = P - dP$$

Rearranging terms

$$dP = \mu N - P K dL$$

The normal force is a function of curvature

$$N = P d\alpha$$

Substituting

$$dP = -\mu P d\alpha - P K dL$$

Put in differential form

$$\frac{dP}{P} = -\mu d\alpha - K dL$$

Integrating both sides over the parameters of the element

$$\int_{P_o}^{P_x} \frac{dP}{P} = -\int_0^{\Sigma\alpha} \mu d\alpha - \int_0^x K dL$$

$$ln P_x - ln P_o = -\mu \Sigma \alpha - K x$$

$$ln \frac{P_x}{P_0} = -\mu \Sigma \alpha - K x$$

This gives the familiar equation

$$\frac{P_x}{P_0} = e^{-(\mu \Sigma \alpha + K x)}$$

or

$$P_x = P_o e^{-(\mu \Sigma \alpha + K x)}$$

P_0	=	known force, jacking end
P_x	=	force at point x
x	=	length from known force
μ	=	modified coefficient of friction
$\Sigma\alpha$	=	total angle change over length x
K	=	wobble coefficient

Figure 1.6 Mathematical model of friction loss.

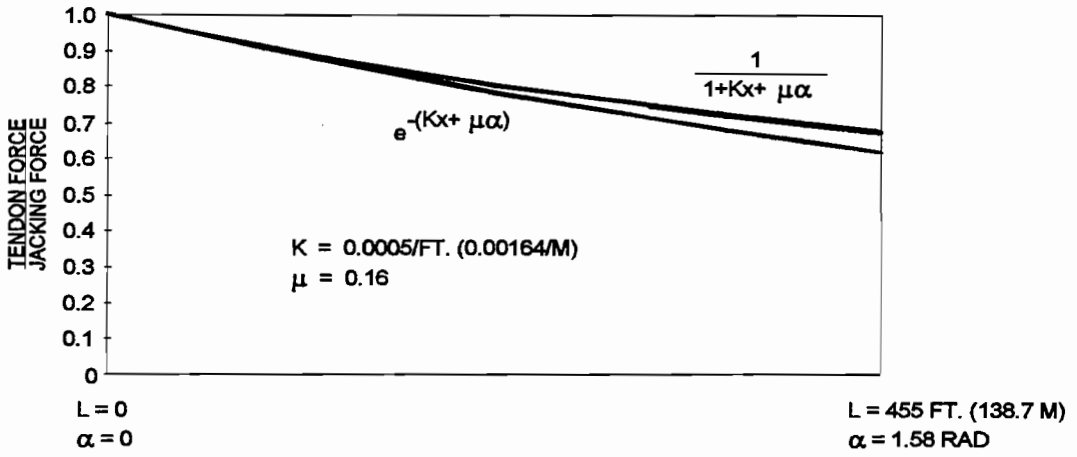

Figure 1.7 Comparison of exact equation and approximate equation for friction reduction.

1.2.3 Previous Tests and Field Data. Many laboratory tests have been performed to evaluate monolithic girder internal tendon friction loss starting in the 1960's. The need was great in the pioneering years of post-tensioned construction to check the approximate friction coefficients suggested by industry officials, such as ACI-ASCE Committee 323 [6].

The "curvature" friction coefficient (μ) and summation of intentional angle change (α), when used in the friction loss equation derived in Section 1.2.2, should accurately predict friction loss in a tendon with no wobble. The wobble term (KL) is added to the equation to estimate losses due to accidental curvature. The magnitude of accidental curvature has been found by experience to be a function of tendon length (L) and construction type (monolithic or segmental). The magnitude of accidental curvature losses would also be expected to be a function of the duct to strand friction coefficient (μ). The wobble term has been simplified to KL, and does not explicitly include the friction coefficient μ. K is given in specifications for the various combinations of duct and tendon.

A commonly used duct in the 1960's was flexible steel tubing. High wobble loss was experienced by the industry, and experimentally verified by Bezouska [7]. Wobble friction coefficients were found to be 0.0015/ft. (0.0049/m) when used with a curvature friction value of 0.25. Soon afterward, the State of California and the rest of the country began using rigid or semi-rigid steel duct in bridge construction. Wobble friction coefficients were then found by Bezouska [8] to drop to 0.0002/ft. (0.00066/m) when used with an assumed curvature friction coefficient of 0.25.

More modern field tests performed by Dywidag [9] gave a curvature friction coefficient of 0.24 in galvanized semi-rigid duct when the wobble coefficient was assumed to be 0.0002/ft. (0.00066/m). Tran [10],

in tests described in Chapter 2, found that the wobble coefficient was closer to 0.0004/ft. (0.0013/m), and the curvature coefficient 0.16. Assuming k = 0.0004/ft. (0.0013/m) in Dywidag's test girder, their curvature coefficient becomes 0.17, similar to Tran's curvature coefficient.

Full scale tests were performed by Harstead, Kummerle, Archer, and Porat [11] in galvanized semi-rigid steel duct with strand tendons. Using as assumed k of 0.0004/ft. (0.0013/m), their test results also give a curvature friction coefficient of 0.17 in a duct with a minimum radius of 65 feet (19.8 m), and 0.24 in another duct with a minimum radius of 20 (6.1 m) feet. Bezouska [8] also saw the relationship between increased curvature per length of girder and increased friction loss. Tests by Yasuno, Kondo, Tadano, Mogami, and Sotomura [12] in specimens with minimum radii of curvature similar to those of Tran (27 ft. - 70 ft.) (8.2 - 21.3 m) gave $\mu = 0.14$ and $k = 0.00033$/ft. (0.00108/m) as friction coefficients. It is well known that friction coefficients for external deviator pipes, with radii usually less than 50 ft. (15 m) are approximately 0.25 for the curvature friction coefficient, and 0.0002/ft. (0.00066/m) or greater for the wobble, or out-of-tolerance, coefficient. The friction coefficient between galvanized semi-rigid duct and strand tendons apparently changes at the normal forces experienced between about 100 ft. to 50 ft (30 m to 15 m) radii in draped ducts, with an upper bound of $\mu = 0.25$ under high normal forces at radii less than 50 ft. (15 m).

1.2.4 Friction and Wobble Coefficients. Friction and wobble coefficients given in codes are generally conservative, and the recommendations do not change in most cases with radius of duct curvature, number of strands per duct, or tendon area to duct area ratio. Many of the coefficients are viewed by the industry as too conservative. Overly conservative friction coefficients result in tendons larger than necessary and out-of-tolerance tendon elongations. Modern construction techniques and experience of contractors have brought wobble losses down to acceptable levels for semi-rigid ducts. Wobble losses in sheathed single-strand tendons remain very high.

1.2.5 Recommended Coefficients. Tables 1.1 through 1.4 give friction and wobble coefficients recommended by different design standards for various combinations of prestressing tendons and bars and duct types. The different standards vary greatly in recommended values, as can be seen in the examples shown later in Section 5.3.

1.3 Objectives and Scope of Research

The research in this report was performed as part of a larger research project sponsored by the Texas Department of Transportation and the Federal Highway Administration. The sub-project topic involved with this study is friction reduction and corrosion protection of internally post-tensioned bridge girder tendons. Tests were reported by Kittleman [16] and detailed in Report 1264-1 [17] to evaluate the corrosion protection capability of various water-soluble lubricants, the effect these lubricants have on strand to grout bond, and the lubricants' effectiveness for reducing friction losses during post-tensioning. Tests were performed by Tran [10] to determine friction factors and the effect of tendon lubrication for monolithic girders with internal tendons. Tests were performed by Davis [18] to determine friction factors and the effect of tendon lubrication for segmentally constructed concrete bridge girders with internal tendons. Both of these latter test series are summarized in this report.

Table 1.1 Friction and Wobble Coefficients for Post-Tensioned Internal Tendons from ACI-ASCE [6].

Type of Steel	Type of Duct or Sheath	Usual Range of Observed Values		Suggested Design Values	
		K /ft (/m)	μ	K /ft (/m)	μ
Wire Cables	Bright metal sheathing Galvanized metal sheathing	0.0005 - 0.0030 (0.0016 - 0.0098)	0.15 - 0.35	0.0020 (0.0066) 0.0015 (0.0049)	0.30 0.25
Wire Cables	Greased or asphalt-coated and wrapped	0.0030 (0.0098)	0.25 - 0.35	0.0020 (0.0066)	0.30
High Strength Bars	Bright metal sheathing Galvanized metal sheathing	0.0001 - 0.0005 (0.00033 - 0.0016)	0.08 - 0.30	0.0003 (0.0010) 0.0002 (0.0007)	0.20 0.15
Galvanized strand	Bright metal sheathing Galvanized metal sheathing	0.0005 - 0.0020 (0.0016 - 0.0066)	0.15 - 0.30	0.0015 (0.0049) 0.0010 (0.0033)	0.25 0.20

Table 1.2 Friction and Wobble Coefficients for Post-Tensioned Internal Tendons from ACI 318-89 [11]

Materials			Wobble Coefficient K /ft (/m)	Curvature Coefficient μ
Grouted tendons in metal sheathing		Wire tendons	0.0010 - 0.0015 (0.0033 - 0.005)	0.15 - 0.25
		High strength bars	0.0001 - 0.0006 (0.0003 - 0.002)	0.08 - 0.30
		7-wire strand	0.0005 - 0.0020 (0.0016 - 0.0066)	0.15 - 0.25
Unbonded tendons	Mastic coated	Wire tendons	0.0010 - 0.0020 (0.0033 - 0.0066)	0.05 - 0.15
		7-wire strand	0.0010 - 0.0020 (0.0033 - 0.0066)	0.05 - 0.15
	Pregreased	Wire tendons	0.0003 - 0.0020 (0.0010 - 0.0066)	0.05 - 0.15
		7-wire strand	0.0003 - 0.0020 (0.0010 - 0.0066)	0.05 - 0.15

Table 1.3 Friction and Wobble Coefficients for Post-Tensioned Internal Tendons from PTI [14].

Type of Duct	Range of Values		Recommended for Calculations	
	μ	K /ft (/m)	μ	K /ft (/m)
Flexible tubing non-galvanized	0.18 - 0.26	$5 - 20 \times 10^{-4}$ ($16 - 66 \times 10^{-4}$)	0.22	7.5×10^{-4} (25×10^{-4})
Flexible tubing galvanized	0.14 - 0.22	$3 - 7 \times 10^{-4}$ ($10 - 23 \times 10^{-4}$)	0.18	5.0×10^{-4} (16×10^{-4})
Rigid thin wall tubing non-galvanized	0.20 - 0.30	$1 - 5 \times 10^{-4}$ ($3.3 - 16 \times 10^{-4}$)	0.25	3.0×10^{-4} (10×10^{-4})
rigid thin wall tubing galvanized	0.16 - 0.24	$0 - 4 \times 10^{-4}$ ($0 - 13 \times 10^{-4}$)	0.20	2.0×10^{-4} (6.6×10^{-4})
Greased and wrapped	0.05 - 0.15	$5 - 15 \times 10^{-4}$ ($16 - 50 \times 10^{-4}$)	0.07	10×10^{-4} (33×10^{-4})

Table 1.4 Friction and Wobble Coefficients for Post-Tensioned Tendons from AASHTO [15].

Materials	Friction Coefficient (μ)	Wobble Coefficient k/ft (K/m)
1. For strand in galvanized metal sheathing	0.15 - 0.25*	0.0002 (0.00066)
2. For deformed high strength bars in galvanized metal sheating	0.15	0.0002 (0.00066)
3. For strand in internal polyethylene duct	0.23	0.0002 (0.00066)
4. For strand in straight polyethylene duct (external to concrete)	0	0
5. Rigid steel pipe deviators	0.25**	0.0002 (0.00066)

*A friction coefficient of 0.25 is appropriate for 12 strand tendons. The coefficient is less for larger tendon and duct sizes.
**Lubricant will probably be required.

1.3.1 Research Objectives. One of the two primary objective of this research is to quantify the differences in wobble and friction loss during post-tensioning between segmentally constructed girders and monolithically constructed girders. Friction loss data for comparable tendons in monolithic construction is provided by Tran [10] while the same type specimen, except for segmental construction, was used in the tests by Davis [18]. Segmental construction will inherently introduce more locations along a duct profile for placement tolerance error, most importantly at the segment joint. Friction loss was expected to increase accordingly.

The second primary objective was to investigate the benefits and side effects from using lubricated tendons in segmental and monolithic construction. Lubricants can be ranked according to their effectiveness in reducing friction, temporarily preventing corrosion, and maintaining strand to grout bond. The efficacy of flushing the lubricants is critical in this last property.

This research is intended to provide the basis for recommending more accurate friction and wobble coefficients for monolithic and segmental design, checking the acceptability of the current duct placement tolerance at segment joints based on its contribution to friction loss, and recommending or rejecting use of lubricants used on tendons for friction reduction.

1.3.2 Variables Studied. The construction of two otherwise identical large-scale friction test specimens (one constructed monolithically and one segmentally) provides friction loss data that can be used to quantify the differences in construction technique. The two specimens have identical length and curvature for two types of duct profiles, one draped and one straight. This study does not include friction losses in external tendons, or internal tendons with curvature change concentrated over very short lengths. The radius of curvature is very tight in the deviator pipe, and normal forces are very high.

The large-scale test specimens have smoothly draped internal tendons with moderately tight radii of curvature when compared to girders usually found in the field. The friction and wobble coefficients found from the test girder should be conservative, since the coefficients have generally been found to increase with decreasing radii of curvature. The straight tendon profiles in the test girders will provide data to facilitate estimating accurate wobble coefficients.

The segmental test specimen also has its ducts placed to provide intentional mismatches at the segment joints. Comparison of data among ducts in the specimen will provide a means for checking the reasonableness of current code duct alignment tolerances.

Tendons and ducts used are of one size and material only. A 7-0.5" (13 mm) ϕ strand tendon is used in a 2"ϕ (51 mm) galvanized semi-rigid duct. This is a commonly used tendon but may not act exactly like some of the very large tendons.

Small-scale friction tests were performed with a normal force of 1000 #/ft. (14.6 kN/m). This is a normal force that would be generated somewhere along the tendon in the large-scale test girders. The lubricants tested are rated at this normal force.

1.4 Report Organization

This report is organized into seven chapters. Chapter 2 describes the preliminary friction and pullout tests used to evaluate the properties of candidate agents both for selection for use in the large-scale tests and to determine the efficacy of flushing. Chapter 3 describes the construction of the specimens and the test procedures and instrumentation used in the full-scale monolithic and segmental girders. Chapter 4 presents the important test results. Chapter 5 evaluates, discusses and analyzes the test results and illustrates the effect of the types of friction losses measured when extended to other applications. Chapter 6 gives specific recommendations for implementation of the results in design and construction including specific language for consideration for AASHTO changes. Chapter 7 summarizes the conclusions.

CHAPTER TWO
PRELIMINARY FRICTION AND PULLOUT TESTS

2.1 General

Several series of tests were performed to evaluate the effectiveness of various lubricants used on strand tendons for corrosion protection, friction reduction, or both. Detailed procedures and results are given in CTR Report 1264-1 [17]. The lubricants tested are identified and described in Table 2.1 The results of these tests provide rankings that could be entered into the decision matrix shown in Table 2.2 [17]. The small scale friction tests were performed expressly for inclusion in this matrix. Lubricants L13 and L14 have been added to the matrix originally developed by Kittleman [16]. L13 and L14 were assumed to be ineffective for corrosion protection. L13 is an effective corrosion inhibitor when used as a coolant during machining operations, but its effectiveness in preventing corrosion on post-tensioning tendons is uncertain. The basis for the rankings based on friction coefficient for L14 was found in the results from the large-scale segmental specimen.

The highest ranking lubricants, as determined from the decision matrix before L13 and L14 were tested, were used in the two large-scale friction test specimens. Only a limited number of ducts were available for tests with lubricated tendons.

Large-scale friction tests were performed by Tran [10] using a monolithically constructed test specimen and by Davis [18] using a segmentally constructed test specimen. Data from both of these tests is directly comparable and is reported herein.

2.2 Small Scale Specimen Friction Tests

The small-scale friction test was developed by Hamilton and Davis [17] to provide a realistic, accurate, and low-cost means of ranking the 13 lubricants shown in Table 2.1.

2.2.1 Test Objectives. The small-scale friction test specimen was designed to be easy to construct, able to be tested quickly, and give repeatable results. The test provided both the static and dynamic coefficients of friction for untreated and lubricated strand bearing on galvanized duct. The change in coefficient of friction for lubricated strand versus bare strand within the same specimen gave an indication of the lubricant's effectiveness for reducing friction for this application. The lubricants could then be ranked.

2.2.2 Test Specimen. The specimen, shown in Figure 2.1, consisted of two 3.5-in. (90 mm) x 3.5-in. (90 mm) x 12-in. (300 mm) concrete blocks with a 1.25-in. (32 mm) x 12-in. (300 mm) strip of duct embedded in opposing faces of each block. A single strand was sandwiched between the two blocks, riding on the duct surfaces. Figure 2.2 shows the specimen ready for testing.

Table 2.1 Lubricant Alternatives.

Identification	Product	Description
L1	Visconorust 8415E	Emulsifiable oil marketed for temporary corrosion protection of post-tensioned tendons before grouting. This oil is no longer manufactured.
L2	Dromus B	Emulsifiable oil designed for use as coolant lubricant and rust preventive in metalworking operations. Has been used for temporary corrosion protection and friction reduction of post-tensioned tendons.
L3	Unocal 10	Emulsifiable oil designed for use as coolant and rust preventive in metalworking operations. Also used as corrosion preventive in hydraulic operations when water is used as the coolant.
L4	Unocal 10MS	Emulsifiable oil designed for use as coolant and rust preventive in metalworking operations. Also used as corrosion preventive in hydraulic operations when water is used as the coolant. Same manufacturer as L3. Recommended because it offers slightly better corrosion protection than L3.
L5	Texaco D	Emulsifiable oil designed for use as coolant lubricant for light metalworking operations where very lean emulsions are required.
L6	Rust Veto FB20	Emulsifiable oil designed for temporary corrosion protection of metals.
L7	Hocut 737	Emulsifiable oil designed for use as coolant lubricant for metalworking applications on a variety of metals.
L8	Hocut 4284	Synthetic emulsifiable oil designed for use as coolant lubricant for difficult machining operations.
L9	Nalco 6667	Emulsifiable oil designed for use as coolant lubricant in heavy drawing of ferrous metals.
L10	Sodium Silicate	Sodium silicate solution designed for various uses including adhesives, detergents, protective coatings and rust inhibitors.
L11	Wright 502	Emulsifiable oil designed for use as coolant lubricant in metalworking of ferrous metals.
L12	Bare Strand	Bare strand with no lubricant
L13	Aqualube MX	Water soluble coolant designed for cutting and grinding use on a variety of metals. This biodegradable soap is formulated to provide maximum performance, be safe to personnel and provide excellent corrosion resistance during machining operations.
L14	Graphite Flakes #2	Dry lubricant used as an additive in other lubricants to reduce friction between mechanical parts.

Table 2.2 Decision Matrix for Lubricant Selection

Alternative	Friction Reduction		Effect on Adhesion		Temporary Corrosion Protection									Safety Hazards			Lub. Cost	Diff. of Use	Total Score
					Unflushed Strands			Flushed Strand			Unflushed Wires								
	Static	Dyn.	Unflush.	Flushed	Strand Protection		Corr. Rate	Strand Protection		Corr. Rate	Amb.	Deion. Water	3.50% NaCl Sol'n.	Health	Flamm.	React.			
					Outer	Inner		Outer	Inner										
Importance	20	20	12.5	12.5	6	2	2	3	1	1	2	1.5	1.5	2	2	2	5	4	100
L14	5.41	5.41	7.54	9.70	0	0	0	0	0	0	0	0	0	10.0	10.0	10.0	6.70	10	565
	108	108	94.3	121	0	0	0	0	0	0	0	0	0	20.0	20.0	20.0	33.5	40.0	
L13	6.81	5.45	4.95	9.60	0	0	0	0	0	0	0	0	0	10.0	10.0	10.0	5.50	9	550
	136	109	61.9	120	0	0	0	0	0	0	0	0	0	20.0	20.0	20.0	27.5	36.0	
L5	8.61	5.58	0.52	0.94	5.00	9.00	7.22	1.00	0.50	5.46	3.50	10.0	9.40	10.0	7.50	10.0	8.81	5.00	529
	172	112	6.50	11.8	30.0	18.0	14.4	3.00	0.50	5.46	7.00	15.0	14.1	20.0	15.0	20.0	44.1	20.0	
L11	7.21	5.58	1.60	2.02	3.75	8.50	8.86	1.00	0.00	8.23	1.75	9.90	8.75	7.50	7.50	10.0	9.24	5.00	517
	144	112	20.0	25.3	22.5	17.0	17.7	3.00	0.00	8.23	3.50	14.9	13.1	15.0	15.0	20.0	46.2	20.0	
Bare Strand	2.33	2.33	7.94	10.00	1.00	1.50	5.46	1.00	1.50	5.46	2.75	4.50	4.00	10.0	10.0	10.0	10.0	10.0	516
	46.6	46.6	99.3	125	6.00	3.00	10.9	3.00	1.50	5.46	5.50	6.8	6.00	20.0	20.0	20.0	50.0	40.0	
L2	6.28	3.70	0.14	2.26	8.75	10.0	5.46	1.00	0.50	5.46	3.50	9.65	9.25	10.0	7.50	10.0	8.58	5.00	475
	126	74.0	1.75	28.3	52.5	20.0	10.9	3.00	0.50	5.46	7.00	14.5	13.9	20.0	15.0	20.0	42.9	20.0	
L3	5.58	3.72	1.44	2.70	5.00	10.0	6.67	1.00	2.00	5.46	3.50	9.00	9.90	10.0	7.50	10.0	8.63	5.00	465
	112	74.4	18.0	33.8	30.0	20.0	13.3	3.00	2.00	5.46	7.00	13.5	14.9	20.0	15.0	20.0	43.2	20.0	
L1	6.28	3.75	0.48	1.44	9.75	1.00	7.86	1.00	0.50	5.46	4.50	7.00	6.75	7.5	7.50	10.0	8.89	5.00	454
	126	75.0	6.00	18.0	58.5	2.00	15.7	3.00	0.50	5.46	9.00	10.5	10.1	15.0	15.0	20.0	44.5	20.0	
L8	6.51	4.65	0.00	2.12	5.00	5.50	5.65	1.00	0.00	5.46	3.50	9.00	8.50	10.0	10.0	10.0	5.41	5.00	451
	130	93.0	0.00	26.5	30.0	11.0	11.3	3.00	0.00	5.46	7.00	13.5	12.8	20.0	20.0	20.0	27.1	20.0	
L4	5.58	3.72	0.29	1.16	5.00	10.0	7.22	1.00	1.00	5.46	4.50	9.95	9.40	10.0	7.50	10.0	8.53	5.00	434
	112	74.4	3.63	14.5	30.0	20.0	14.4	3.00	1.00	5.46	9.00	14.9	14.1	20.0	15.0	20.0	42.7	20.0	
L9	5.12	2.77	0.00	0.00	9.75	10.0	7.86	1.00	10.0	5.46	9.75	10.0	10.0	7.50	7.50	10.0	3.12	2.00	394
	102	55.4	0.00	0.00	58.5	20.0	15.7	3.00	10.0	5.46	19.5	15.0	15.0	15.0	15.0	20.0	15.6	8.00	
L10	0.00	0.00	3.82	9.39	5.00	0.50	6.35	5.00	3.00	6.54	2.75	8.50	6.75	10.00	10.00	5.00	9.36	0.00	359
	0.00	0.00	47.8	117	30.0	1.00	12.7	15.0	3.00	6.54	5.50	12.8	10.1	20.0	20.0	10.0	46.8	0.00	
L6	2.33	0.91	0.46	0.42	5.00	10.0	6.82	1.00	1.00	5.46	4.50	9.95	9.75	10.0	7.50	10.0	7.11	5.00	298
	46.6	18.2	5.75	5.25	30.0	20.0	13.6	3.00	1.00	5.46	9.00	14.9	14.6	20.0	15.0	20.0	35.6	20.0	
L7	0.23	0.86	0.25	0.68	5.00	1.50	3.33	1.00	0.00	5.46	3.50	9.80	9.70	7.50	7.50	10.0	6.33	5.00	219
	4.60	17.2	3.13	8.50	30.0	3.00	6.66	3.00	0.00	5.46	7.00	14.7	14.6	15.0	15.0	20.0	31.7	20.0	

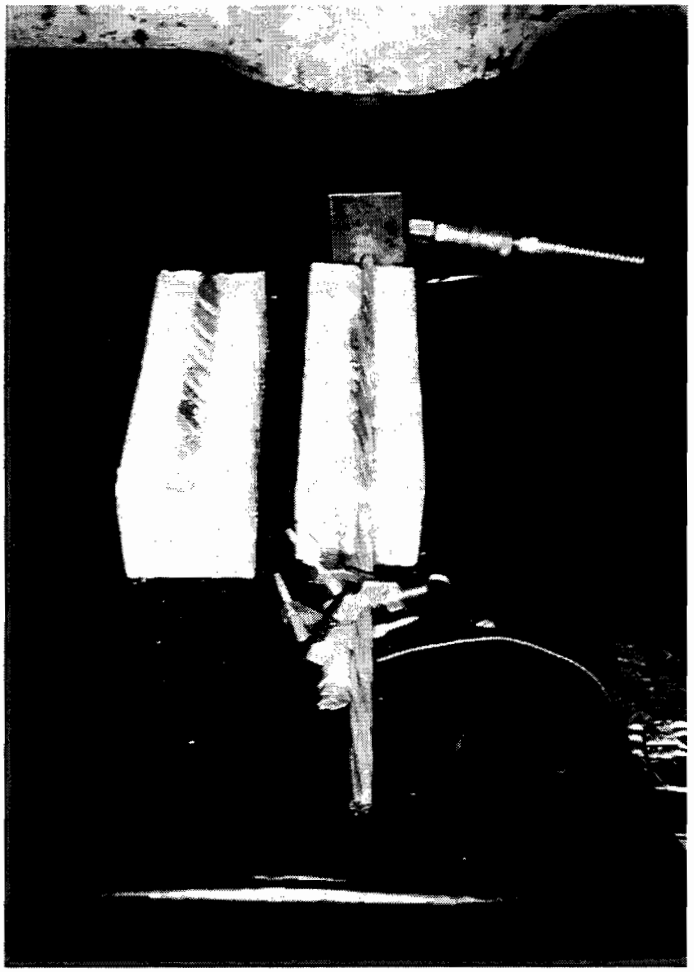

Figure 2.1 Small-scale friction test specimen.

2.2.3 Test Procedure. The blocks and strand were assembled in a 60-kip (267 kN) testing machine. Both dry and lubricated tests were performed. Lubricant was applied to the strand as shown in Figure 2.3, and a 1000-lb. (4.45 kN) force was applied normal to the strand. A hydraulic ram was attached to the strand on one end to apply a tension force along the strand axis. A linear potentiometer was attached to the strand on the other end to measurement movement. Ram force, measured by a pressure transducer, divided by the normal force gave the coefficient of friction. Force versus strand movement was recorded on a plotter.

The specimen was disassembled after each test. Each specimen was tested twice without an applied lubricant, and then twice with a lubricant. Additional tests of the specimen were performed only if the results of a test were inconsistent with previous tests. A typical plot is shown in Figure 2.4.

2.2.4 Test Results. The static coefficient of friction was determined by dividing the ram load at first slip of the strand by the 1000-lb. (4.45 kN) normal force. The dynamic coefficient of friction was found by dividing the ram load recorded as the strand first went into steady state motion by the 1000-lb. (4.45 kN) normal force. The repeated test values for each test specimen were averaged together. Static friction coefficients are given in Table 2.3, and dynamic friction coefficients are given in Table 2.4.

2.2.5 Analysis and Conclusions. Average coefficients of friction, both static and dynamic, for unlubricated strand on galvanized duct are 0.24 or larger. This is somewhat higher than what is actually seen in the field in draped ducts, and corresponds to the upper limit of the curvature coefficient of friction recommended by AASHTO [15]. In all cases, visual inspection showed that the strand cut into the duct surfaces and essentially screwed itself out of the specimen under the ram load. Coefficients of friction for each block could be consistently obtained with little scatter for about five test repetitions. Coefficients of friction for additional tests were larger. This behavior can be attributed to removal of the galvanization, and continued deeper grooving of the duct surfaces.

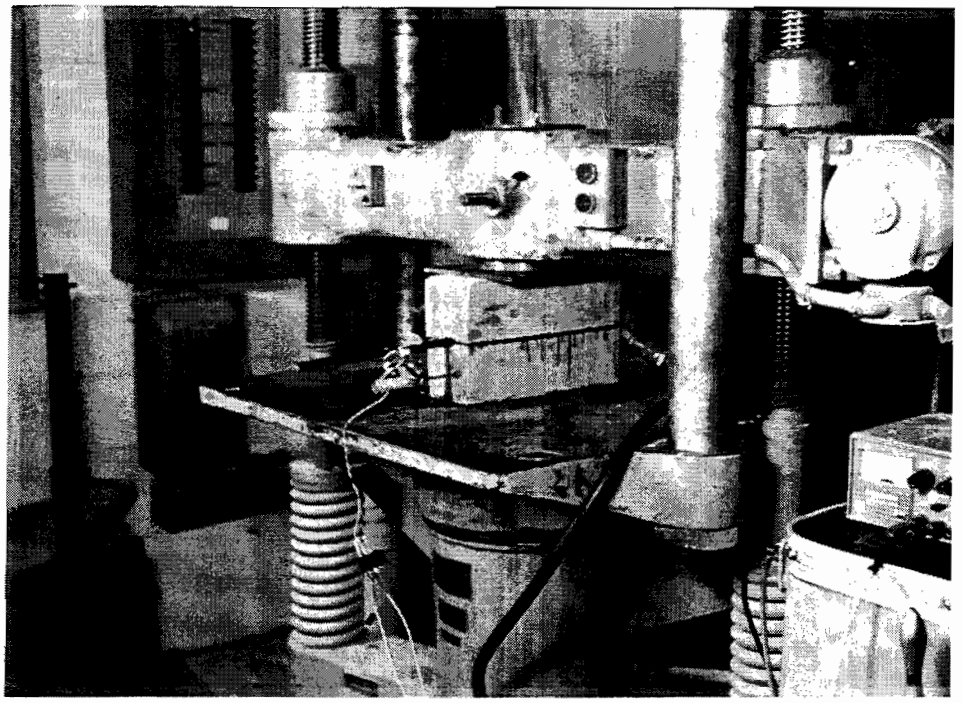

Figure 2.2 Small-scale friction test setup.

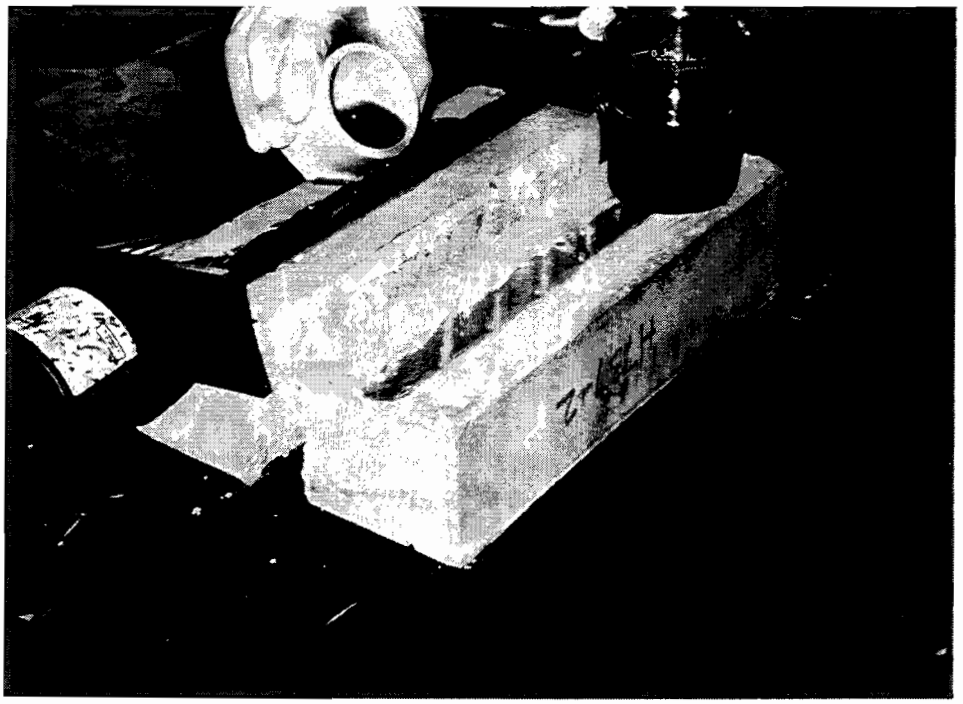

Figure 2.3 Applying lubricant to small-scale friction specimen.

Table 2.3 Static Coefficients of Friction from Small-Scale Specimens.

Lubricant		Static Friction Factor[1]		Percent Reduction in Friction	Average
		Bare	Lubricated		%
L5	(1)	0.26	0.19	27	27
L5	(2)	0.25	0.18	28	
L11	(1)	0.26	0.20	23	21
L11	(2)	0.27	0.22	18	
L13	(1)	0.23	0.21	11	19
L13	(2)	0.30	0.22	26	
L8	(1)	0.25	0.18	28	18
L8	(2)	0.24	0.22	8	
L1	(1)	0.26	0.22	15	17
L1	(2)	0.26	0.21	15	
L2	(1)	0.26	0.22	15	17
L2	(2)	0.27	0.22	18	
L4	(1)	0.26	0.23	11	14
L4	(2)	0.23	0.19	17	
L3	(1)	0.27	0.23	15	14
L3	(2)	0.24	0.21	12	
L9	(1)	0.27	0.23	15	12
L9	(2)	0.24	0.22	8	
L6	(1)	0.25	0.25	0	0
L6	(2)	0.25	0.25	0	
L7	(1)	0.26	0.26	0	-9
L7	(2)	0.22	0.26	-18[2]	
L10	(1)	0.27	0.36	-33	-31
L10	(2)	0.28	0.36	-29	

[1] Force required to extract strand from specimen divided by normal force. "Static" indicates friction values for initial slip of strand.

[2] Indicates an increase in friction with strand lubricated with oil.

Table 2.4 Dynamic Coefficients of Friction from Small-Scale Specimens.

Lubricant		Dynamic Friction Factor[1]		Percent Reduction in Friction	Average
		Bare	Lubricated		%
L5	(1)	0.25	0.21	16	14
L5	(2)	0.24	0.21	13	
L11	(1)	0.25	0.21	16	14
L11	(2)	0.26	0.23	11	
L13	(1)	0.26	0.25	6.0	13
L13	(2)	0.32	0.26	20	
L8	(1)	0.25	0.23	8.0	10
L8	(2)	0.25	0.22	12	
L1	(1)	0.24	0.23	4.2	6.1
L1	(2)	0.25	0.23	8	
L2	(1)	0.25	0.24	4.0	5.9
L2	(2)	0.26	0.24	7.7	
L4	(1)	0.26	0.25	3.8	6.0
L4	(2)	0.24	0.22	8.3	
L3	(1)	0.25	0.24	4.0	6.0
L3	(2)	0.25	0.23	8.0	
L9	(1)	0.26	0.25	3.8	1.9
L9	(2)	0.25	0.25	0	
L6	(1)	0.26	0.27	-3.8[2]	-6.1
L6	(2)	0.24	0.26	-8.3	
L7	(1)	0.24	0.26	-8.3	-6.3
L7	(2)	0.24	0.26	-4.2	
L10	(1)	0.26	0.31	-19	-26
L10	(2)	0.25	0.33	-32	

1 Force required to extract strand from specimen divided by normal force. "Dynamic" indicates friction values for steady movement of the strand.

2 Indicates an increase in friction with strand lubricated with oil.

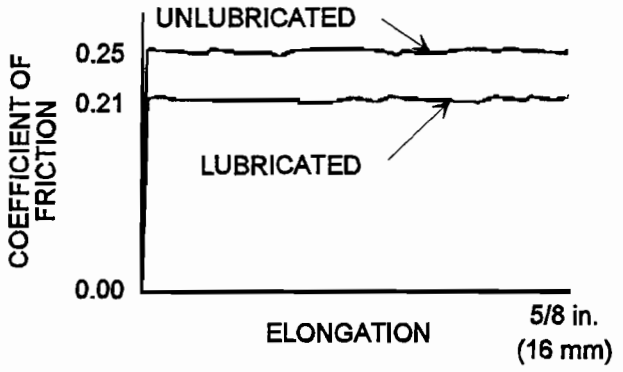

Figure 2.4 Typical test result small-scale friction test.

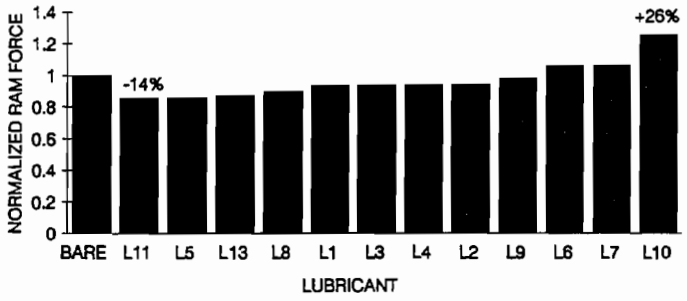

Figure 2.5 Small-scale friction test results - dynamic.

Lubricants tested either decreased the coefficients of friction or increased them. As shown in Figure 2.5, the greatest average de crease in dynamic coefficient of friction was 0.035 or 14%. This related to a 14% decrease in ram load needed to keep the strand moving steadily through the specimen. Static coeffi cients of friction were smaller than the dynamic coefficients of friction when lubricants were used. The overall reduction in static friction of 27% for L5 approached friction reduction seen by Dywidag [9] in field tests in draped ducts with lubricants L13 (35%) and L2 (28%). Several lubricants acted like cutting agents and actually increased friction by increasing duct grooving. Duct grooves on the small-scale friction specimen are shown in Figure 2.6.

Many of the water soluble lubricants were difficult to remove from the strand and duct surface. Emulsification of the oil by rinsing alone proved ineffective. Some of the lubricants were retested in the small-scale friction test specimen after the specimens had been flushed with water to remove the lubricant from the duct surfaces. New bare strand was used with the lubricated and flushed specimen duct surfaces. The friction reduction seen after flushing was similar to that of the fully lubricated test. The results of the flushed test are shown in Figure 2.7. This behavior can be attributed to residual traces of lubricant remaining on the duct surfaces, and the removal of dirt and grit by flushing. Overall the effectiveness of most lubricants tested was marginal to poor.

2.3 Pullout Tests

A pullout test was developed by Kittleman [16, 17] to study the effect each lubricant had on the adhesion between seven-wire strand and cement grout with and without flushing. Internal post-tensioning bridge tendons are generally grouted in the duct for both corrosion protection after stressing and to provide greater ultimate strength for the girder section. Lubricant remaining on the strand surfaces may increase development length of the tendon near regions of high moment, and decrease ultimate moment capacity.

Figure 2.6 Small-scale friction test duct grooving.

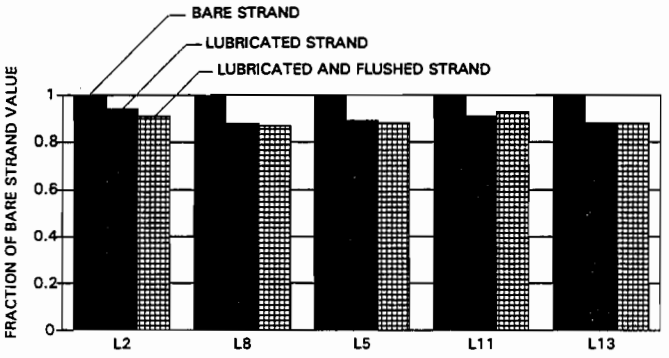

Figure 2.7 Small-scale friction test results - flushed.

2.3.1 Test Objectives. The pullout test was designed to give repeatable results at low cost. Lubricants tested were to be ranked by their influence on strand to grout bond, which also gives an indication of their ability to be flushed clean from the strand. These results were entered in the decision matrix in Table 2.2.

Effect on adhesion was given a high importance factor in Table 2.2, second only to friction reduction capability. Flushing techniques used in the field are of questionable effectiveness for removing water soluble lubricants from tendons. Lubricant remaining on the strand may destroy bond and may chemically react with the steel or grout over the long term.

2.3.2 Test Specimen. The test specimen consisted of a 12-in. (300 mm) x 8-in. (200 mm) x 8-in. (200 mm) concrete block with a 12-in. (300 mm) piece of 2-in. (50 mm) ϕ galvanized semi-rigid duct cast down the longitudinal axis. A length of 0.5-in. (13 mm) ϕ seven-wire strand was then grouted in place down the center of the duct using cement grout with a water to cement ratio of 0.45.

2.3.3 Test Procedure. Strand in the specimens was either (1) grouted in place with no lubricant, (2) lubricated by submersion then installed in the duct and grouted, or (3) lubricated then installed in the duct, flushed through the grout tubes with clean water for five minutes, and grouted. The bare strand specimen

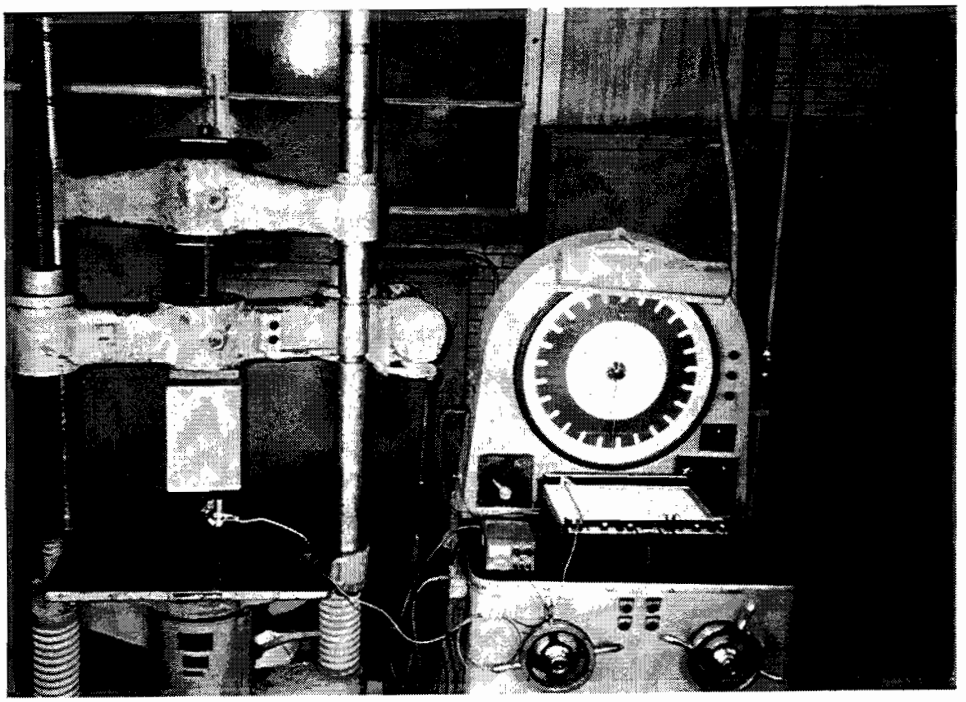

Figure 2.8 Bond test specimen.

provided a control, the unflushed strand specimen represented the worst case possible, and the flushed strand specimen gave an indication of the lubricant's flushability.

The grout was allowed to cure for a minimum of seven days before testing. The specimens were installed vertically in a 60-kip (267 kN) test machine so that an axial tension force could be applied to the strand while holding the block in place. A linear potentiometer was installed on the opposite end of the strand from which load was applied by the top crosshead of the test machine. Strand movement versus pullout force was plotted. Figure 2.8 shows the specimen installed in the 60 kip (267 kN) test machine. Figure 2.9 shows a lubricated strand being flushed in place with the use of the grouting hoses.

2.3.4 Test Results. Slip loads are plotted in Figures 2.10 and 2.11 as a percentage of the bare strand specimen slip load for both the unflushed and flushed strand tests. Figure 2.12 shows the slip loads for strand that was lubricated and flushed in the large-scale monolithic friction test specimen described in Section 2.4. This strand was cut to length then installed and grouted in the pullout specimen.

2.3.5 Analysis and Conclusions. Figure 2.10 clearly shows that nearly all the lubricants tested have the capability of substantially reducing strand to grout bond strength. Only L14 has less than 1/3 reduction. Figure 2.11 more importantly shows that most of the lubricants tested were unable to be flushed clean of the strand. Only three of the lubricants/corrosion inhibitors tested (L10, L14, and L13) had minimal impact on bond strength after flushing. Use of the other lubricants should be questioned when development of the tendon is required by design. Strand flushed in the large scale specimen gave somewhat better results for lubricants L11 and L5 in the pullout test than strand flushed in the pullout specimen. However, even then Figure 2.12 shows that less than 55% of bare strand bond strength could be recovered.

Figure 2.9 Flushing bond test specimen.

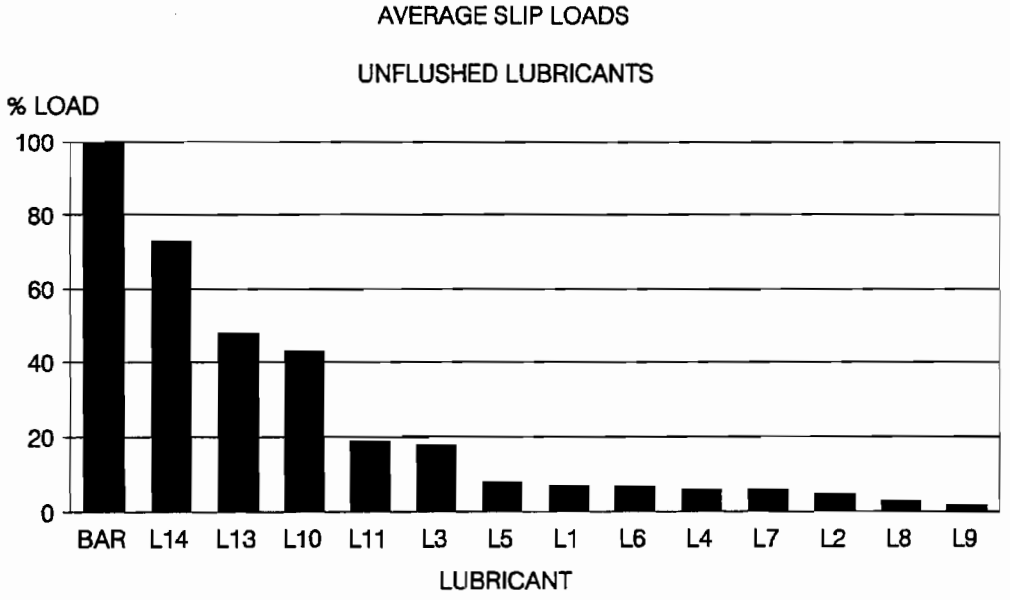

Figure 2.10 Average slip loads for unflushed lubricants.

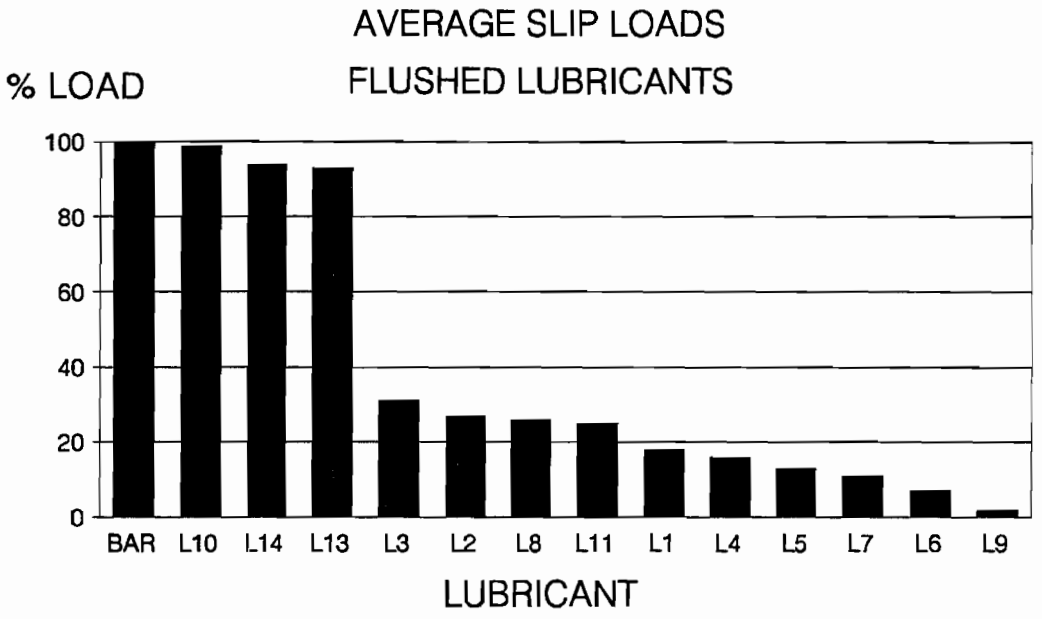

Figure 2.11 Average slip loads for flushed lubricants.

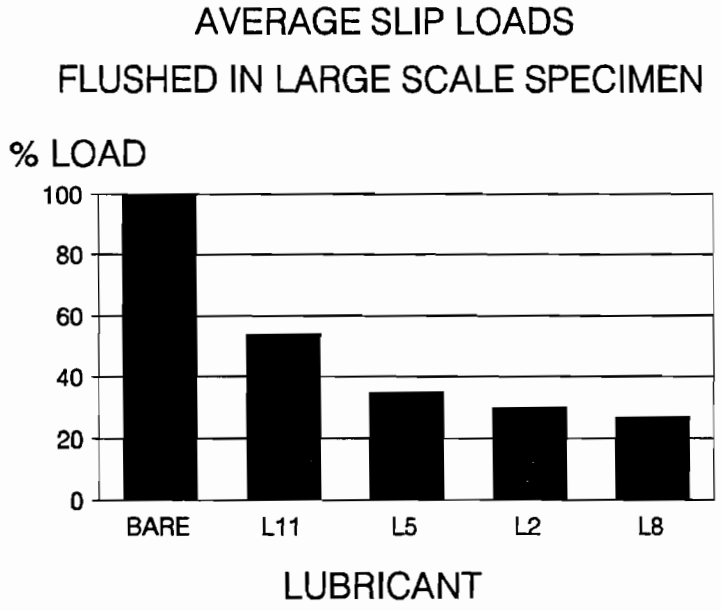

Figure 2.12 Average slip loads for lubricated strand flushed in large-scale specimen.

CHAPTER THREE
LARGE SCALE MONOLITHIC AND SEGMENTAL SPECIMEN FRICTION TESTS

3.1 Test Objectives

This study deals with multi-strand post-tensioning systems in monolithic and segmental girders, primarily in the following areas:

1) stress distribution along the tendon;

2) wobble coefficients;

3) friction coefficients;

4) the effect of selected lubricants on the friction and wobble coefficients; and,

5) the effect of the lubricants on the adhesion between the strand and grout after flushing the tendon.

The large scale segmental specimen was constructed with geometry nearly identical to the large-scale monolithic specimen. Construction procedure was the major variable studied between the two major specimens. The large scale segmental specimen also was designed to provide information on the adequacy of current duct placement tolerances.

3.1.1 Behavior Compared to Monolithic Construction. Field experience has shown that higher friction losses occur during post-tensioning of internal tendons in segmentally constructed girders than would be predicted for monolithic girders. The segmental test specimen was designed and constructed to simulate actual construction conditions. Friction loss data from the segmental and monolithic specimens can be directly compared, and the relationship between friction loss and construction technique evaluated.

Friction losses in segmental girders are higher for several reasons. Continuous tendons in monolithic construction are more rigid longitudinally than the short pieces of duct used in segmental construction, and therefore tend to remain in place better during concrete placement. Also, short pieces of duct placed with small curvature or alignment errors at each end of a segment will increase the wobble friction loss over the length of a segmental girder. This increase in friction will be measured in the segmental test specimen.

3.1.2 Impact of Duct Placement Tolerance. Current AASHTO [19] tolerance for matching ducts at segment joints is 1/8-in. (3.2 mm). To determine whether duct placement at this tolerance would greatly increase friction, the segmental test specimen has ducts placed with intentional offsets of 0-in., 1/8-in. (3.2 mm), and 1/4-in. (6.4 mm) at every segment joint along the length of the girder. This direct comparison

testing will give the relationship between the offset and friction loss. The adequacy of the current tolerance can then be evaluated.

3.1.3 Use of Lubricants. The four highest ranking water soluble oils from Table 2.2 were used in the monolithic specimen. Two of the best lubricants tested in the monolithic test specimen, as well as a water soluble soap and graphite, were tested in the segmental girder. These tests were performed to verify the effectiveness of the lubricants recommended by Tran [10], and to study any difference in performance of the lubricants when used in a segmental girder.

3.2 Specimen Design and Construction

The monolithic and segmental specimens were very much alike. Unless a specific difference is highlighted herein, the dimensions and procedures for both tests can be assumed as the same. The large-scale monolithic specimen was designed to generally comply with the recommendations of AASHTO [15] and to represent fairly tight radius of curvature tendons in a cast-in-place post-tensioned bridge girder.

The large-scale segmental friction test specimen was nearly identical in design to the monolithic specimen with the exception of construction technique and the number of straight tendon profiles. The segmental girder was designed and constructed to satisfy the AASHTO Guide Specifications for Design and Construction of Segmental Concrete Bridges [19]. Great effort was taken to use realistic construction procedures and good craftsmanship so that the test results would be similar to those of the same girder constructed in the field.

3.2.1 Monolithic Test Specimen. The specimen was a girder 78-ft. (23.77 m) long, 48-in. (1220 mm) high and 18-in. (958 mm) wide. There were ten internal duct profiles. Eight were draped with identical curvature, and two were straight for measuring wobble loss. The girder was formed with wood and cast in a single placement. The post-tensioning hardware was identical to that used in the segmental specimen. A detailed description of the post-tensioning hardware used in both specimens is given later. An elevation and end view of the monolithic specimen are shown in Figures 3.1 and 3.2.

The monolithic test specimen was identical to the segmental test specimen with the exception of the construction procedure and the number of ducts. Figures 3.3 and 3.4 show the girder under construction with one side form removed.

3.2.2 Segmental Test Specimen. The segmental specimen had eight draped profiles and three straight profiles. A typical draped profile is shown in Figure 3.5. The straight profiles were used to measure wobble loss. Each of the three straight ducts was constructed with an intentional duct mismatch at each of the nine segment joints along the duct. Offsets used for each duct are shown in Figure 3.6. The eight draped duct profiles were also constructed with intentional mismatched ducts at the segment joints. The offset was made with the use of a hard rubber gasket set shown in Figure 3.7. During stressing the tendon always is pulled into the offset so that friction loss is maximized.

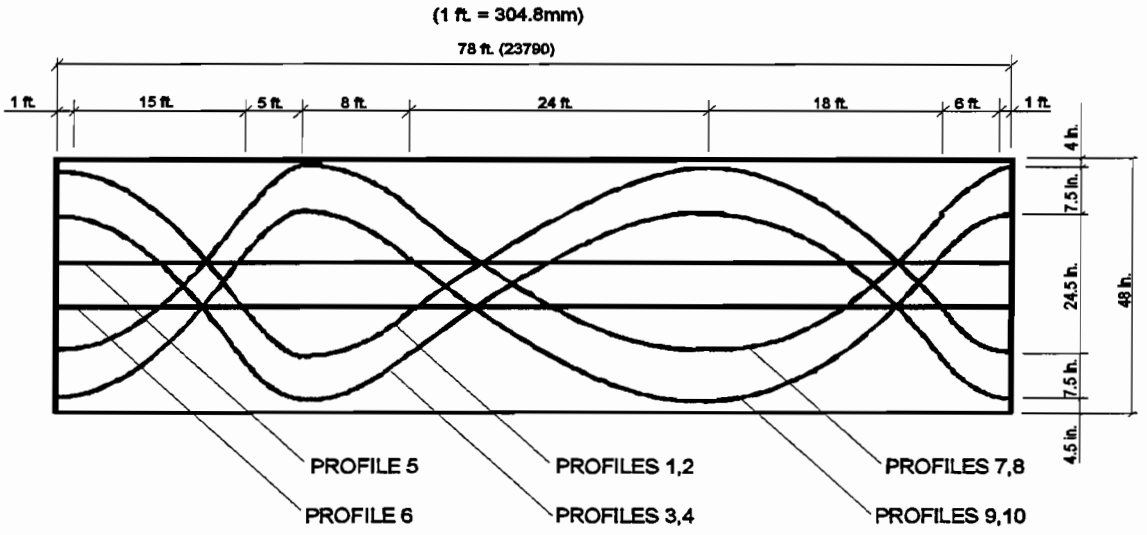

Figure 3.1 Large-scale monolithic friction specimen - elevation.

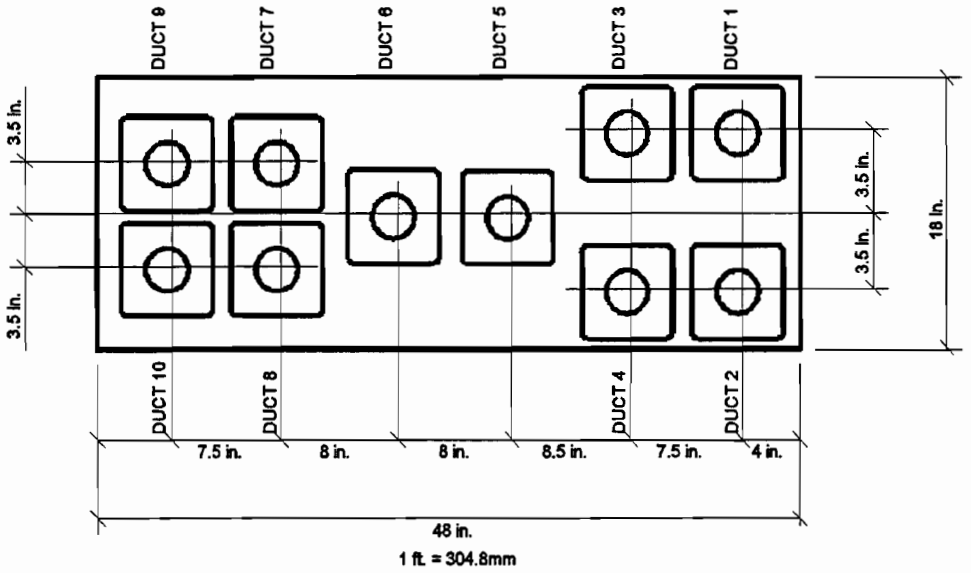

Figure 3.2 Large-scale monolithic friction specimen - end view.

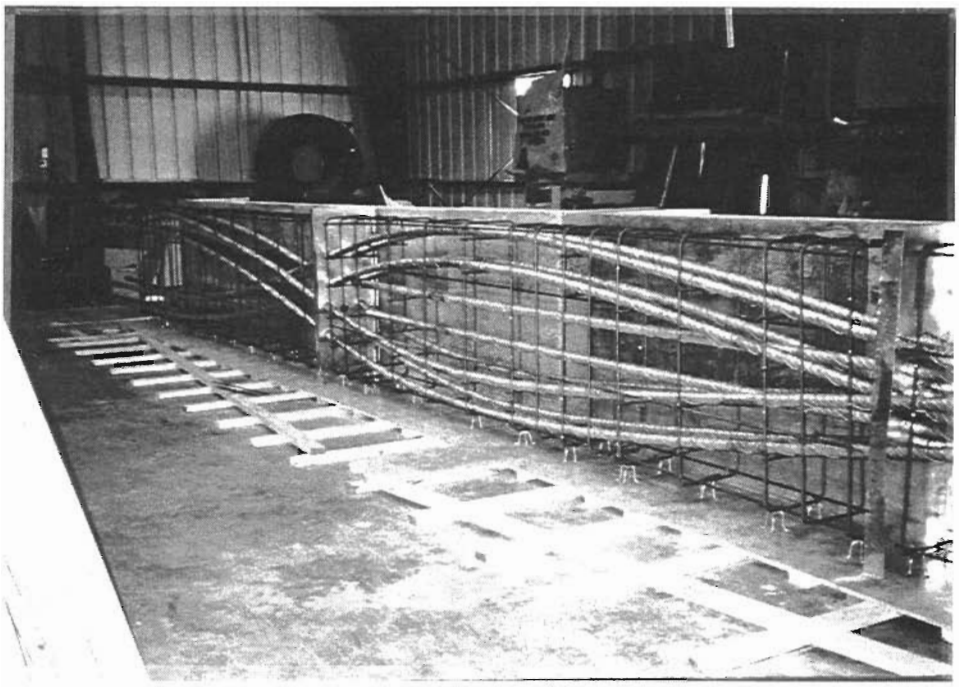

Figure 3.3 Large-scale monolithic friction test specimen - under construction.

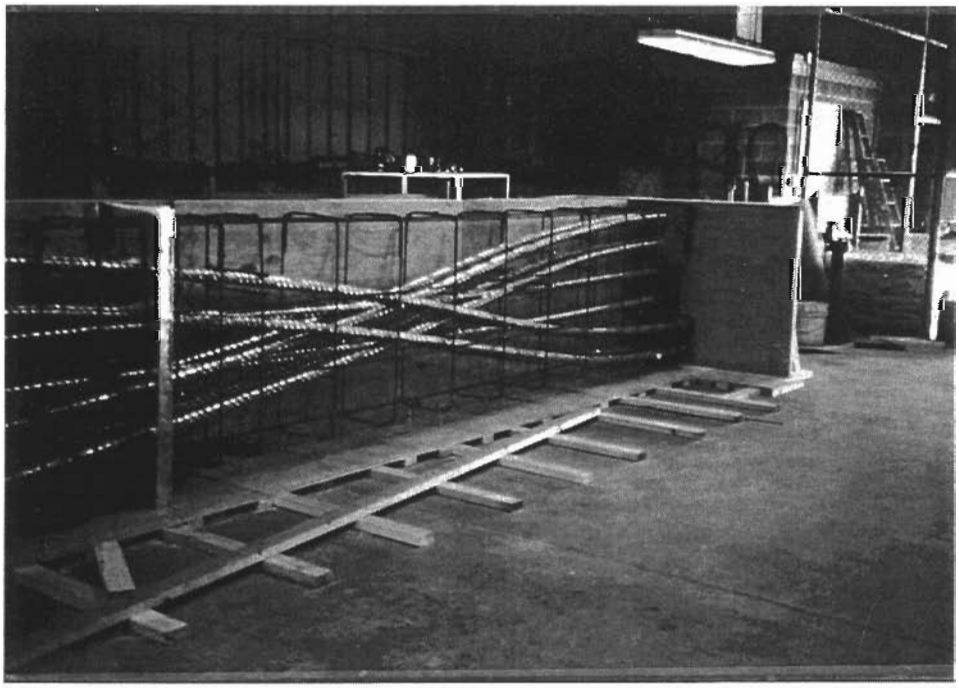

Figure 3.4 Large-scale monolithic friction specimen - under construction.

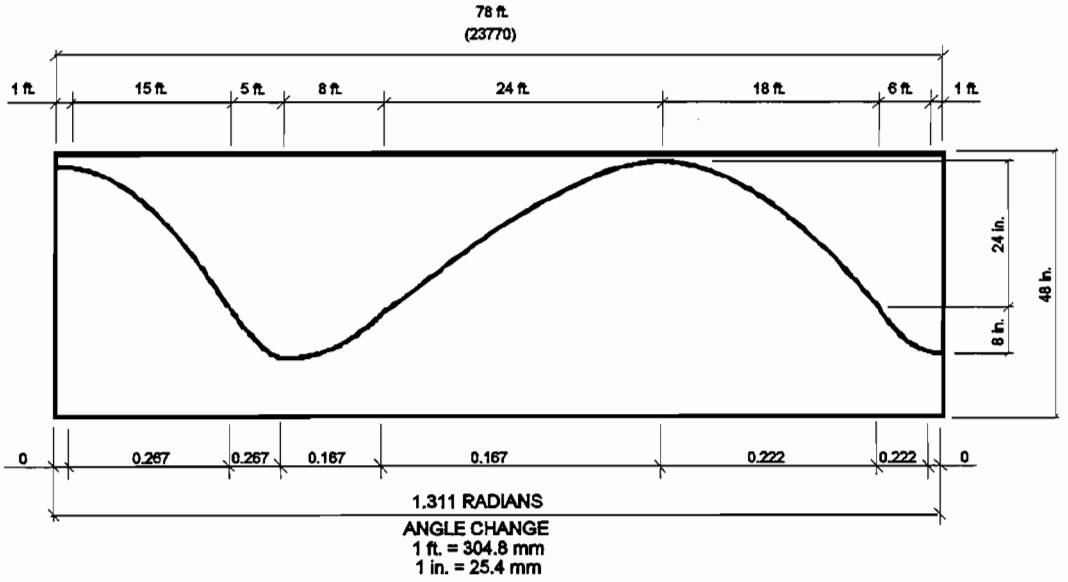

Figure 3.5 Large-scale segmental friction specimen elevation - curvature data.

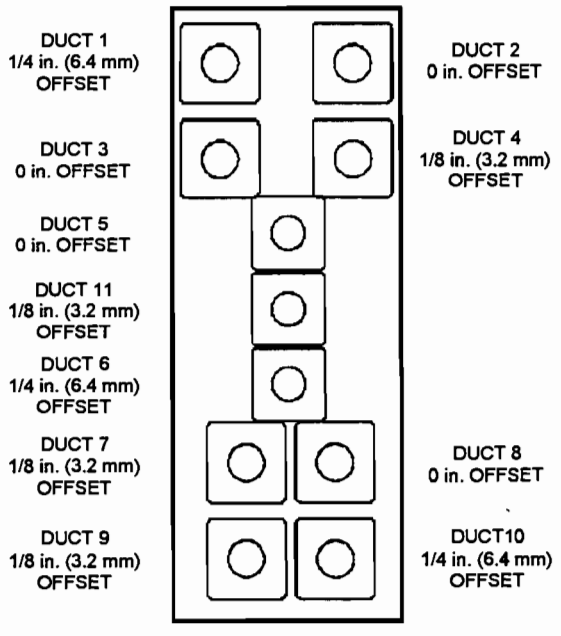

Figure 3.6 Large-scale segmental friction specimen elevation - offset data.

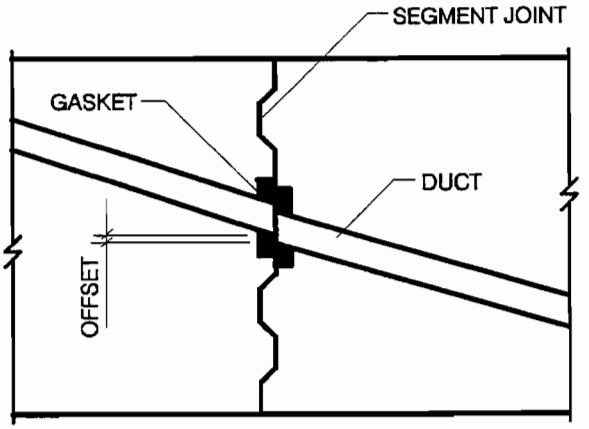

Figure 3.7 Duct offsets.

The parabolic draped tendon profile used is shown in Figure 3.5. The radii of curvature along the tendon are smaller than those found on a typical highway box girder and will have conservative friction coefficients. The eight draped tendon profiles are identical to those used in the monolithic test specimen with the exception of the offsets at the segment joints.

The segmental girder was constructed in ten segments. The interior eight segments were 8-ft. (2438 mm) long and the anchorage segments measured 7-ft. (2134 m) long. An elevation and end view of the girder is given in Figures 3.8 and 3.9.

The first constructed segment, Segment 1, was located in the center of the girder. This segment was constructed with wingwalls to stabilize the rest of the girder during construction. Construction proceeded outward from Segment 1, with segments match cast mostly two at a time.

Segment 1 was constructed on forms placed directly on the concrete lab floor. The remaining nine segments were cast on forms resting on bar rollers so that the match cast joint could be separated and the joints epoxied.

Figures 3.10 and 3.11 show typical segments under construction.

3.2.3 Components. All components constructed into the girders are commonly used in post-tensioned construction in the United States. Some components used were required by the test program to facilitate taking measurements, or to set test parameters. These components were constructed or installed so as not to interfere with normal construction or stressing operations.

Strand used was from Florida Wire and Cable. Properties are listed in Table 3.1. A 7-1/2-in. (13 mm) ϕ strand tendon was used in all tests. Figure 3.12 shows tendons installed in a specimen.

All duct used was 2-in. (51 mm) I.D. galvanized semi-rigid steel duct supplied by VSL. The duct came in 20-ft. (6.1 m) lengths. Ducts were shaped to the curvature required prior to installation, then checked in the form before concrete was placed. Duct ends were cut plumb and flush after the bulkheads were removed. Figure 3.13 shows ducts passing through the bulkhead and gaskets.

Anchorage system components were also supplied by VSL. Figures 3.14 through 3.16 give details.

The gasket system used in the segmental specimen was developed to firmly hold the ducts in place at the match cast face at the specified duct offset. The system also kept concrete paste and epoxy out of the duct. Epoxy intruded into only one duct at one joint. See Figures 3.7 and 3.17 for gasket details.

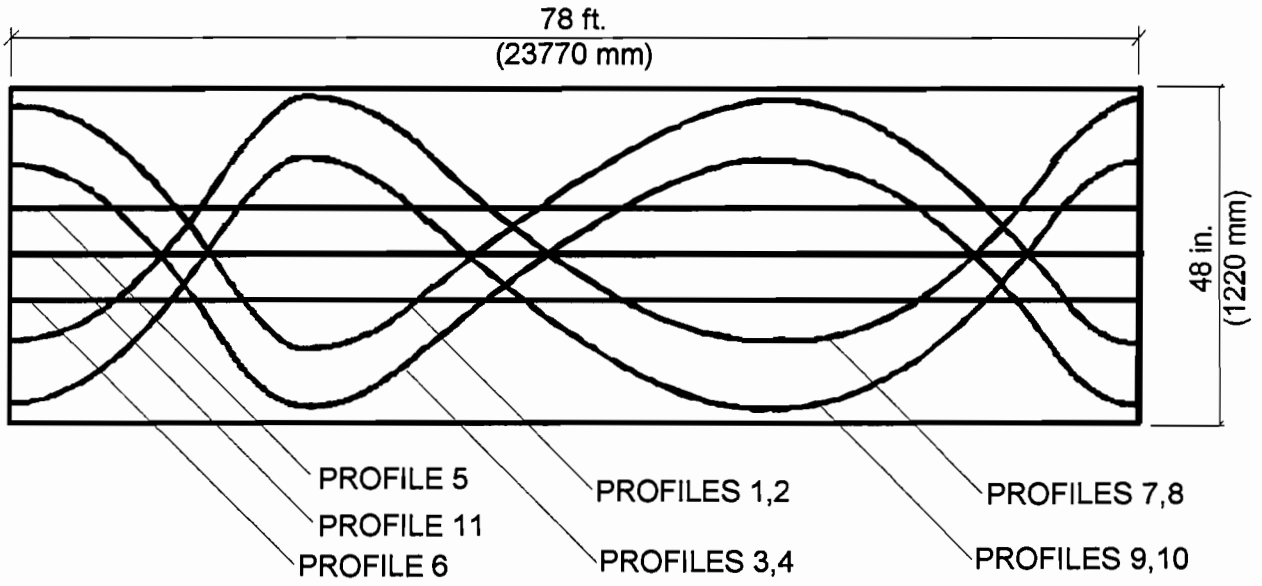

Figure 3.8 Large-scale segmental friction specimen - elevation.

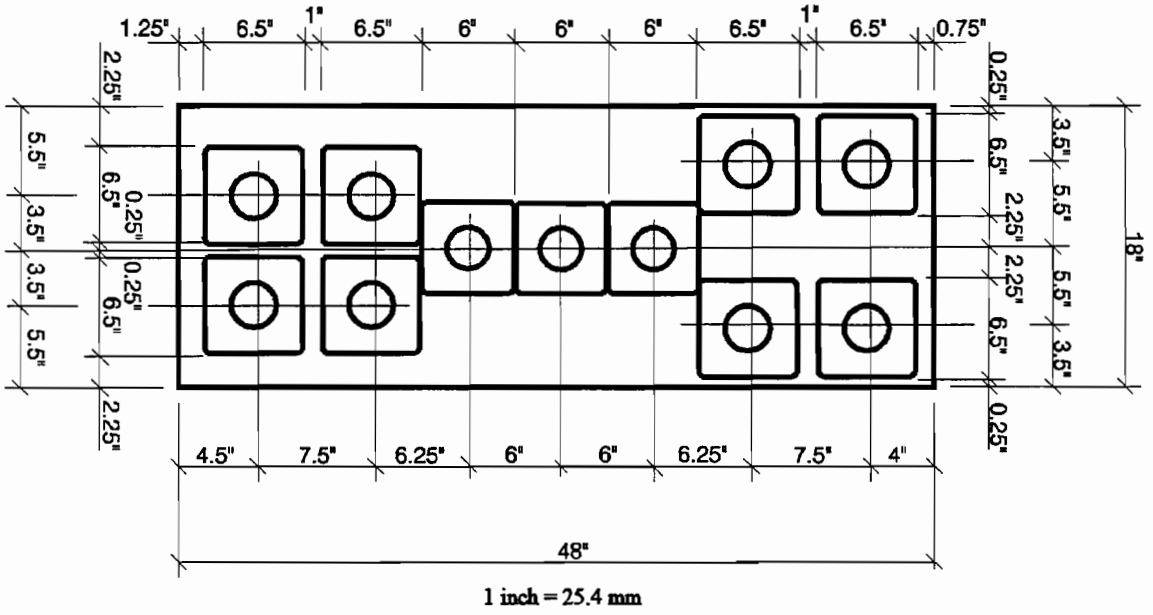

Figure 3.9 Large-scale segmental friction specimen - end view.

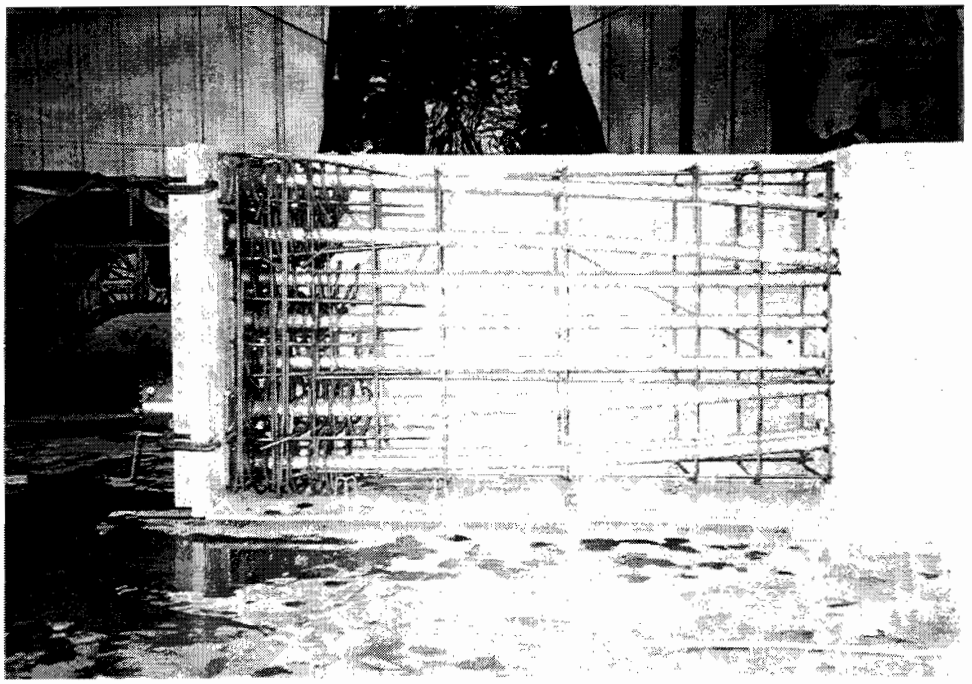

Figure 3.10 Segment 10 under construction.

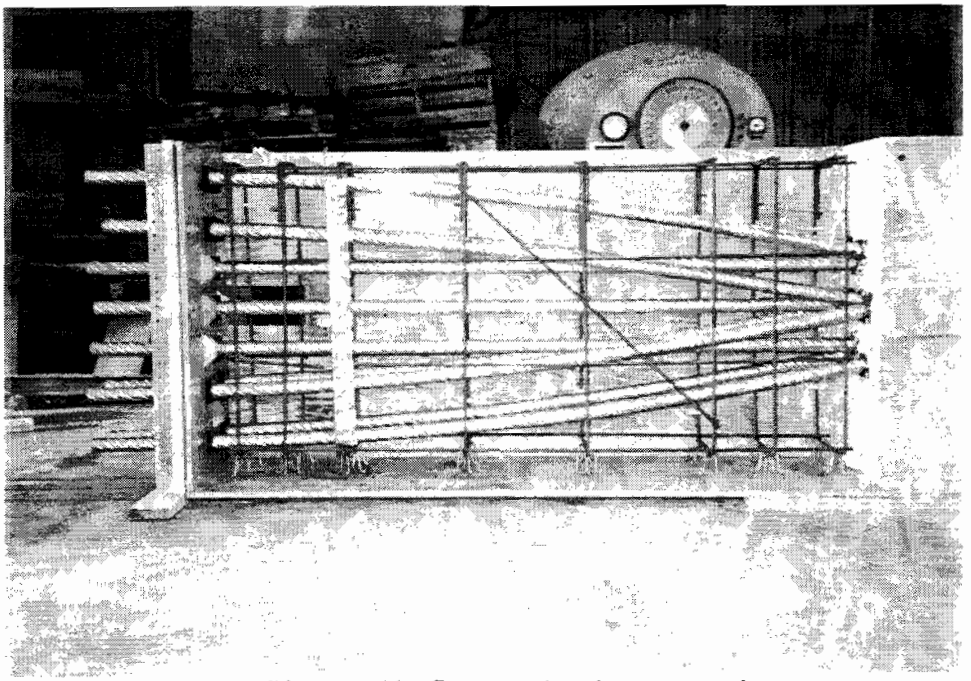

Figure 3.11 Segment 4 under construction

Table 3.1 Prestressing Strand Characteristics.

GRADE 270 UGPAATED SEVEN-WIRE, STRESS-RELIEVED LOW-RELAXATION STRAND PROPERTIES		
Nominal Diameter	0.502 in.	(12.75 mm)
Steel Area	0.153 sq. in.	(98.7 mm^2)
Breaking Strength	43,505 lb.	(193.5 kN)
Guaranteed Ult. Break Strength	41,300 lb.	(183.7 kN)
Load at 1% Extension	40,447lb.	(180 kN)
Elongation at 30,975 lb. (136 kN) or in 10 ft. (3 m) (%)	7.08	
Modulus of Elasticity	28.6 x 10^6 psi	(197.2 Gpa)

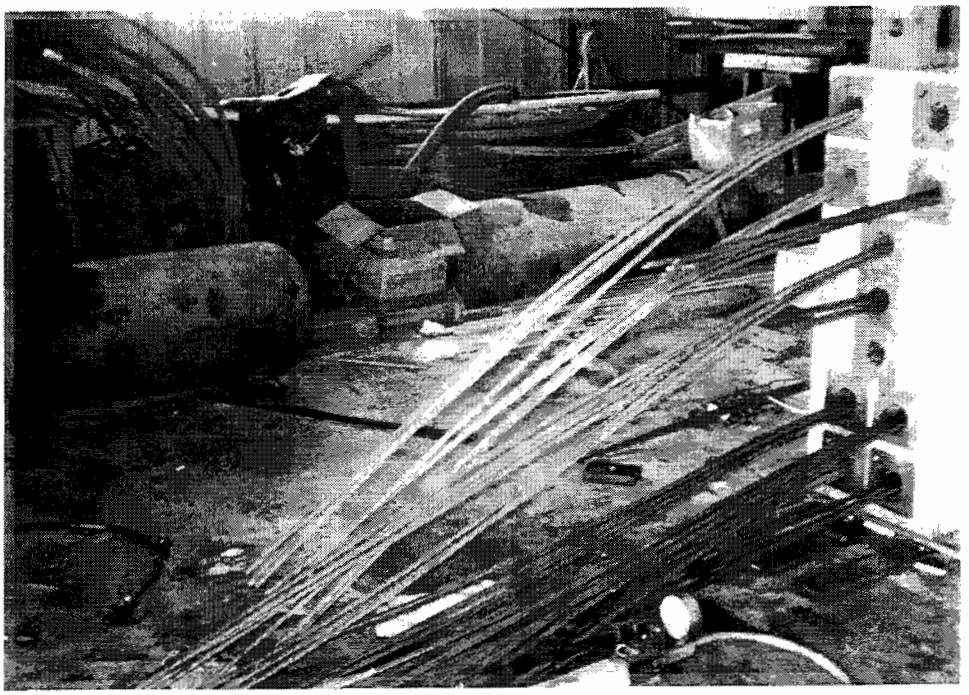

Figure 3.12 Prestressing strand

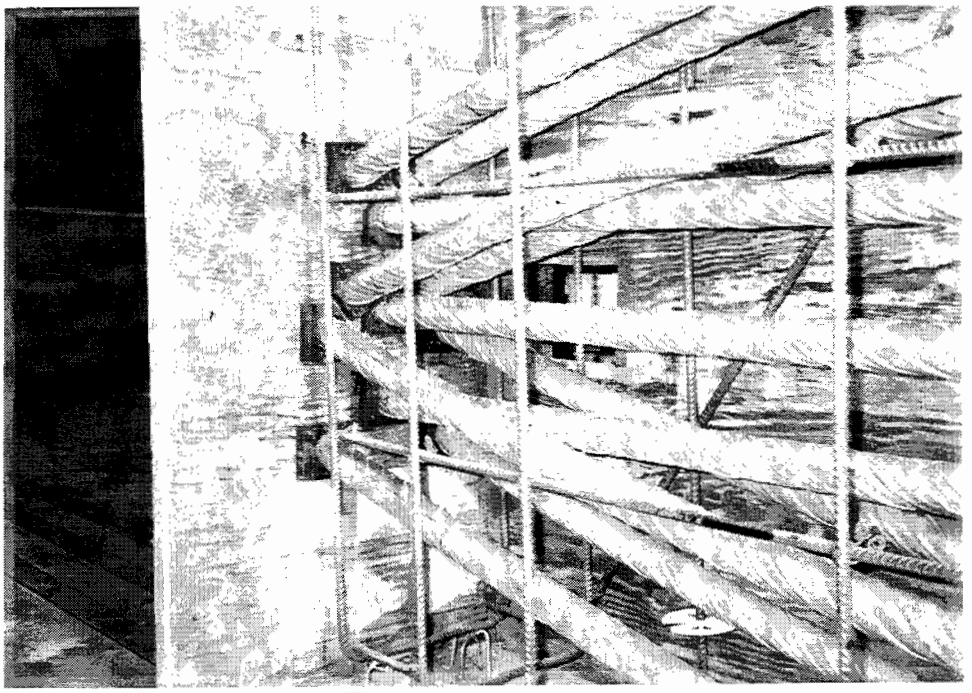

Figure 3.13 Ducts.

The monolithic girder tendons were instrumented by strain gages placed on the strands at various stations along their length after the strands were inserted into the ducts. In order to provide room for mounting the strain gages so that measurements of the actual strand strains could be made, 4-in. (100 mm) by 7-in. (180 mm) polyethylene styrofoam blockouts were placed at various locations along the duct layouts. The primary blockout locations were at the points of inflection, as well as the uppermost and the lowermost points of the layouts. If the distance between two points was great, then secondary blockout locations were positioned between the two primary points. Next, at the locations marked for the blockouts, about 1/4 of the duct perimeter was cut away with an electric cutting disc. Before the ducts were installed in the reinforcement cages, the cutouts were sealed with tape. After they were installed the styrofoam blockouts were contoured and tapered to fit tightly around the duct cuts at the blockout locations. Because the strain gages gave great difficulty in the first specimen, the tendon elongations were measured by potentiometers along the tendons in the segmental specimen. Ducts had to have access openings for measuring tendon elongations at seven places in four of the draped profiles, and at three places in all the straight profiles. Openings were precut into the ducts before placement. Styrofoam blocks and duct tape insured access into the duct from the exterior of the girder after concrete placement. These elongation measurement blockouts can be seen in Figure 3.18.

3.2.4 Adherence to the AASHTO Guide Specification for Design and Construction of Segmental Concrete Bridges. To ensure a realistic construction procedure was used, segment design and construction closely followed the AASHTO Guide Specification [19] in all but one instance.

The specification required that steel side forms be used for a good concrete surface finish and also for form rigidity. Wooden forms were used during the construction of both the monolithic and the

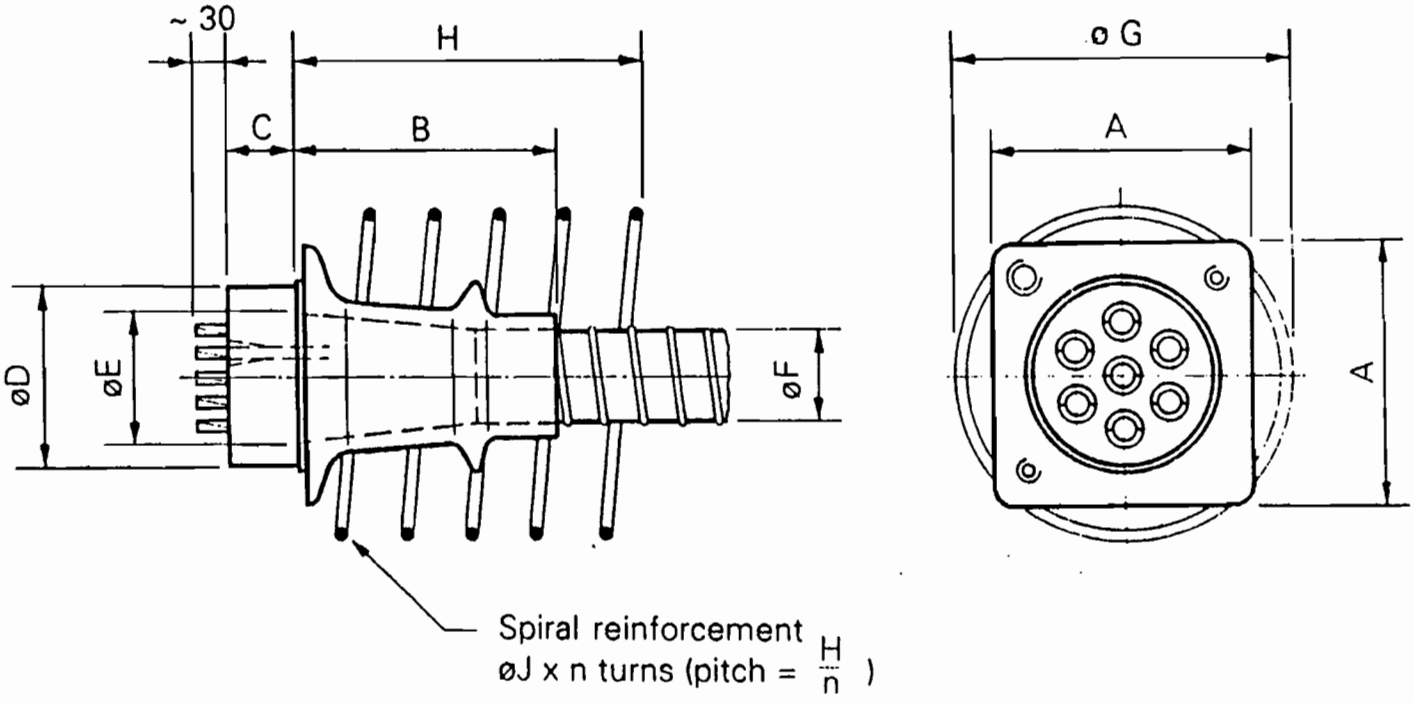

Type	Str. Dia. in. (mm)	No. Str.	A in. (mm)	B in. (mm)	C in. (mm)	ϕD in. (mm)	ϕE in. (mm)	ϕF in. (mm)
EC 5-7	0.5 (12.7)	5 - 7	6.50 (165)	6.10 (155)	2.91 (74)	4.33 (110)	2.91 (74)	2.36 (60)

ϕG in. (mm)	H in. (mm)	ϕJ in. (mm)	n
7.50 (19)	9.00 (229)	0.50 (13)	6

Figure 3.14 Anchorage system.

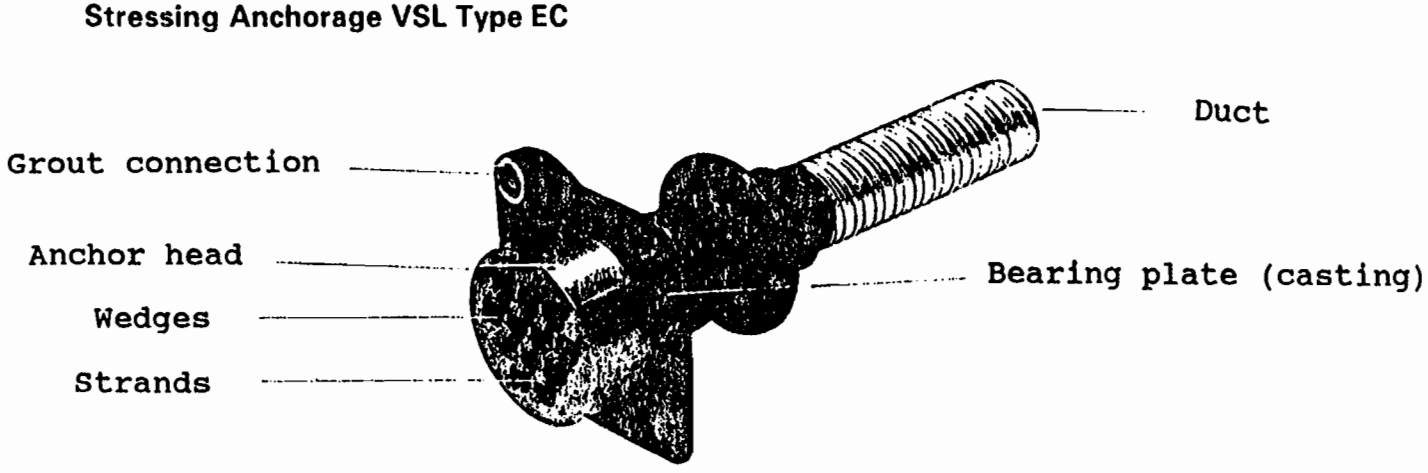

Figure 3.15 Anchorage components

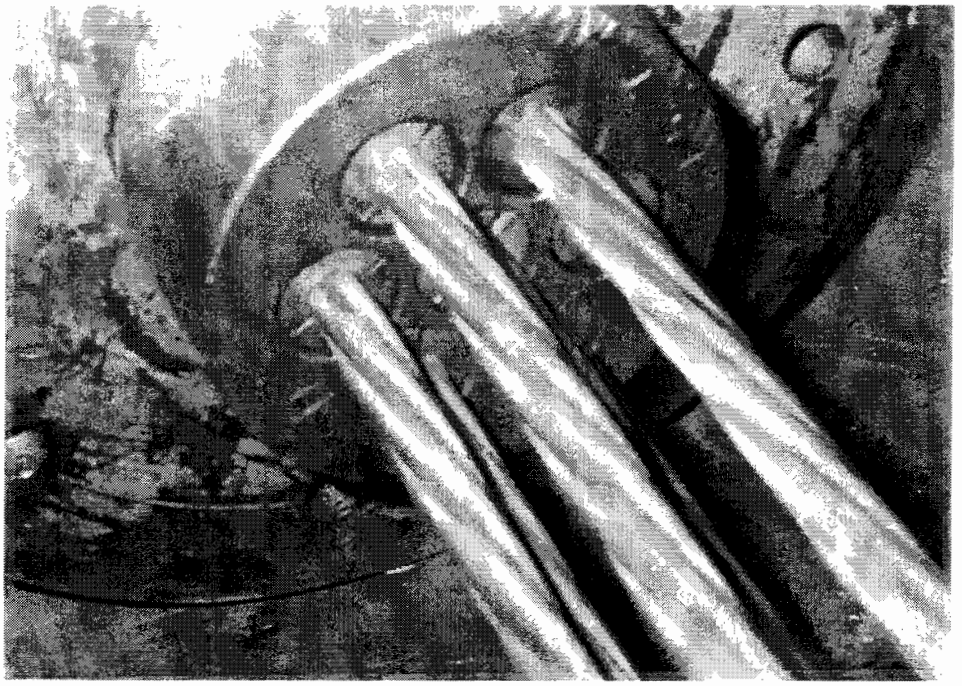

Figure 3.16 Wedges

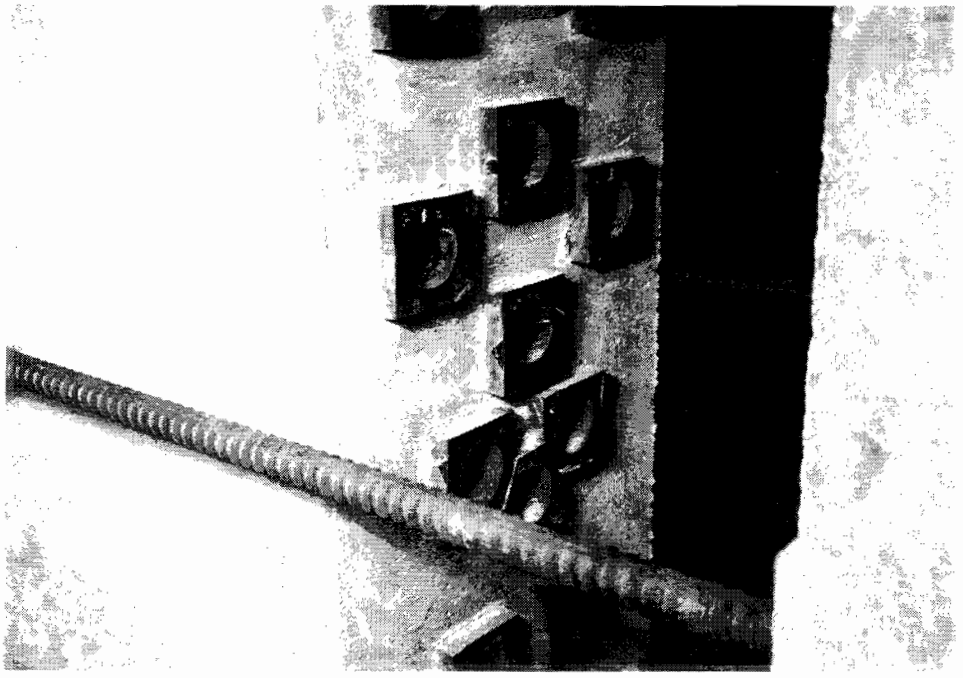

Figure 3.17 Gaskets

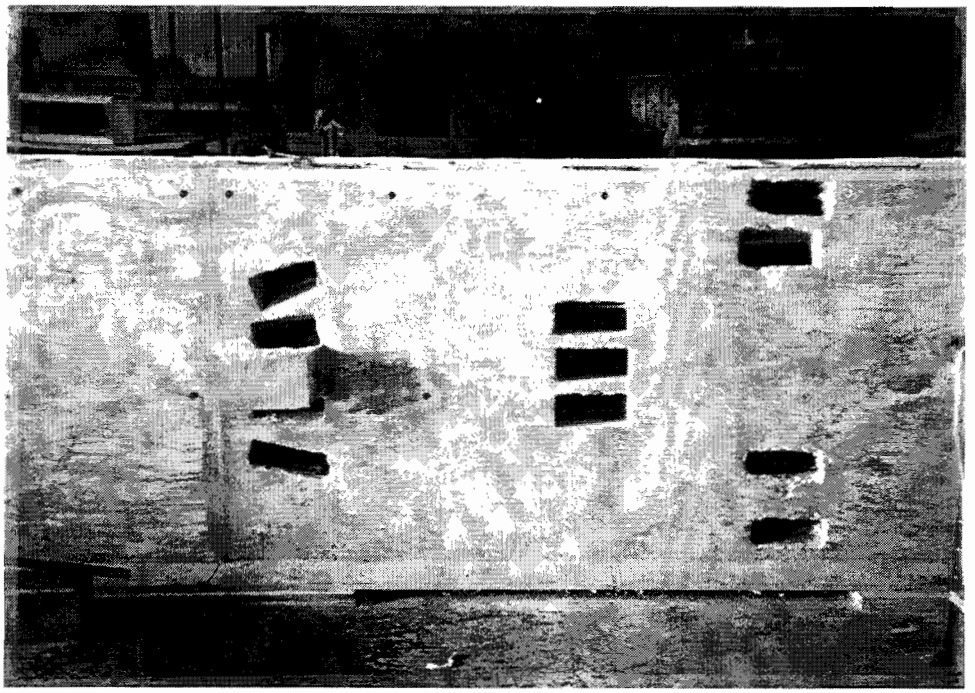

Figure 3.18 Elongation measuring blockouts.

segmental test specimen since concrete finish would have no impact on test results. Supporting form members were redundant and sufficiently rigid. Bulkhead forms were lacquered to simulate a steel form finish.

Ducts were secured to stirrups at intervals not exceeding four feet (1.2 m) and often as close as two (0.6 m) feet. A 1-in. (25 mm) placement tolerance within the girder was easily maintained.

Inflated hose mandrels were used in the segmental specimen during concrete placement and extended at least two feet (0.6 m) into the ducts of the previously cast segment. Mandrels were retrieved easily from all ducts, therefore it was assumed no mandrel had to take any force during concrete placement.

Shear keys followed the height to width ratio and spacings recommended in the specification.

Anchorage zones were designed to safely carry a ram load of 80% of the tendon capacity. Stirrups, ties, and spirals were designed based on bursting criteria or as specified by the anchorage supplier.

Concrete for the monolithic girder specimen was a 4500 psi (31 MPa) mix design. Twenty-eight-day cylinders averaged over 5500 psi (38 MPa) and 270-day cylinders at completion of testing averaged over 5850 psi (40.3 MPa). Concrete for the segmental girder specimen was a 7000 (48 MPa) psi mix design. At least 6000 psi (41.4 MPa) was achieved in all segments by 28 days. The anchorage zones were designed for 6000 psi (41.4 MPa) concrete. Concrete was adequately compacted to ensure voidless segments.

For the proper conducting of segmental operations, early concrete strengths were important. A concrete strength of 2500 psi (17.2 MPa) was achieved overnight, so forms could be removed without damage to the girder. 3000 psi (20.7 MPa) was reached before segments were separated and epoxied. Temporary force blisters were designed by the strut-and-tie method with 3000 psi (20.7 MPa) concrete strength.

Bond breaker used on match cast faces consisted of a talc and vegetable oil soap mixture. The bond breaker was tested on a 2-ft. (0.6 m) x 4-ft. (1.2 m) specimen to prove its effectiveness. The bond breaker worked flawlessly at all match cast joints. Bond break was easily applied by hand.

Joint epoxy supplied by Industrial Coatings was used on all joints. The epoxy was mixed and applied by hand. This epoxy was used on the San Antonio "Y" project.

Temporary force blisters were constructed on each segment on the end opposite to the face to be epoxied. Force was provided on each side of the segment at mid-height by a threadbar and hydraulic ram apparatus. Temporary force on the segment face was 40 psi (276 kPa) and was maintained for at least 12 hours.

3.3 Test Procedure

Tests on the large scale segmental girder were conducted using essentially the same tendon feeding and stressing procedure as used on the monolithic girder by Tran [10]. This eliminates unwanted variability of the results between the two girders. Some improvements in instrumentation and stressing equipment were used based on experience gained during testing the monolithic girder. For instance, the strain gages on the tendon were eliminated and replaced with a hand measurement of elongation at selected points along the girder.

3.3.1 Schedule of Tests. A summary of the testing sequence for the monolithic girder is given in Table 3.2. The tendons were installed into the ducts either as a seven-strand group or one strand at a time. Care was taken not to tangle the strand group. A load cell was installed at the dead end between the anchor plate and the anchor head. A linear potentiometer was then installed on one of the strands to measure movement of the strand with respect to the anchor head as the wedges gripped and moved. A hydraulic ram with pressure transducer was centered on the anchor plate at the live end of the tendon. An anchor head was moved into place behind the ram. Each strand was initially stressed independently to a low seating force to get equal force on the strands before the large ram stressed the whole tendon. This would ensure consistent reading by the strain gages placed on the strands at various locations along the tendon. A linear potentiometer was also installed at the live end to measure strand movement with respect to the anchor head.

All instruments were tied into a data acquisition system, where voltage outputs are converted to digital information and processed by a personal computer. After a system check and zero readings were taken, the tendon was stressed in increments up to 80% of the tendon ultimate load, or 230 kips (1023 kN). Data was recorded at each increment.

The test schedule for the segmental specimen is shown in Table 3.3. Tendon 2 profiles to be tested with lubricants were tested only once with bare tendons prior to the lubricated test. Lubricants selected for testing in the segmental specimen were:

Table 3.2 Large-Scale Monolithic Friction Specimen - Test Schedule.

Duct	Profile	Test	Lubricant
5	Straight	1	Bare
		2	L5
6	Straight	1	Bare
		2	L11
1	Draped	1	Bare
		2	L2
2	Draped	1	Bare
		2	L5
		3	L5
3	Draped	1	Bare
		2	L2
		3	L2
4	Draped	1	Bare
		2	L5
7	Draped	1	Bare
		2	L11
8	Draped	1	Bare
		2	L11
		3	L11
		4	Flushed
9	Draped	1	Bare
		2	L8
10	Draped	1	Bare
		2	L8
		3	L8
		4	Flushed
		5	L13

Table 3.3 Large-Scale Segmental Friction Specimen - Test Schedule.

Duct	Profile	Offset in. (mm)	Test	Lubricant
5	Straight	0	1	Bare
			2	Bare
11	Straight	1/8 (3.2)	1	Bare
			2	L11 - Wright
6	Straight	1/4 (6.4)	1	Bare
			2	L13 - Aqualube
1	Draped	1/4 (6.4)	1	Bare
			2	L13 - Aqualube
2	Draped	0	1	Bare
			2	Bare
3	Draped	0	1	Bare
			2	Bare
			3	L13 - Aqualube
4	Draped	1/8 (3.2)	1	Bare
			2	Bare
			3	L14 - Graphite
7	Draped	1/8 (3.2)	1	Bare
			2	L11 - Wright
8	Draped	0	1	Bare
			2	L11 - Wright
9	Draped	1/8 (3.2)	1	Bare
			2	L13 Aqualube
10	Draped	1/4 (6.4)	1	Bare
			2	L11 - Wright

- L11 - Wright 502 - Top ranked lubricant from previous monolithic girder tests.
- L13 - Aqualube MX-1 - Biodegradable soap lubricant commonly used in California bridges.
- L14 - Graphite - Commonly used dry lubricant.

3.3.2 Tendon Installation and Stressing Procedure. Strand was pushed into the ducts one at a time, two at a time, or as a complete 7-strand tendon. Care was taken not to tangle the strands during installation. A great increase in force needed to install the strands usually indicated unwanted entanglement. This could be verified visually through the elongation measurement blockouts in some ducts. Lubricant was applied to each strand, regardless of installation method, to ensure complete coverage. In one test, two gallons (7.6 ℓ)of lubricant were poured into the low point of a duct and the strands pushed through it. Figures 3.19 and 3.20 show the application of lubricant to strands pushed through one at a time. In all lubricated tests, strands came out of the ducts at the opposite end dripping with lubricant (oil or soap) or carrying graphite flakes between wires.

With the tendon in place, a load cell and anchor head were secured in place. The seven sets of wedges were installed in the anchor head to equivalent positions using a pipe and hammer. This would help ensure consistent movement or take up of each strand at the dead end. This movement was measured on one strand with a linear potentiometer. Other strands were marked at the back end of the wedges to check whether all strands were moving equally.

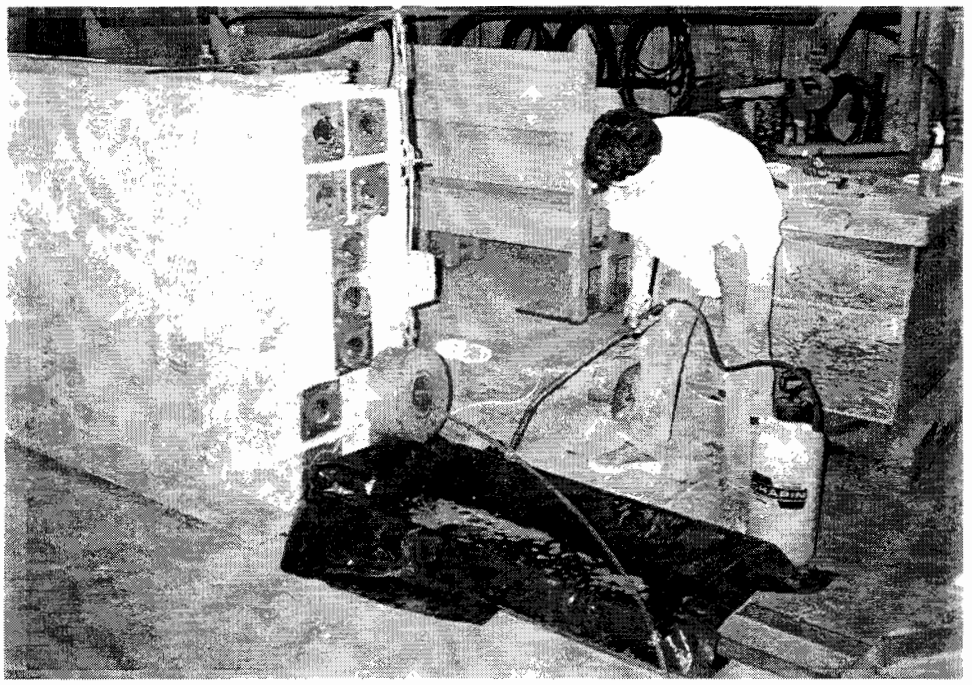

Figure 3.19 Installing strand

Figure 3.20 Application of lubricant

Without distorting the position of the load cell and anchor head at the dead end, a hydraulic ram was moved into place. The ram was positioned with the piston against the anchor plate. This allowed m44-easier measurement, by a linear potentiometer, of the movement of the ram body with respect to the end of the girder, and also made the ram easier to center on the anchor. No permanent anchorage of the tendon at the live end was to be performed.

In both the monolithic and the segmental test specimen, the anchor head was preloaded to the ram body by stressing each strand separately and setting the wedges using a small hydraulic ram. Since wedge set was measured at the live end on one strand only, equal force on the strands was essential. The preload force was then taken off the large ram by opening the pressure valve on the hydraulic pump. The data acquisition system was then assembled, checked, and zeroed.

3.3.3 Pertinent Data. The most essential data from a test was the live end force and dead end force on the tendon. Measurement of strains along the tendons or of the total tendon elongation and tendon forces at many increments during a test allowed the friction behavior of the tendon and duct to be plotted and compared against other tests in the same duct.

Instruments recorded forces and strains or elongations during stressing in 20-kip (89 kN) increments up to 150 kips (667 kN), then in 10-kip (45 kN) increments up to 230 kips (1023 kN), or 80% of ultimate. In the segmental specimen data was gathered for five minutes with the jacking force held at 230 kips (1023 kN).

On some tests without lubrication, elongations were measured at points along the tendon. Elongations were measured only at 0 kip (kN) and 230 kip (1023 kN) jack loads.

3.3.4 Data Acquisition. Data was collected and stored electronically with a data acquisition system that has been used successfully on many projects at the Ferguson Structural Engineering Laboratory. All instruments were tested and calibrated prior to use in the specimen. Instruments either measured force or displacement. A schematic of the data acquisition system and instrument location is shown in Figure 3.21. Complete information on equipment, data processing, calibrations and all detailed data for each specimen are given in Refs. 10 and 18.

3.4 Flushing

In some tests an evaluation of the adequacy of flushing was made. In these tests, after the tension of the tendon was released, the ram and the load cell were removed and the tendon was flushed with water in the following manner. First, all the blockouts were closed with styrofoam and sealed with silicone. Then the live end of the girder was connected to a long hose by a coupler sleeve. This hose was used to transport the used water to outside the laboratory. The dead end of the girder was shut by a wooden doughnut; it had a small hole which served as a water jet head. After the silicone was hardened, water was introduced trough the

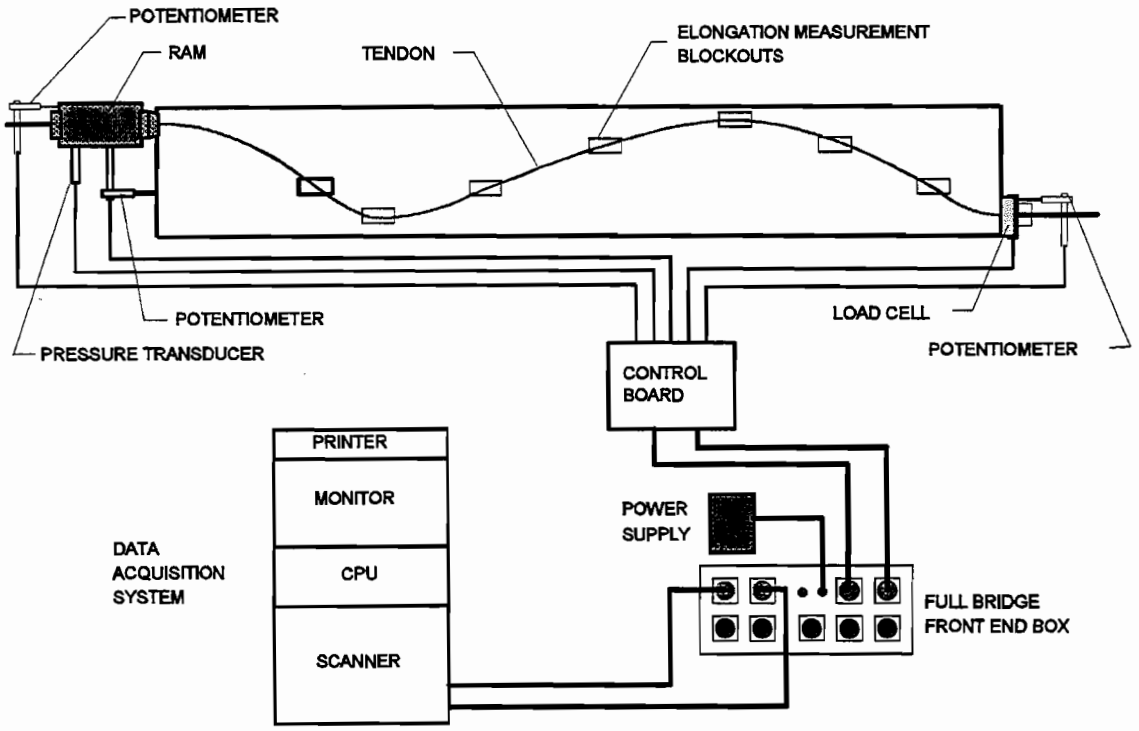

Figure 3.21 Data acquisition system schematic

doughnut into the duct. All the blockouts and ends were closed so tightly that there were no leaks when the water ran through the duct. The water was kept flowing through the duct until it was clear. Water flow rate was about 3.5 gpm (13.2 ℓpm) and flushing continued for about 45 minutes. After the water flushing was stopped, the tendon was removed from the girder and two samples were cut from both ends of one of seven strands so that adhesion tests could be conducted.

CHAPTER FOUR
TEST RESULTS

4.1 Introduction

The detailed data collected in the stressing of all of the tendons is presented in Ref. 10 for the monolithic girder tests and Ref. 18 for the segmental girder tests. These references are permanently filed in the library of The University of Texas at Austin should access to this very detailed data be required. In this report, representation samples from these voluminous data tables and figures are presented to illustrate basic behavior. A detailed analysis of the complete test results is presented in Chapter 5.

4.2 Monolithic Girder Results

4.2.1 Wobble Friction Coefficient. Two straight duct profiles, Profile No. 5 and Profile No. 6, were chosen to study the wobble effect, which is essentially accidental friction in a supposedly straight duct. During this study, the live end jacking force was derived from a pressure transducer placed on the precalibrated stressing system, while the dead end holding force was measured by a load cell installed at the dead end of the girder. Two strands were selected to be instrumented by strain gages at three locations: 19 (5.8), 43 (13.1), and 59 (18) feet (m) from the live end of the girder. The wobble coefficient was computed from the following equation:

$$K = \left[\ln \left(\frac{F_j}{F_h} \right) \right] \Big/ L \qquad (4.1)$$

where K = the wobble coefficient

F_j = the measured prestress tendon force at the jacking end of the girder

F_h = the measured prestress tendon force at the holding end

L = the known tendon profile length, 78 feet (23.77 m)

Results of the wobble coefficient test for Profile No. 5 are shown in Table 4.1 and in Figure 4.1. For this profile, the values of the wobble coefficient range from 10.55×10^{-4} to 3.85×10^{-4} /ft. (34.6×10^{-4} to 12.6×10^{-4}/m). Note that the initial friction is quite high but stabilizes above 50-60 percent of GUTS. This is typical in most tests. The average of the last three values, defined as the practical wobble coefficient, is 3.86×10^{-4} /ft. (12.66×10^{-4}/m). This value is higher than that specified by AASHTO, which is 2.0×10^{-4}/ft (6.6×10^{-4}/m, but is in the range recommended by PTI, which is 3 - 7 $\times 10^{-4}$/ft. (9.8 - 23 $\times 10^{-4}$/m). The stresses derived from the measured strain values are shown in Figure 4.2. These values are lower than those predicted by the theory and do not decrease uniformly, as expected.

Table 4.1 Bare Strand in Straight Duct 5 of the Monolithic Girder - Wobble Coefficient Test Results

Holding Force			Jacking Force			Wobble Coefficient	
Voltage (mV)	Load kip	(kN)	Voltage (mV)	Load kip	(kN)	1 Ft.	1 m.
3.851	19.64	(87.4)	6.883	21.33	(94.9)	10.55×10^{-4}	34.6×10^{-4}
7.790	39.73	(176.7)	13.606	42.16	(187.5)	7.60×10^{-4}	24.9×10^{-4}
11.414	58.21	(258.9)	19.835	61.46	(273.4)	6.95×10^{-4}	22.8×10^{-4}
15.013	76.57	(340.6)	26.042	80.69	(358.9)	6.72×10^{-4}	22.0×10^{-4}
18.902	96.40	(428.8)	32.528	100.78	(448.3)	5.70×10^{-4}	18.7×10^{-4}
22.772	116.14	(516.6)	39.083	121.09	(538.1)	5.36×10^{-4}	17.6×10^{-4}
26.455	134.92	(600.1)	45.307	140.38	(624.4)	5.08×10^{-4}	16.7×10^{-4}
28.648	146.11	(649.9)	48.950	151.66	(674.6)	4.78×10^{-4}	15.7×10^{-4}
30.556	155.84	(693.2)	52.129	161.51	(718.4)	4.59×10^{-4}	15.0×10^{-4}
32.490	165.70	(737.0)	55.279	171.27	(761.8)	4.24×10^{-4}	13.9×10^{-4}
34.351	175.19	(779.2)	58.436	181.05	(805.3)	4.22×10^{-4}	13.8×10^{-4}
36.536	186.34	(828.8)	61.973	192.01	(854.0)	3.85×10^{-4}	12.6×10^{-4}
37.970	193.65	(861.1)	64.409	199.56	(887.6)	3.85×10^{-4}	12.6×10^{-4}
40.293	205.49	(914.0)	68.358	211.79	(942.0)	3.87×10^{-4}	12.7×10^{-4}

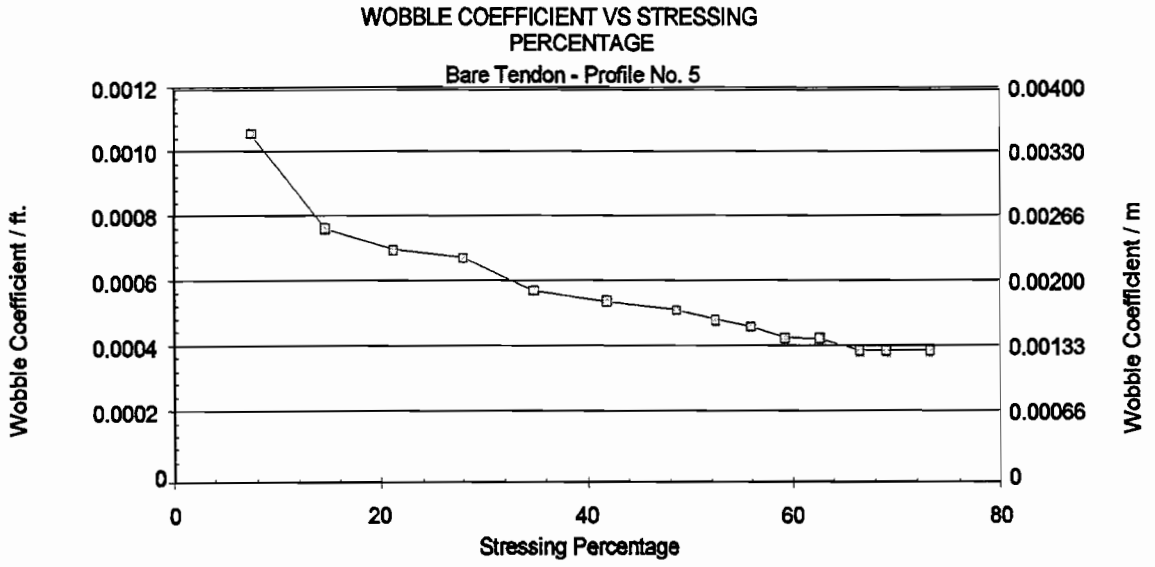

Figure 4.1 Bare strand in Straight Duct 5 of the monolithic girder - wobble coefficient vs. stressing percentage

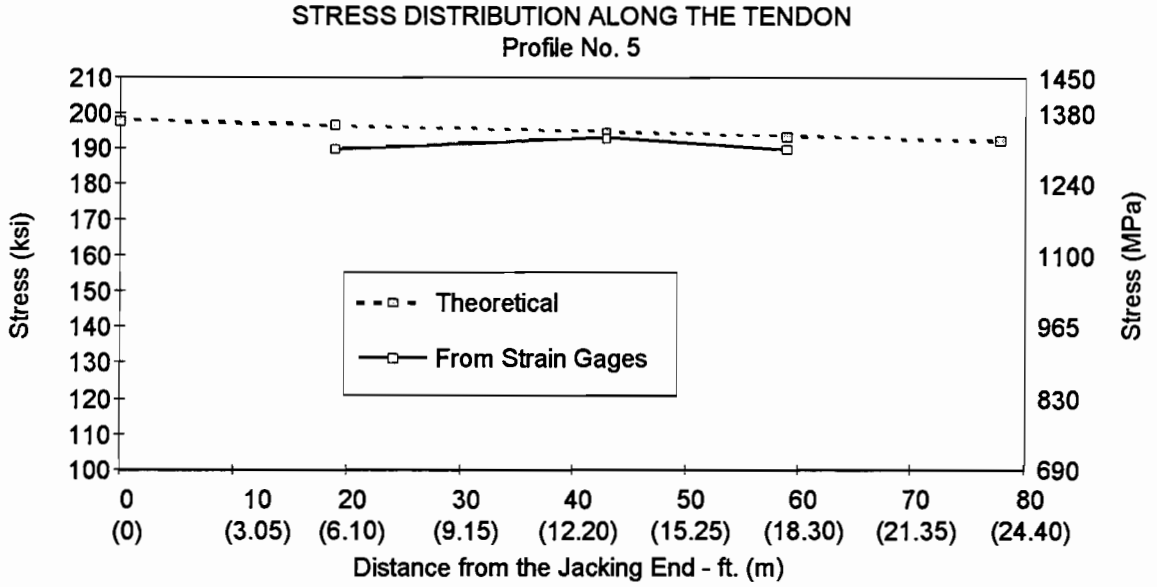

Figure 4.2 Bare strand in Straight Duct 5 of monolithic girder - stress distribution along the tendon.

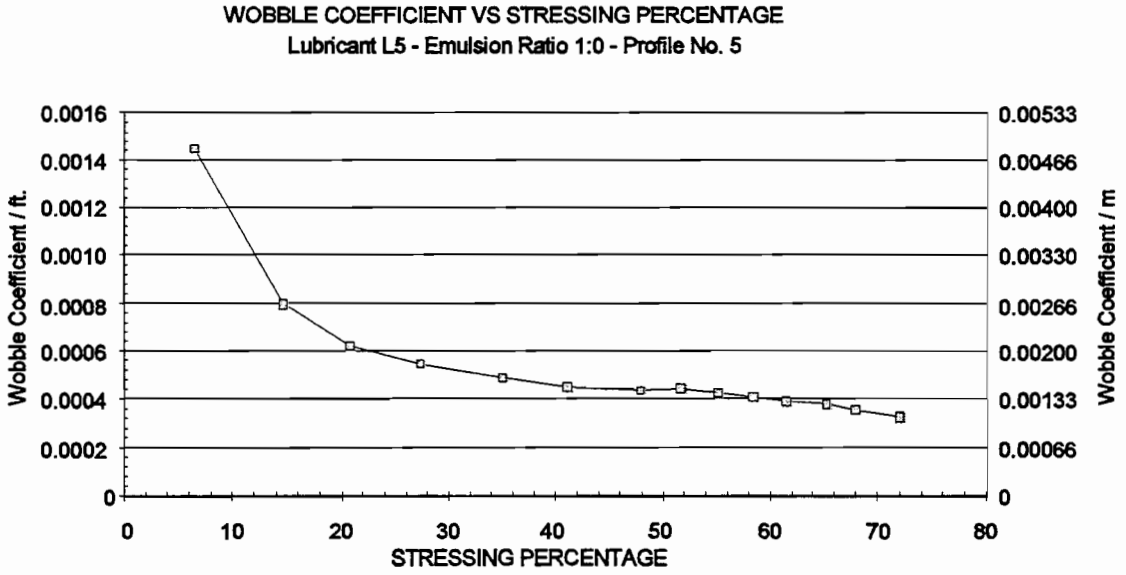

Figure 4.3 Lubricated strand (L5) in Straight Duct 5 of monolithic girder - wobble coefficient vs. stressing percentage.

Table 4.2 Lubricated Strand (L5) in Straight Duct 5 of Monolithic Girder - Wobble Coefficient Test Results

Holding Force			Jacking Force			Wobble Coefficient	
Voltage (mV)	Load kip	(kN)	Voltage (mV)	Load kip	(kN)	1 Ft.	(1 m)
3.302	16.84	(74.9)	6.088	18.86	(83.9)	14.50×10^{-4}	(47.5×10^{-4})
7.818	39.87	(177.3)	13.694	42.43	(188.7)	7.96×10^{-4}	(26.1×10^{-4})
11.210	57.17	(254.2)	19.371	60.02	(267.0)	6.23×10^{-4}	(20.4×10^{-4})
14.870	75.84	(337.3)	25.538	79.12	(351.9)	5.44×10^{-4}	(17.8×10^{-4})
19.086	97.34	(433.0)	32.627	101.09	(449.6)	4.85×10^{-4}	(15.9×10^{-4})
22.542	114.96	(511.3)	38.422	119.04	(529.5)	$4.47 \times 10^{-}$	(14.7×10^{-4})
26.218	133.71	(594.7)	44.641	138.31	(615.2)	4.33×10^{-4}	(14.2×10^{-4})
28.319	144.43	(642.4)	48.239	149.46	(664.3)	4.39×10^{-4}	(14.4×10^{-4})
30.231	154.18	(685.8)	51.441	159.38	(708.9)	4.25×10^{-4}	(13.9×10^{-4})
32.050	163.45	(727.0)	54.458	168.73	(750.5)	4.07×10^{-4}	(13.4×10^{-4})
33.848	172.63	(767.8)	57.431	177.94	(791.5)	3.88×10^{-4}	(12.7×10^{-4})
35.954	183.37	(815.6)	60.947	188.83	(839.9)	3.77×10^{-4}	(12.4×10^{-4})
37.499	191.25	(854.7)	63.451	196.59	(874.4)	3.54×10^{-4}	(11.6×10^{-4})
39.814	203.05	(903.2)	67.221	208.27	(926.4)	3.25×10^{-4}	(10.7×10^{-4})

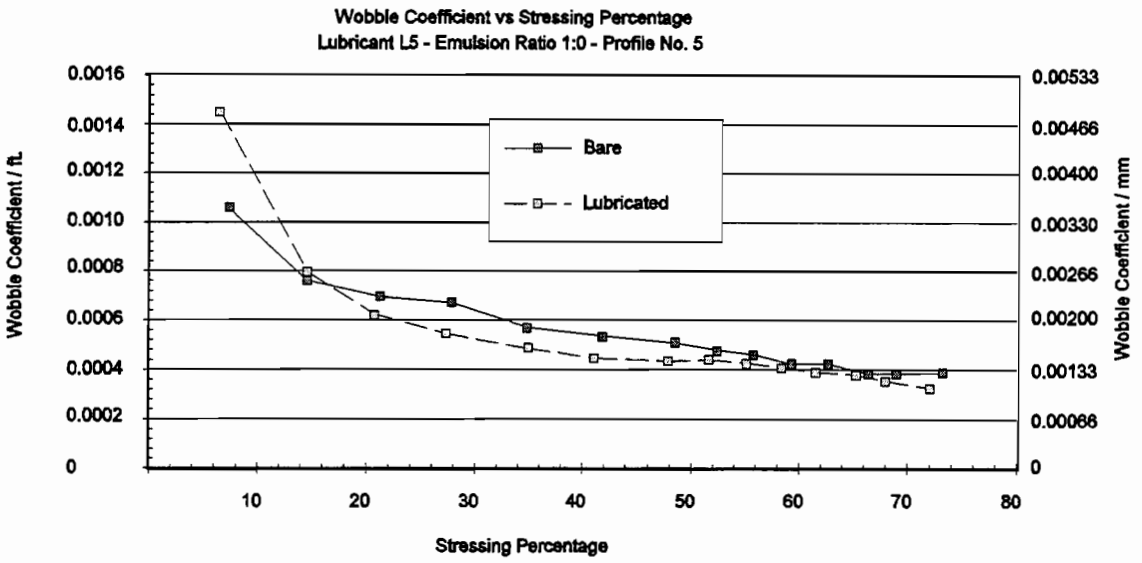

Figure 4.4 Wobble coefficient - stressing percentage for straight duct in monolithic girder

The same straight duct was used to measure wobble friction coefficient with lubricant L5. The test results are given in Table 4.2 and shown in Figure 4.3. After very high initial friction, the values somewhat stabilize above 50-60 percent and end up about 10 percent lower than the bare strand values given in Table 4.1. A comparison of the bare and lubricated wobble test results is shown in Figure 4.4.

4.2.2 Curvature Friction Coefficient. All tendons except those tested for wobble coefficient were stressed up to the limit of 0.8 f_{pu} in accordance with ACI 318 Sec. 18.5 [13]. In the wobble coefficient tests the limit, about 0.73 f_{pu}, was set by the capacity of the load cell.

Because the application of the strain gages consumed a great deal of time and because the eight curved duct profiles had the same curvature and length, bare tendons were instrumented with strain gages in only three duct profiles. These profiles were Nos. 2, 8 (which is the inverse of 2), and 1, which shows a significant friction loss.

Three types of data were collected in these tests: strain measurements, jacking loads, and holding forces. Strains were obtained from strain gage measurements which were unique to an individual wire of a particular strand at a specified point. The jacking loads were based upon data collected by the data acquisition system from the pressure transducer connected to the ram at the live end of the girder. The holding forces were derived from the output voltages of the load cell at the holding or dead end of the girder.

A series of three figures describe test results for each duct profile. The first figure (Figure 4.5) in the series gives, for each of two instrumented strands at specific locations along the duct, the strain as a function of the jacking load. It also gives the average of the two strains. The second figure (Figure 4.6)

A series of three figures describe test results for each duct profile. The first figure (Figure 4.5) in the series gives, for each of two instrumented strands at specific locations along the duct, the strain as a function of the jacking load. It also gives the average of the two strains. The second figure (Figure 4.6) illustrates the percentage of variation in the strains on the two selected strands at different blockouts. The third figure (Figure 4.7) shows the theoretical and measured distribution of the tendon stress along the tendon length.

In Figure 4.7, tendon stresses at the jacking and holding ends of the girder represent the overall averages of stresses for the strands, while the stresses at other points were based upon the strain measurements and upon the strain calibrated modulus of elasticity E_s. In this figure, a solid line connects the measured strand stresses, determined from the strain gages at specified blockouts. A dashed line represents the theoretical stress distribution along the length of the girder. This stress is based upon the friction coefficient, μ (which was computed from the jacking and holding end forces) and is computed from the equation:

$$f_x = f_j e^{-KL_x - \mu\alpha} \tag{4.2}$$

where

f_x	=	the stress at a point x on the tendon
f_j	=	the measured stress at the jacking end
e	=	the base of Napierian logarithms
K	=	the wobble coefficient (here taken as 0.0002/ft and 0.00066/m)
L_x	=	the length in feet of the tendon from the jacking end to point x
μ	=	the friction coefficient
α	=	the total angular change in radians from the jacking end to point x

The load-strain curves for Profile No. 2 are shown in Figures 4.5a to 4.5g. The largest variation in the strain functions, about 21 percent, occurs near the jacking end of the girder (Figures 4.5a, 4.5b, and 4.6). At the other locations the variation is minimal, about 4 percent. The strain variations at different locations are shown in Figure 4.6. As shown in Figure 4.7a, these measured stresses did not exactly match those predicted by friction loss theory as expressed by Equation 4.2. It is true that, from the 29-ft. (8.8 m) mark to the holding end of the girder, the strains measured by the red strain gages are very close to the theoretical ones, but near the jacking end of the girder they show values higher than those predicted by the theory. On the other hand, the strains measured by the blue strain gages are lower than the theoretical values at all locations, especially near the jacking end. As shown in Figure 4.7b, the average values of the two measured strains are comparable to the theoretical values except for a value at the 16-ft. (4.9 m) mark. Thus, in general, a theoretical uniform friction effect is evident in the measured data.

Summarizing the strain measurement test results lead to the following observations:

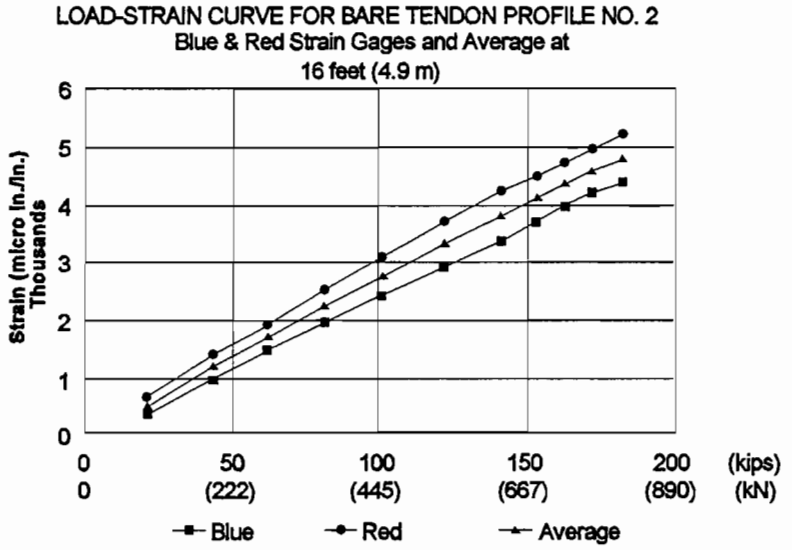

Figure 4.5a P2B1:BL16 and P2B1:RD16 load-strain curves.

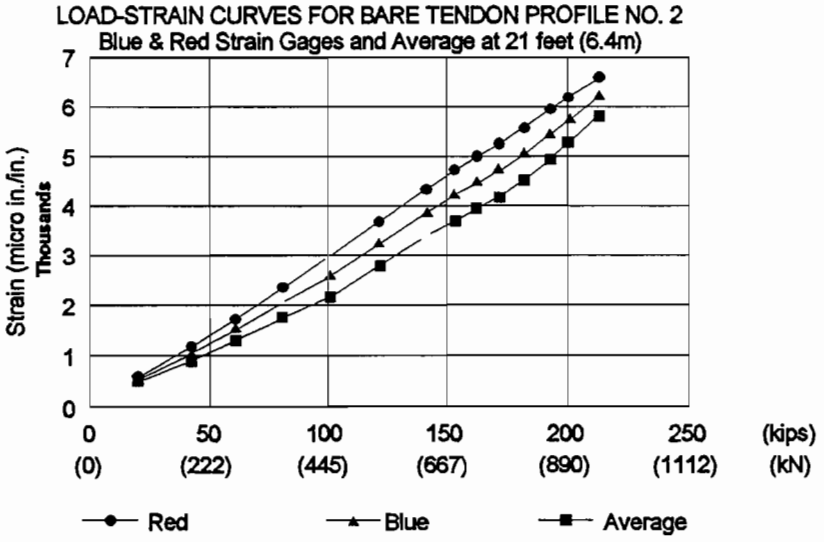

Figure 4.5b P2B1:BL21 and P2B1:RD21 load-strain curves.

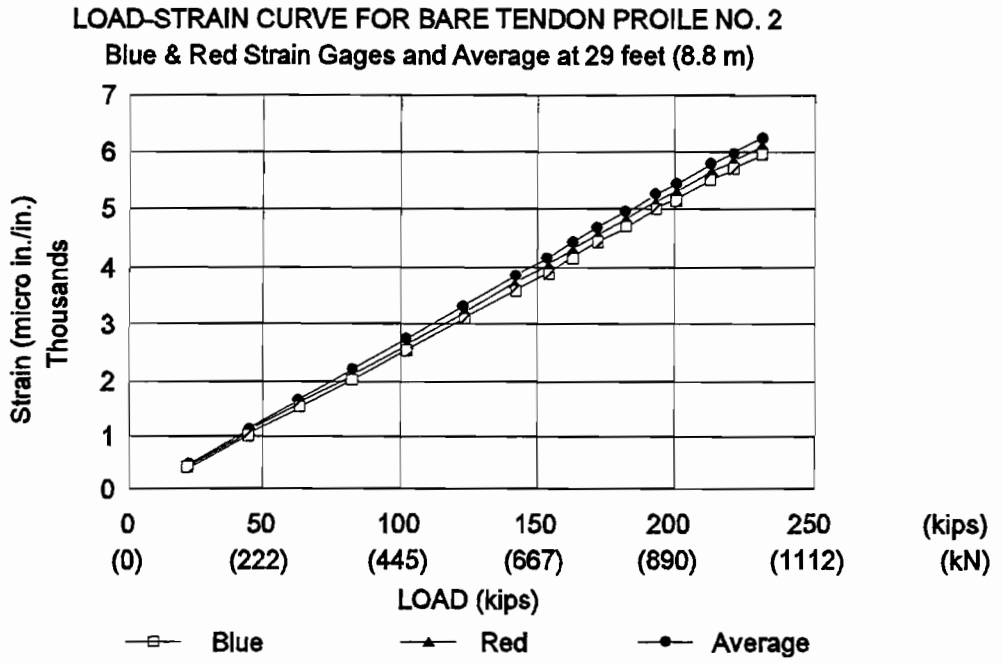

Figure 4.5c P2B1:BL29 and P2B1:RD29 load-strain curves

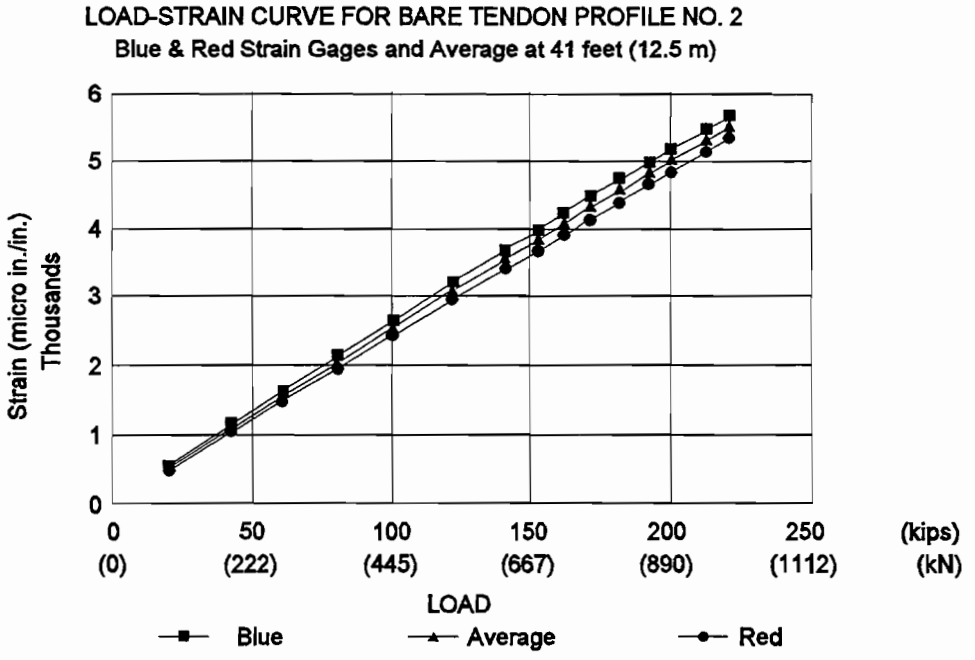

Figure 4.5d P2B1:BL41 and P2B1:RD41 load-strain curves

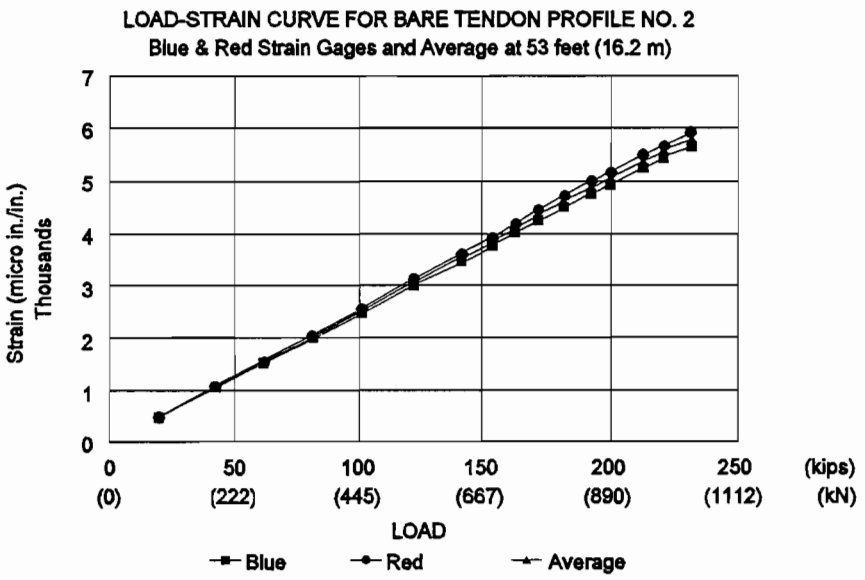

Figure 4.5e P2B1:BL53 and P2B1:RD53 load-strain curves

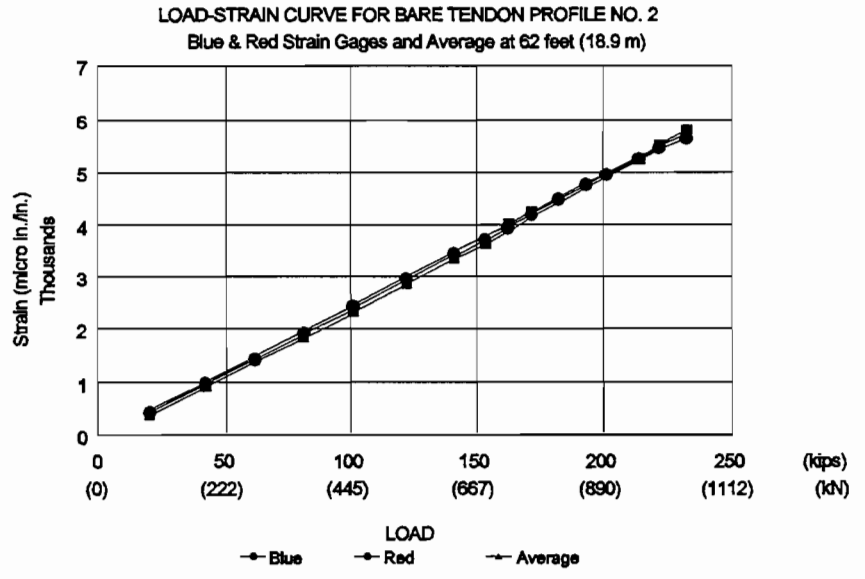

Figure 4.5f P2B1:BL62 and P2B1:RD62 load-strain curves

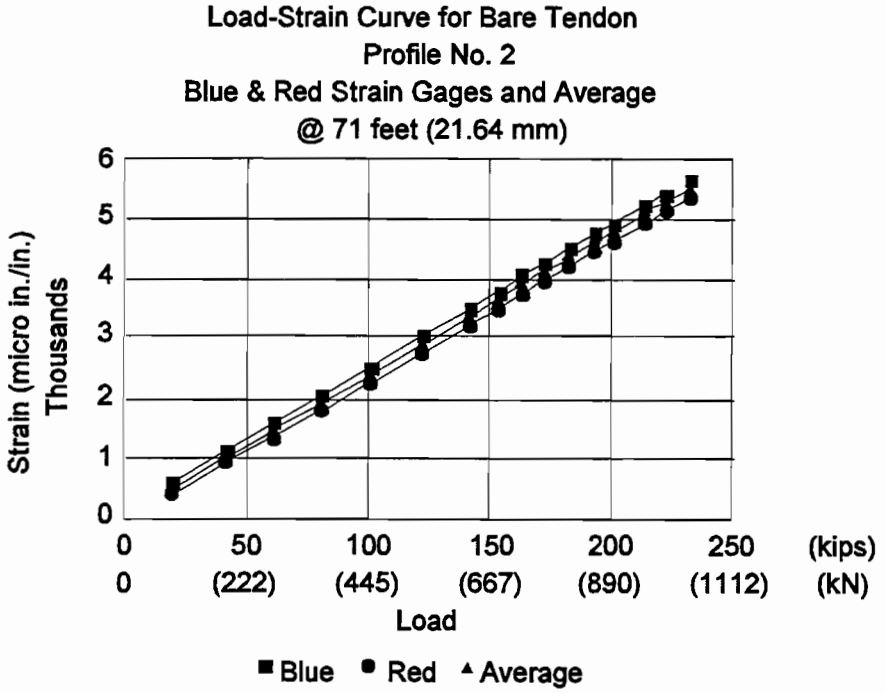

Figure 4.5g P2B1:BL71 and P2B1:RD71 load-strain curves

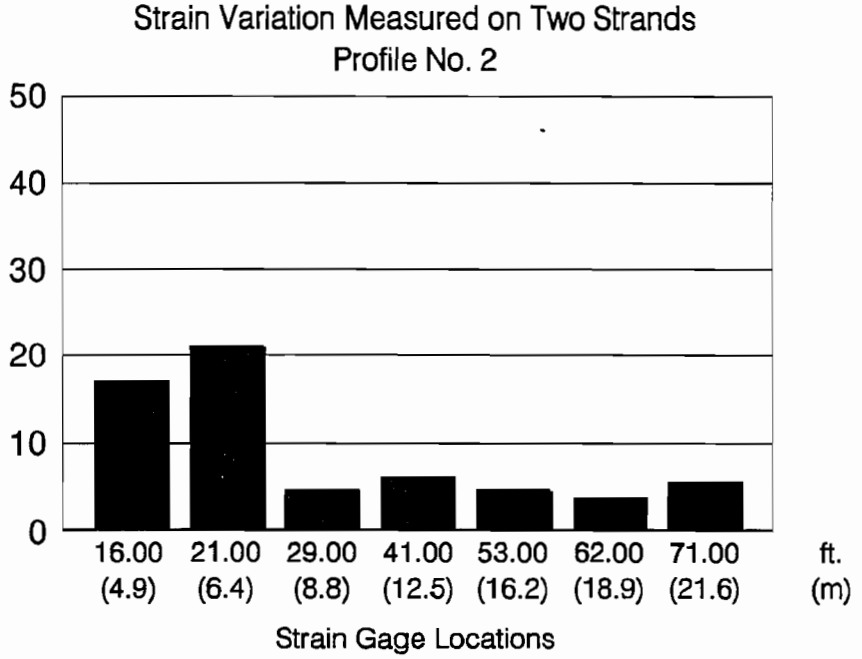

Figure 4.6 P2B1 Strain Variation Measured on Two Strands

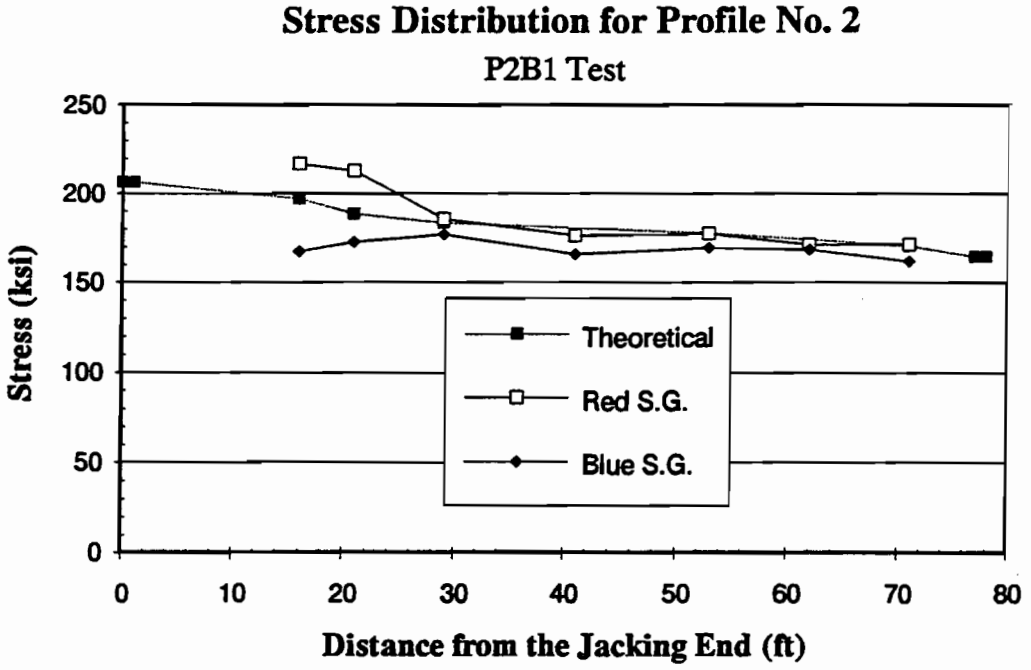

(a) With two strain gages

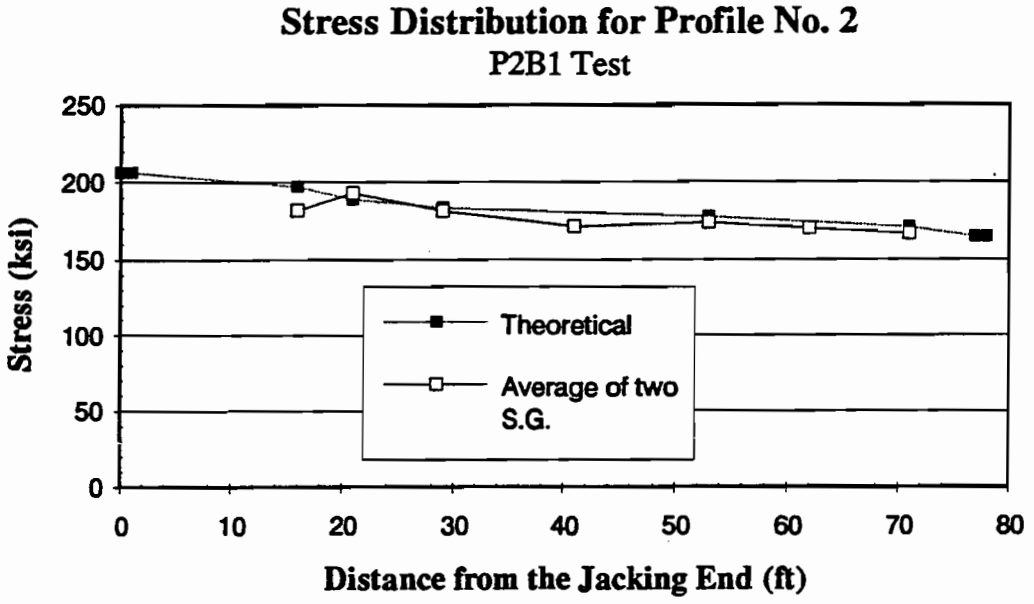

(b) With average of two strain gages

1 ft. = .3048 m

Figure 4.7 P2B1 stress distribution along the tendon

First, sometimes the strains on the two marked strands were very different even at the same blockout and in the same test. The distribution of stresses for the two instrumented strands in the same tendon can be affected by local frictional contact with the duct and by local forces caused by interaction with the surrounding strands. Different strains in the wires of the same strand have been documented by Yates [23]. The variations are due to small differences in the seating of the gripping chucks in the anchorages and would be most noticeable in this study near the tendon ends where the largest differences were generally noted. For these several reasons and because of their relative locations in the tendon, even though they should be subjected to the same nominal stress, the strands could have slightly different total angular changes and therefore could be acted upon by different parallel and normal forces.

Second, although the individual strand stress distributions did not exactly match the theoretical pattern in accordance with friction loss theory, friction did, except near the jacking end, uniformly and consistently reduce the average of the measured tendon stresses over the entire length of the girder in such way that the average of the two measured strains are comparable to the predicted value. Therefore, predicted values would be a reasonable assumption for design along the length of the girder.

Finally, measuring the strains in one strand was not an accurate way to determine the friction coefficient of the overall tendon because the variation in strain measurements was strictly applicable only to that one wire on that one strand and not to the entire tendon. When the measured strains of two instrumented strands at the same location show a great deal of difference, this could indicate that there has been improper workmanship in duct placement, during concreting, or in tendon feeding.

A more direct measurement was possible for determining the curvature friction coefficient. Eight duct profiles of the same total curvature and length were used to study the friction coefficient. In this study, the live end jacking force was measured from a pressure transducer placed on the stressing system and the dead end holding force was measured by a load cell installed at the dead end of the girder. These measurements were used to calculate the friction coefficient. The friction coefficient was obtained from the following equation:

$$\mu = \left[\ln\left(\frac{F_j}{F_h} \right) - KL \right] \Big/ \alpha \qquad (4.3)$$

where μ = the friction coefficient

F_j = the measured prestress tendon force at the jacking end of the girder

F_h = the measured prestress tendon force at the holding end

K = the wobble coefficient, taken as 3.9×10^{-4}/ft (12.8×10^{-4}/m)

L = the known tendon profile length, 78.55 ft. (23.94 m)

α = the total angular change of the centerline of the tendon in radians from the jacking end to the holding end, 1.27 radians.

The resulting friction coefficients for the bare tendon in duct profile 2 are listed in Table 4.3 and are plotted as a function of stressing percentages in Figure 4.9. From this figures it can be seen that the coefficient varied with the stressing percentages. In practice, most tendons will be stressed to the maximum allowable temporary stressing forces. For example, ACI 318-89 Section 18.5.1 [13] states that the tensile stress in prestressing tendons shall not exceed 0.80 f_{pu}. In general agreement with this, the practical friction coefficient of this study is defined as the average of the last three coefficients, which correspond to stressing percentages from 70 to 80.

The friction coefficients for bare strand in Profile No. 2 are listed in Table 4.3. These coefficients varied from 0.174 at low stressing to 0.146 at the middle, with an average value of 0.152 and a practical value of 0.156. Figure 4.9 shows that there is a wide plateau corresponding to the 20-70 stressing percentage with a small rise in the value at either end.

The friction coefficients of lubricated tendons treated with lubricant L5 and tested in Profile No. 2 are listed in Table 4.4 and are shown in Figure 4.10. Except for the first three values, Figure 4.10 shows a fairly flat horizontal line from 27.3 percent to high stressing. The practical range values for friction coefficients for lubricated tendons in Profile No. 2 is 0.127 which is about 81 percent of the value for the bare tendon.

The elongation of the strands was also measured at the live end. A plot of elongation versus the ratio of holding force to maximum live end force is shown in Figure 4.8. The lubricated strand test developed about 19 percent less friction loss than the bare strand.

4.3 Segmental Girder Results

Because of the generally poor performance of the strain gages along the tendons in the monolithic girder tests and in consideration of the extensive labor required to place and waterproof the gages, the measurement system for the segmental tests was changed so that the strain gages were replaced with potentiometers to measure elongation at various stations. Live end and holding end measurements of load remained the same. Plotted elongations are calculated based on an interpolated ram extension at which the tendon is assumed to be drawn tight to overcome minor nonlinearity in the very initial stages [18].

The graphs use the calculated elongation so that the plot will fall through the origin on all tests. Holding forces divided by jacking force is used for the vertical axis. The normalized force allows each test in the same duct to be directly comparable on the same plot.

Elongation is calculated at the face of the girder at the live end as follows:

Elongation	=	ram extension (measured)
	-	dead end wedge set (measured)
	-	elastic deflection of strand in load cell (calculated)
	-	elastic deflection of strand in ram body (calculated)

Table 4.3 P2B1 Friction Coefficient Test Results

Holding Force			Jacking Force			Friction Coefficient
Voltage (mV)	Load kip	(kN)	Voltage (mV)	Load kip	(kN)	
3.112	15.87	(70.6)	6.583	20.40	(90.7)	0.174
6.677	34.05	(151.4)	13.768	42.66	(189.8)	0.153
9.675	49.34	(219.5)	19.853	61.51	(273.6)	0.149
12.789	65.22	(290.1)	26.182	81.12	(360.8)	0.148
15.925	81.22	(361.2)	32.606	101.02	(449.3)	0.148
19.290	98.38	(437.6)	39.421	122.14	(543.3)	0.146
22.258	113.51	(504.9)	45.676	141.52	(629.5)	0.149
24.008	122.44	(544.4)	49.518	153.42	(682.4)	0.153
25.600	130.56	(580.7)	52.521	162.73	(723.8)	0.149
27.095	138.18	(614.6)	55.502	171.96	(764.9)	0.148
28.639	146.06	(649.7)	58.849	182.33	(811.0)	0.150
30.329	154.68	(688.0)	62.241	192.84	(857.7)	0.149
31.425	160.27	(712.9)	64.741	200.59	(892.2)	0.153
33.324	169.95	(755.9)	68.803	213.17	(948.2)	0.154
34.543	176.17	(783.6)	71.406	221.24	(984.1)	0.155
35.927	183.23	(815.0)	74.723	231.52	(1029.8)	0.160

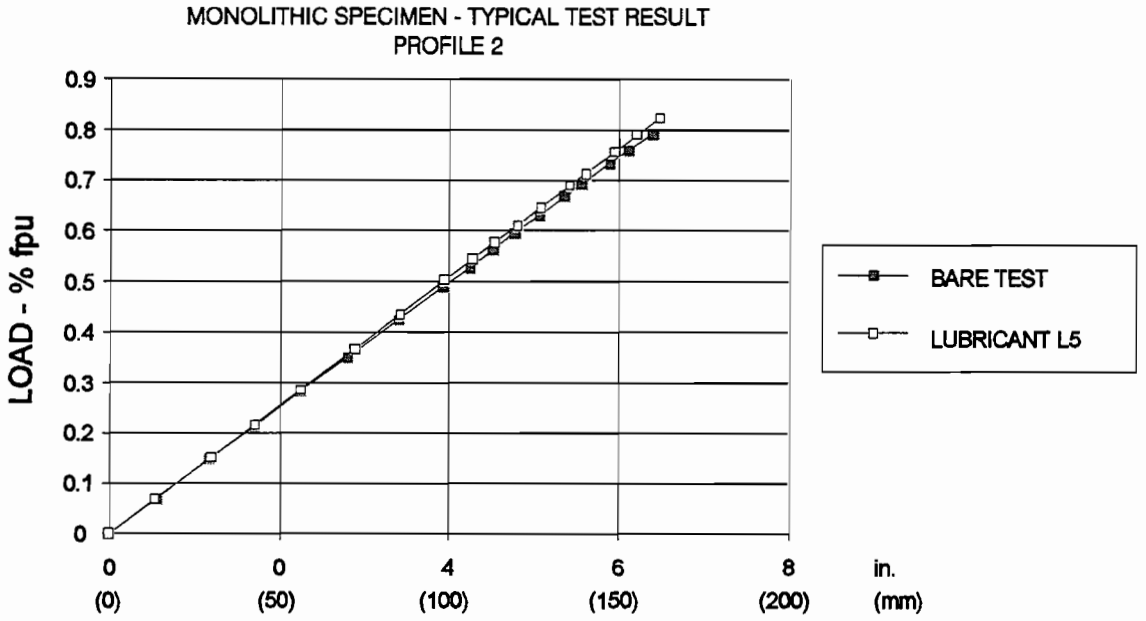

Figure 4.8 Monolithic specimen - typical test result elongation - Profile 2

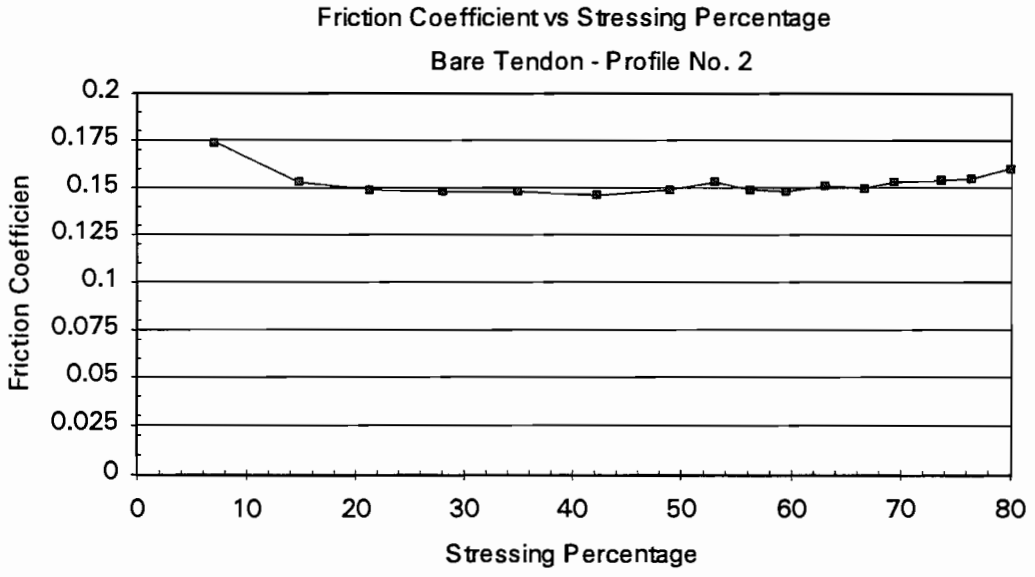

Figure 4.9 P2B1 friction coefficient vs. stressing percentage

Table 4.4 P2L5:ER10 Friction Coefficient Test Results

Holding Force			Jacking Force			Friction Coefficient
Voltage (mV)	Load kip	(kN)	Voltage (mV)	Load kip	(kN)	
3.039	15.50	(68.9)	6.364	19.72	(89.7)	0.165
6.760	34.48	(153.4)	13.750	42.60	(189.5)	0.142
9.666	49.30	(219.3)	19.396	60.10	(267.3)	0.132
12.814	65.35	(290.7)	25.524	79.08	(351.7)	0.126
16.441	83.85	(373.0)	32.710	101.35	(450.8)	0.125
19.507	99.49	(442.5)	38.762	120.10	(534.2)	0.124
22.561	115.06	(511.8)	44.718	138.55	(616.3)	0.122
24.373	124.30	(552.9)	48.511	150.30	(668.5)	0.125
25.858	131.88	(586.6)	51.406	159.27	(708.4)	0.124
27.370	139.59	(620.9)	54.561	169.05	(751.9)	0.127
28.916	147.47	(655.9)	57.691	178.74	(795.0)	0.127
30.883	157.50	(700.6)	61.501	190.55	(847.6)	0.126
31.909	162.74	(723.9)	63.676	197.29	(872.5)	0.127
33.927	173.03	(769.6)	67.514	209.18	(930.4)	0.125
35.382	180.45	(802.6)	70.539	218.55	(972.1)	0.127
36.885	188.12	(836.8)	73.681	228.29	(1015.4)	0.128

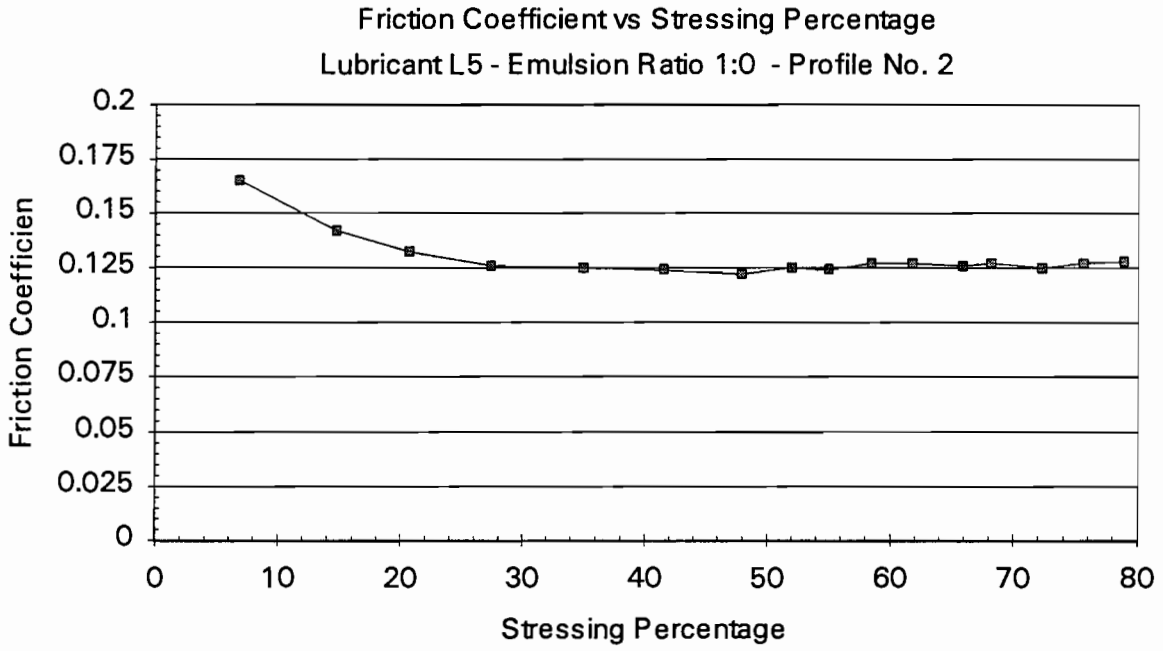

Figure 4.10 P2L5:ER10 friction coefficient vs. stressing percentage

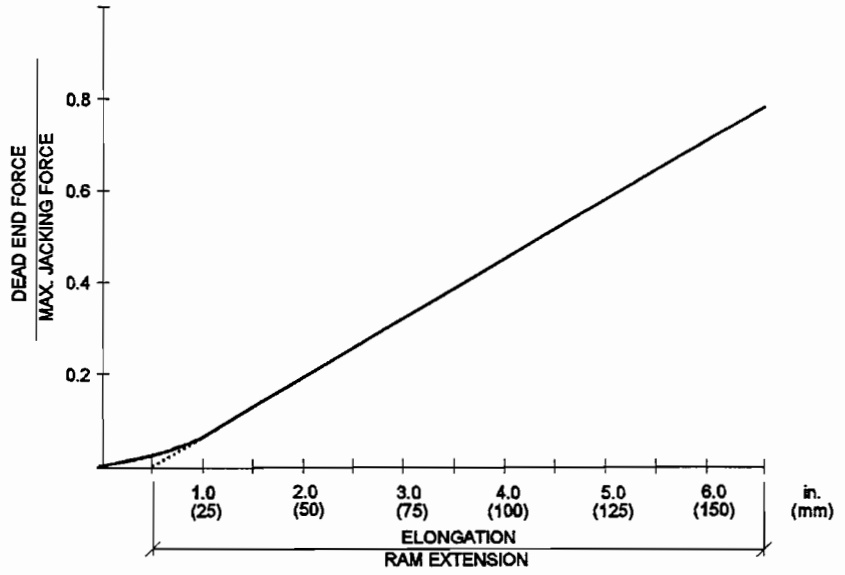

Figure 4.11 Interpolated elongation

- elastic deflection of strand in ram piston (calculated)
- live end wedge set (measured)
- beam elastic shortening (calculated)
- interpolated initial elongation correction with ram force equal to 0.

As shown in Figure 4.11, the force vs. elongation curve is extrapolated back toward the origin using the slope of the curve at the beginning of the test. As the force in the tendon increase, the coefficient of friction tends to change. The interpolated elongation at a ram force of zero eliminates elongation perceived from pulling a slack tendon.

The elongations at intermediate points along the tendons are calculated in a similar manner. Only terms in the equation that apply, or fractions thereof, are used. Elongation is only measured at the beginning and end of stressing at the intermediate points.

4.3.1 Wobble Friction Coefficient. Data for tests in Duct 11, which had offsets at segment joints of 1/8-in. (3.2 m) (the current AASHTO tolerances), are given in Tables 4.5 through 4.8 and shown in Figures 4.12 and 4.13. The first test is for bare strand. Table 4.6 indicates that at maximum live end load there is about a 4% stress loss at the holding end. Table 4.8 shows that in the second test with lubricated strand this loss actually increased to approximately 5%. The corresponding wobble friction coefficients are $K = 4.77 \times 10^{-4}$/ft. (15.6×10^{-4}/m) for the bare strand and $K = 4.15 \times 10^{-4}$/ft. (13.6×10^{-4}/m) for the strand lubricated with L11. The increase is due to duct scarring which roughened the duct and increased subsequent stressing.

4.3.2 Curvature Friction Coefficient. Data for tests in Duct 4, which had offsets at segment joints of 1/8-in. (3.2 mm) (the current AASHTO tolerance), are given in Tables 4.9 through 4.14 and shown in Figures 4.14 and 4.15. The first two tests are for bare strand. Table 4.10 indicates that at maximum stressing load there is about a 21% friction loss at the holding end. Table 4.11 indicates that in a second test with bare strand, this loss increased to about 23% at maximum jacking force, again due to scarring of the ducts. When the tendon was lubricated with graphite powder (L14), Table 14 indicates the loss was reduced slightly to about 20% of the maximum jacking force or a reduction in friction of about 15 percent as compared to the previous test.

Table 4.5 Duct 11, Test Parameters

Duct No.	11
Offset at Segment Joints	1/8" (3.2 mm)
Total Angle Change	0 rad
Duct Length	78' - 0" (23.77 m)

Test	Lubricant
1	None
2	L11 - Wright

Table 4.6 Duct 11, Test 1 Data

Tendon Force				Wedge Set				Ram Extension		Elongation	
Jacking		Holding		Live		Dead					
kips	(kN)	kips	(kN)	in.	(mm)	in.	(mm)	in.	(mm)	in.	(mm)
20.97	(93.3)	18.65	(82.9)	0.366	(9.3)	0.000	(0)	1.022	(25.9)	0.614	(15.6)
40.73	(181.2)	37.38	(166.3)	0.376	(9.6)	0.012	(0.30)	1.645	(41.8)	1.193	(30.3)
60.41	(268.7)	56.68	(252.1)	0.382	(9.7)	0.020	(0.51)	2.278	(57.9)	1.789	(45.4)
80.72	(359.0)	76.52	(340.4)	0.388	(9.8)	0.032	(0.81)	2.930	(74.4)	2.399	(60.9)
100.19	(445.6)	95.58	(425.1)	0.393	(10.0)	0.041	(1.04)	3.559	(90.4)	2.989	(75.9)
120.70	(536.9)	115.70	(514.6)	0.397	(10.1)	0.053	(1.35)	4.183	(106.2)	3.571	(90.7)
140.35	(624.3)	134.23	(597.0)	0.401	(10.2)	0.061	(1.55)	4.787	(121.6)	4.137	(105.1)
150.56	(669.7)	143.03	(636.2)	0.403	(10.2)	0.066	(1.68)	5.147	(130.7)	4.476	(113.7)
160.10	(712.1)	153.43	(682.4)	0.405	(10.3)	0.072	(1.83)	5.449	(138.4)	4.757	(120.8)
170.24	(757.2)	163.65	(727.9)	0.406	(10.3)	0.076	(1.93)	5.781	(146.8)	5.070	(128.8)
280.07	(801.0)	173.38	(771.2)	0.408	(10.4)	0.079	(2.01)	6.106	(155.1)	5.376	(136.6)
190.06	(845.4)	182.97	(813.8)	0.410	(10.4)	0.084	(2.13)	6.428	(163.3)	5.676	(144.2)
200.07	(889.9)	192.81	(857.6)	0.411	(10.4)	0.089	(2.26)	6.761	(171.7)	5.989	(152.1)
197.81	(879.8)	197.71	(879.4)	0.413	(10.5)	0.093	(2.36)	6.930	(176.0)	6.149	(156.2)

Table 4.7 Duct 11, Test 1 Elongation Data

Point	Distance from Dead End Anchorage		Measured Tendon Movement		Elongation	
	Ft	(m)	in.	(mm)	in.	(mm)
0	78.00	(23.77)	--	(--)	6.151	(156)
1	59.08	(18.01)	5	(127)	4.839	(123)
2	35.17	(10.72)	3-1/8	(79)	2.978	(76)
3	19.17	(5.84)	1-7/8	(48)	1.737	(44)

Table 4.8 Duct 11, Test 2 Data

Tendon Force				Wedge Set				Ram Extension		Elongation	
Jacking		Holding		Live		Dead					
kips	(kN)	kips	(kN)	in.	(mm)	in.	(mm)	in.	(mm)	in.	(mm)
19.77	(87.9)	18.82	(83.7)	0.260	(6.6)	0.016	(0.4)	0.434	(11.0)	0.597	(15.2)
40.00	(177.9)	37.95	(168.8)	0.272	(6.9)	0.033	(0.8)	1.096	(27.8)	1.208	(30.7)
59.71	(265.6)	57.08	(253.9)	0.281	(7.1)	0.048	(1.2)	1.727	(43.9)	1.793	(45.5)
79.82	(355.0)	75.97	(337.9)	0.290	(7.4)	0.059	(1.5)	2.370	(60.2)	2.392	(60.7)
99.00	(440.3)	94.22	(419.1)	0.297	(7.5)	0.072	(1.8)	2.992	(76.0)	2.971	(75.5)
119.93	(533.4)	114.15	(507.7)	0.304	(7.7)	0.082	(2.1)	3.621	(92.0)	3.556	(90.3)
139.65	(591.2)	132.91	(591.7)	0.310	(7.9)	0.094	(2.4)	4.239	(107.6)	4.131	(104.9)
149.66	(665.7)	142.4	(633.6)	0.313	(8.0)	0.102	(2.6)	4.550	(115.6)	4.417	(112.2)
159.72	(710.4)	152.02	(676.2)	0.315	(8.0)	0.102	(2.6)	4.867	(123.8)	4.719	(119.9)
169.88	(755.6)	161.55	(718.6)	0.317	(8.1)	0.109	(2.8)	5.191	(131.8)	5.020	(127.5)
179.68	(799.2)	171.70	(763.7)	0.321	(8.2)	0.114	(2.9)	5.499	(139.7)	5.305	(134.7)
183.49	(816.2)	180.35	(802.2)	0.323	(8.2)	0.115	(2.9)	5.812	(147.6)	5.601	(142.3)
199.74	(888.4)	190.35	(846.7)	0.327	(8.3)	0.120	(3.0)	6.238	(158.4)	6.003	(152.5)
203.41	(904.8)	198.00	(880.7)	0.331	(8.4)	0.127	(3.2)	6.541	(166.1)	6.287	(159.7)

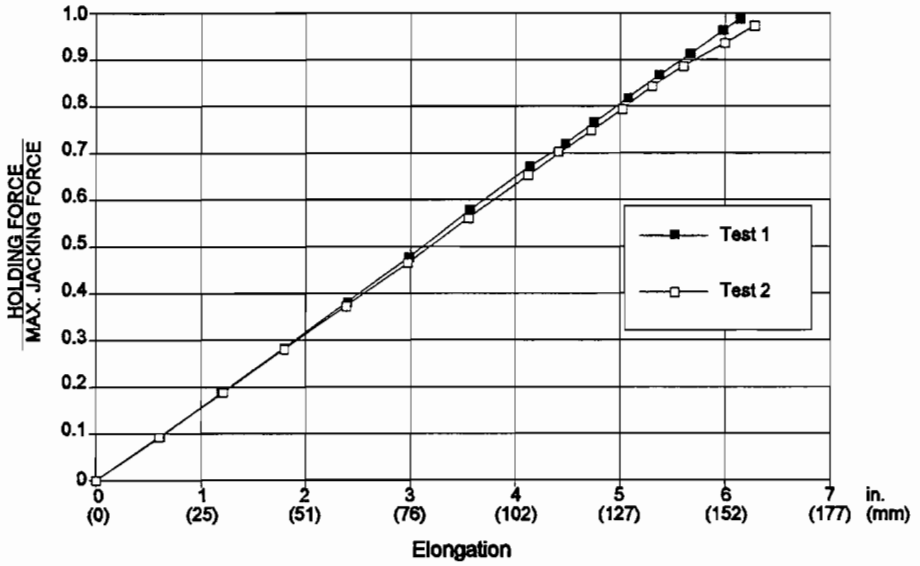

Figure 4.12 Duct 11 - P_D / P_J vs. elongation

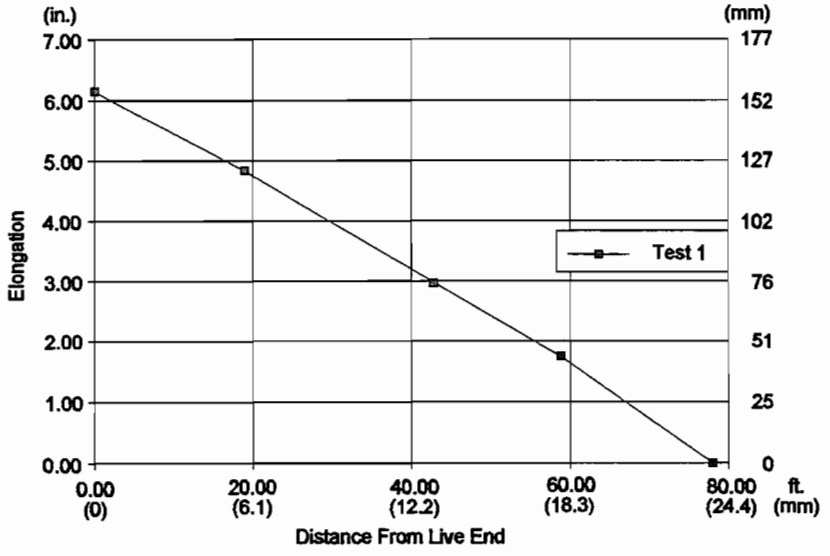

Figure 4.13 Duct 11 - elongation vs. length

Table 4.9 Duct 4 Test Parameters

Duct No.	4
Offset at Segment Joints	1/8 " (3.2 mm)
Total Angle Change	1.31 rad
Duct Length	78' - 7" (23.95 m)
Test	Lubricant
1	None
2	None

Table 10 Duct 4, Test 1 Data

Tendon Force				Wedge Set				Ram Extension		Elongation	
Jacking		Holding		Live		Dead					
kips	(kN)	kips	(kN)	in.	(mm)	in.	(mm)	in.	(mm)	in.	(mm)
21.32	(94.8)	12.05	(53.6)	0.108	(2.7)	0.016	(0.2)	0.774	(19.6)	0.587	(14.9)
41.39	(184.1)	28.51	(126.8)	0.109	(2.8)	0.038	(1.0)	1.372	(34.8)	1.140	(28.9)
61.18	(272.1)	45.32	(201.6)	0.139	(3.5)	0.053	(1.3)	1.972	(50.0)	1.673	(42.5)
80.86	(359.7)	61.62	(272.2)	0.145	(3.7)	0.064	(1.6)	2.546	(64.7)	2.208	(56.1)
100.51	(947.1)	78.22	(347.9)	0.152	(3.9)	0.074	(1.9)	3.136	(79.6)	2.757	(70.0)
120.86	(537.6)	94.88	(422.0)	0.157	(4.0)	0.083	(2.1)	3.739	(95.0)	3.322	(84.4)
140.60	(625.4)	110.36	(490.9)	0.162	(4.1)	0.092	(2.3)	4.277	(108.6)	3.821	(97.0)
150.35	(668.8)	118.26	(526.0)	0.164	(4.2)	0.094	(2.4)	4.561	(115.8)	4.089	(103.9)
160.44	(713.6)	126.02	(560.5)	0.166	(4.2)	0.098	(2.5)	4.849	(123.2)	4.358	(110.7)
170.14	(756.8)	134.07	(596.3)	0.170	(4.3)	0.100	(2.5)	5.142	(130.6)	4.632	(117.6)
180.17	(801.4)	142.38	(633.3)	0.172	(4.4)	0.105	(2.7)	5.442	(138.2)	4.911	(124.7)
190.42	(847.0)	150.02	(667.3)	0.174	(4.4)	0.109	(2.8)	5.729	(145.5)	5.179	(131.5)
200.43	(891.5)	157.80	(701.9)	0.176	(4.5)	0.113	(2.9)	6.016	(152.8)	5.446	(138.3)
109.98	(934.0)	165.24	(735.0)	0.179	(4.5)	0.115	(2.9)	6.295	(159.9)	5.707	(144.9)
220.43	(980.5)	173.71	(772.7)	0.181	(4.6)	0.118	(3.0)	6.618	(168.1)	6.010	(152.6)
230.71	(1023.8)	181.23	(806.1)	0.183	(4.6)	0.123	(3.1)	6.907	(175.4)	6.277	(159.4)
230.48	(1023.7)	184.36	(820.0)	0.184	(4.7)	0.126	(3.2)	6.907	(175.4)	6.273	(159.3)
228.87	(1018.0)	185.32	(824.3)	0.184	(4.7)	0.127	(3.2)	6.907	(175.4)	6.271	(159.3)
229.90	(1022.6)	185.44	(824.8)	0.184	(4.7)	0.128	(3.3)	6.907	(175.4)	6.270	(159.2)

Table 4.11 Duct 4, Test 1 Elongation Data

Point	Distance from Dead End Anchorage		Measured Tendon Movement		Elongation	
	Ft	(m)	in.	(mm)	in.	(mm)
0	78.00	(23.77)	----	(----)	6.271	(159.3)
1	62.17	(18.95)	5-3/16	(131.8)	4.990	(126.7)
2	57.17	(17.42)	----	(----)	----	(----)
3	49.08	(14.96)	4-5/16	(109.5)	4.123	(104.7)
4	37.08	(11.30)	3	(76.2)	2.818	(71.6)
5	25.08	(7.64)	2-3/16	(55.6)	2.012	(51.1)
6	16.25	(4.95)	1-1/2	(38.1)	1.330	(33.8)
7	7.33	(2.23)	3/4	(19.0)	0.586	(14.9)

Table 4.12 Duct 4, Test 2 Data

Tendon Force				Wedge Set				Ram Extension		Elongation	
Jacking		Holding		Live		Dead					
kips	(kN)	kips	(kN)	in.	(mm)	in.	(mm)	in.	(mm)	in.	(mm)
20.56	(91.4)	13.61	(60.5)	0.409	(10.4)	0.012	(0.3)	1.155	(29.3)	0.582	(14.8)
40.56	(180.4)	29.63	(131.8)	0.427	(10.8)	0.022	(0.5)	1.771	(45.0)	1.148	(29.2)
60.24	(267.9)	45.65	(203.1)	0.437	(11.1)	0.030	(0.8)	2.360	(59.9)	1.697	(43.1)
80.34	(357/4)	61.8	(274.9)	0.446	(11.3)	0.037	(0.9)	2.944	(74.8)	2.242	(56.9)
100.37	(446.4)	77.72	(345.7)	0.453	(11.5)	0.045	(1.1)	3.526	(89.6)	2.785	(70.7)
120.47	(535.8)	94.00	(418.1)	0.460	(11.7)	0.050	(1.3)	4.126	(104.6)	3.349	(85.1)
140.17	(623.5)	109.43	(486.7)	0.465	(11.8)	0.054	(1.3)	4.701	(119.4)	3.890	(98.8)
150.40	(669.0)	117.37	(522.1)	0.468	(11.9)	0.056	(1.4)	4.960	(126.0)	4.131	(104.9)
160.37	(713.3)	125.34	(559.5)	0.469	(11.9)	0.058	(1.5)	5.243	(133.2)	4.398	(111.7)
170.55	(758.6)	133.17	(592.3)	0.472	(12.0)	0.060	(1.5)	5.533	(140.5)	4.670	(118.6)
180.15	(801.3)	140.41	(624.5)	0.474	(12.0)	0.063	(1.6)	5.802	(147.4)	4.921	(125.0)
190.08	(845.5)	148.11	(658.8)	0.476	(12.1)	0.065	(1.6)	6.087	(154.6)	5.188	(131.8)
200.23	(890.6)	156.11	(694.4)	0.479	(12.2)	0.068	(1.7)	6.385	(162.2)	5.466	(138.8)
210.18	(934.9)	163.10	(725.5)	0.481	(12.2)	0.070	(1.8)	6.651	(168.9)	5.751	(146.1)
219.93	(978.2)	170.86	(760.0)	0.483	(12.3)	0.072	(1.8)	6.951	(176.5)	5.997	(152.3)
230.40	(1024.8)	178.95	(796.0)	0.487	(12.4)	0.075	(1.9)	7.266	(184.4)	6.290	(159.8)
229.62	(1021.3)	183.15	(814.6)	0.486	(12.3)	0.078	(2.0)	7.264	(184.5)	6.285	(159.6)
232.36	(1033.5)	183.24	(815.0)	0.486	(12.3)	0.078	(2.0)	7.261	(184.4)	6.280	(159.5)
229.68	(1021.6)	183.42	(815.8)	0.486	(12.3)	0.079	(2.0)	7.261	(184.4)	6.279	(159.5)

Table 4.13 Duct 4, Test 2 Elongation Data

Point	Distance from Dead End Anchorage Ft	(m)	Measured Tendon Movement in.	(mm)	Elongation in.	(mm)
0	78.00	(23.77)	----	(----)	6.281	(159.5)
1	62.17	(18.95)	5-1/4	(133.3)	5.103	(129.6)
2	57.17	(17.42)	----	(----)	----	(----)
3	49.08	(14.96)	4-3/16	(106.4)	4.048	(102.8)
4	37.08	(11.30)	3-1/8	(79.4)	2.993	(76.0)
5	25.08	(7.64)	2-5/16	(58.7)	2.187	(55.5)
6	16.25	(4.95)	1-9/16	(39.7)	1.443	(36.6)
7	7.33	(2.23)	3/4	(19.0)	0.636	(16.2)

Table 4.14 Duct 4, Test 3 Data

Tendon Force				Wedge Set				Ram Extension		Elongation	
Jacking kips	(kN)	Holding kips	(kN)	Live in.	(mm)	Dead in.	(mm)	in.	(mm)	in.	(mm)
21.08	(93.8)	17.01	(75.7)	0.000		0.011	(0.3)	1.106	(28.1)	0.706	(17.9)
40.51	(180.2)	32.62	(145.1)	0.000		0.020	(0.5)	1.787	(45.3)	1.357	(34.5)
60.17	(267.6)	49.07	(218.3)	0.000		0.026	(0.7)	2.432	(61.8)	1.974	(50.1)
80.19	(356.7)	65.97	(293.4)	0.000		0.036	(0.9)	3.040	(77.2)	2.549	(64.7)
100.35	(446.4)	81.97	(364.6)	0.000		0.040	(1.0)	3.630	(92.2)	3.111	(79.0)
121.18	(539.0)	98.77	(439.3)	0.000		0.050	(1.3)	4.188	(106.4)	3.634	(92.3)
140.04	(622.9)	114.03	(507.2)	0.000		0.051	(1.3)	4.737	(120.3)	4.158	(105.6)
149.88	(666.7)	121.91	(542.2)	0.000		0.055	(1.4)	5.024	(127.6)	4.428	(112.5)
159.22	(708.2)	129.37	(575.4)	0.000		0.058	(1.5)	5.300	(134.6)	4.689	(119.1)
170.06	(756.4)	137.60	(612.0)	0.000		0.060	(1.5)	5.600	(142.2)	4.973	(126.3)
179.66	(799.1)	145.67	(647.9)	0.000		0.064	(1.6)	5.889	(149.6)	5.245	(133.2)
188.63	(839.0)	153.12	(681.0)	0.000		0.067	(1.7)	6.167	(156.6)	5.507	(139.9)
198.45	(882.7)	160.77	(715.1)	0.000		0.069	(1.8)	6.446	(163.7)	5.771	(146.6)
207.87	(924.6)	168.08	(747.6)	0.000		0.075	(1.9)	6.722	(170.7)	6.028	(153.1)
217.06	(965.5)	175.40	(780.2)	0.000		0.079	(2.0)	7.008	(178.0)	6.297	(159.9)
225.68	(1003.8)	181.76	(808.5)	0.000		0.079	(2.0)	7.251	(184.2)	6.527	(165.8)
224.66	(999.3)	183.04	(814.2)	0.000		0.082	(2.1)	7.275	(184.8)	6.548	(166.3)
224.96	(1000.6)	183.30	(815.3)	0.000		0.083	(2.1)	7.275	(184.8)	6.547	(166.3)
225.90	(1004.8)	183.54	(816.4)	0.000		0.084	(2.1)	7.275	(184.8)	6.546	(166.3)
225.08	(1001.1)	183.74	(817.3)	0.000		0.084	(2.1)	7.275	(184.8)	6.545	(166.2)
225.27	(1002.0)	183.79	(817.5)	0.000		0.084	(2.1)	7.275	(184.8)	6.545	(166.2)

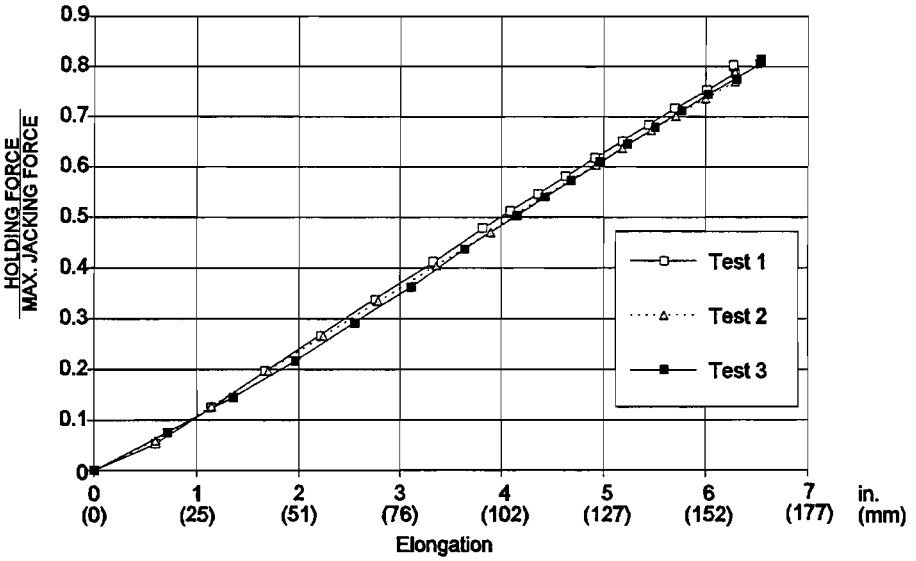

Figure 4.14 Duct 4 - P_D / P_J vs. elongation

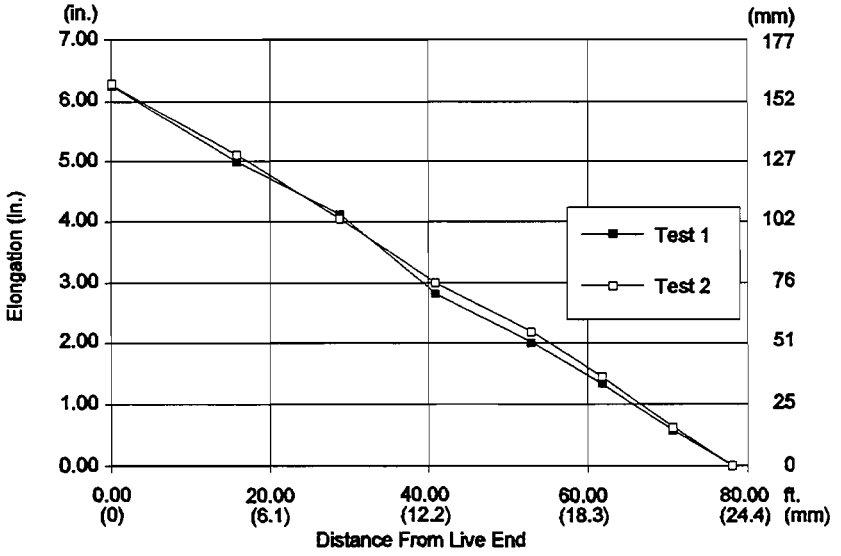

Figure 4.15 Duct 4 - elongation vs. length

CHAPTER FIVE
ANALYSIS OF TEST RESULTS

5.1 Introduction

The testing procedure for both the monolithic test specimen and the segmental test specimen was essentially the same as far as the major parameter measured. In both test series, the accurate measurement of ram force at the active stressing end through a carefully calibrated ram equipped with sensitive pressure transducers and the accurate measurement of tendon force at the dead or holding end by a calibrated load cell, allowed direct comparison of the total wobble friction in straight ducts and indirect comparison of the curvature friction in curved ducts. The latter is termed indirect since measured difference in force between active and dead end (or between jacking and holding end) was corrected by deducting the wobble effect measured in the straight ducts. In the two series different measures of the deformation along the length of the tendons were made. Strain gages were used in the earlier monolithic series. Because the data was erratic and not of value commensurate with the effort, the measurement system was changed to emphasize elongation measurements in the segmental girder. Sample data has been given in Chapter 4 to illustrate typical observations in the test series. In this Chapter most emphasis will be given to direct comparisons between bare and lubricated strand as well as between monolithic and segmental girders based on ratios of dead end to jacking force and resultant μ and K factors for calculating friction and wobble losses.

5.2 Monolithic Girder Results

5.2.1 Wobble Effect. Wobble friction loss among straight tendon profiles was fairly consistent. Among the draped tendon profiles the curvature friction loss was also fairly consistent with the exception of one damaged draped duct. Paste entered that one duct and greatly increased the friction loss in that test. Data from the strain gauges located along the tendon had great scatter and did not provide much useful information. Difficult installation conditions were to blame.

Wobble coefficients are summarized in Table 5.1, and the ratio of dead end force to jacking end force is shown in Figures 5.1 and 5.2 for each straight duct. Wobble friction coefficients calculated from the results of the unlubricated straight profile tests were consistent with a 95% fractile (mean plus 1.7 standard deviations) of about 3.85×10^{-4} / ft. (12.6×10^{-4}/m). This relates to about a 3% tendon force loss over 78 ft. (24 m) for unlubricated strand.

The lubricated strand tests shown had somewhat more scatter but with a 95% fractile of about 3.69×10^{-4} / ft. (12.1×10^{-4}/m). This again results in about a 2.8% tendon force loss over 78 ft. (24 m) for the lubricated strand. Thus, as also shown in Figure 5.2, lubricating the tendon in a monolithic girder with the best of the water soluble oil has an insignificant effect on the wobble loss coefficient.

Table 5.1 Monolithic Wobble Friction Results - Straight Ducts

Duct	Test	Lubricant	P_{dead} / P_{jack}	K (/ft)	K (/m)
5	1	Bare	0.970	3.84×10^{-4}	12.6×10^{-4}
	2	L5	0.975	3.23×10^{-4}	10.6×10^{-4}
6	1	Bare	0.970	3.82×10^{-4}	12.5×10^{-4}
	2	L11	0.972	3.57×10^{-4}	11.7×10^{-4}

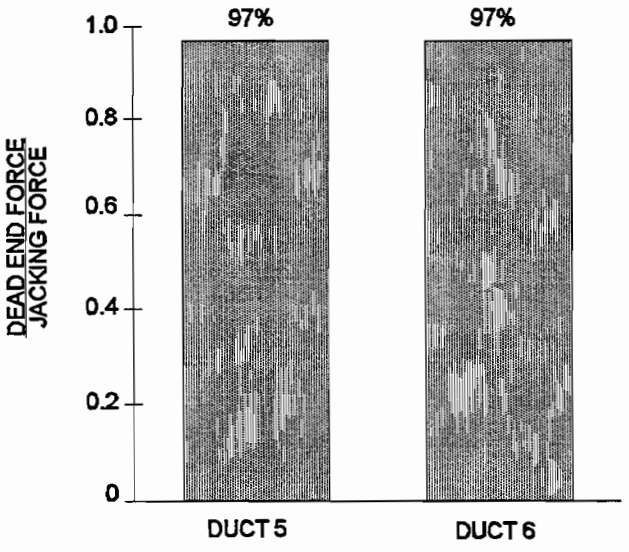

Figure 5.1 Bare strand monolithic friction test results - straight ducts

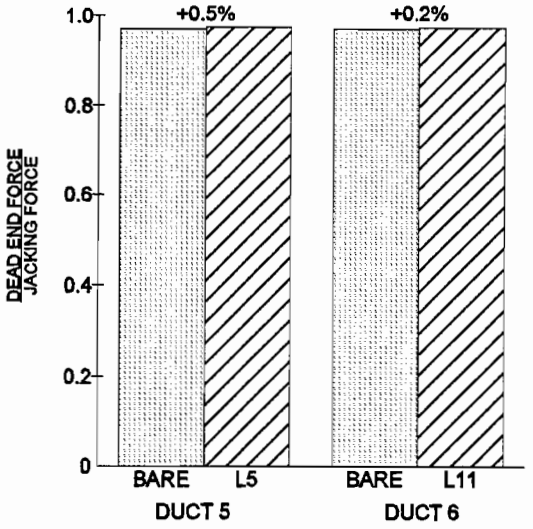

Figure 5.2 Lubricated strand monolithic friction test results - straight ducts

5.2.2 Curvature Effect. In the tests of curved tendons both intentional and accidental curvature (wobble) are present. In order to determine intentional curvature coefficients, the results of wobble effects must first be deducted. Curvature friction coefficients were calculated assuming a wobble coefficient of 3.9×10^{-4} / ft. (12.8×10^{-4}/m). As shown in Table 5.2, bare strand curvature friction coefficients, μ, generally ranged from 0.146 to 0.162 with a single very high value of 0.245 for the damaged duct profile, Duct 1. Excluding that outlier, the mean is 0.155 and standard deviation is 0.0058. The 95% fractile would be 0.165. Again excluding the damaged Duct 1, curvature coefficients for lubricated duct and tendons ranged from 0.106 to 0.138. The means is 0.131 and 95% fractile is 0.153. Thus the average lubricant effect is 0.153/0.165 or about a 7 percent reduction in friction coefficient. The best product, L11, approached a 14 percent reduction on the same calculation basis. Ducts tested after very thorough flushing showed similar reduction in friction as the ducts with lubricant on all contacting surfaces. Curvature coefficients are summarized in Table 5.2, and dead and forces for dry and lubricated tendons in each draped duct are shown in Figures 5.3 and 5.4

5.2.3 Indications. The wobble coefficient (K) for galvanized semi-rigid duct and unlubricated multi-strand tendon can conservatively be taken as 4×10^{-4} / ft. (13×10^{-4}/m) for monolithic construction. The curvature coefficient (μ) can conservatively be taken as 0.16 for girders with duct radii of curvature similar to or greater than that of the present test specimen. These coefficients conservatively include all the test results from the bare strands in the monolithic specimen except that of the damaged duct. The actual average curvature coefficient for bare strand was 0.155. These values can be confirmed from the data of the field tests by Dywidag [9] in galvanized semi-rigid duct which gave unlubricated tendon curvature friction coefficients of $\mu = 0.17$ when the curvature coefficient was recalculated using an assumed wobble coefficient of 0.0004/ft. (0.00131/m), as suggested by Tran [10], instead of the 0.0002/ft. (0.00066/m) assumed originally by Dywidag.

Table 5.2 Monolithic Friction Specimen Results - Curved Ducts

Duct	Test	Lubricant	P_{dead}/P_{jack}	μ *
1	1	Bare	0.711	0.245
	2	L2	0.724	0.231
2	1	Bare	0.791	0.160
	2	L5	0.824	0.128
	3	L5	0.810	0.142
3	1	Bare	0.792	0.159
	2	L2	0.814	0.138
	3	L2	0.795	0.157
4	1	Bare	0.789	0.162
	2	L5	0.823	0.129
7	1	Bare	0.804	0.147
	2	L11	0.848	0.106
8	1	Bare	0.796	0.155
	2	L11	0.840	0.113
	3	L11	0.815	0.137
	4	Flushed	0.849	0.105
9	1	Bare	0.795	0.157
	2	L8	0.826	0.126
10	1	Bare	0.806	0.146
	2	L8	0.819	0.133
	3	L8	0.814	0.138
	4	Flushed	0.821	0.132
	5	L13	0.828	0.125

* μ computed assuming $K = 3.9 \times 10^{-4}$/ft. (1.28×10^{-3}/m)

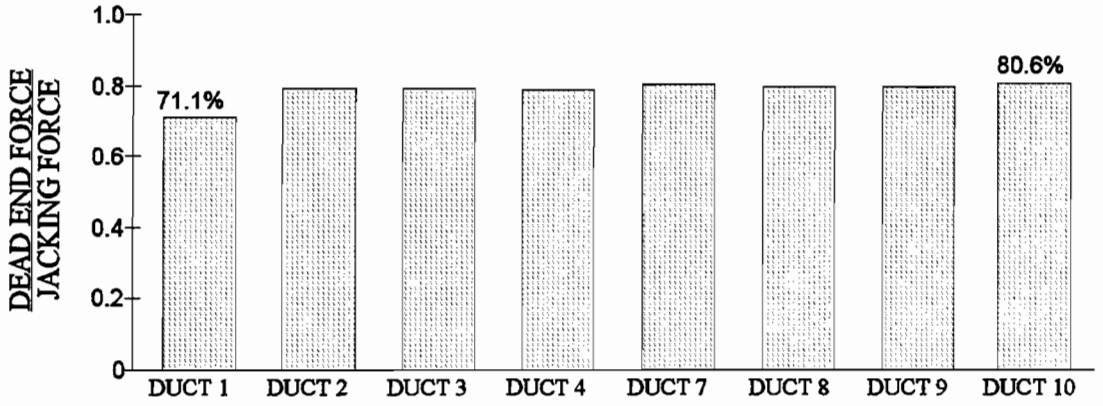

Figure 5.3 Bare strand monolithic friction test results - draped ducts

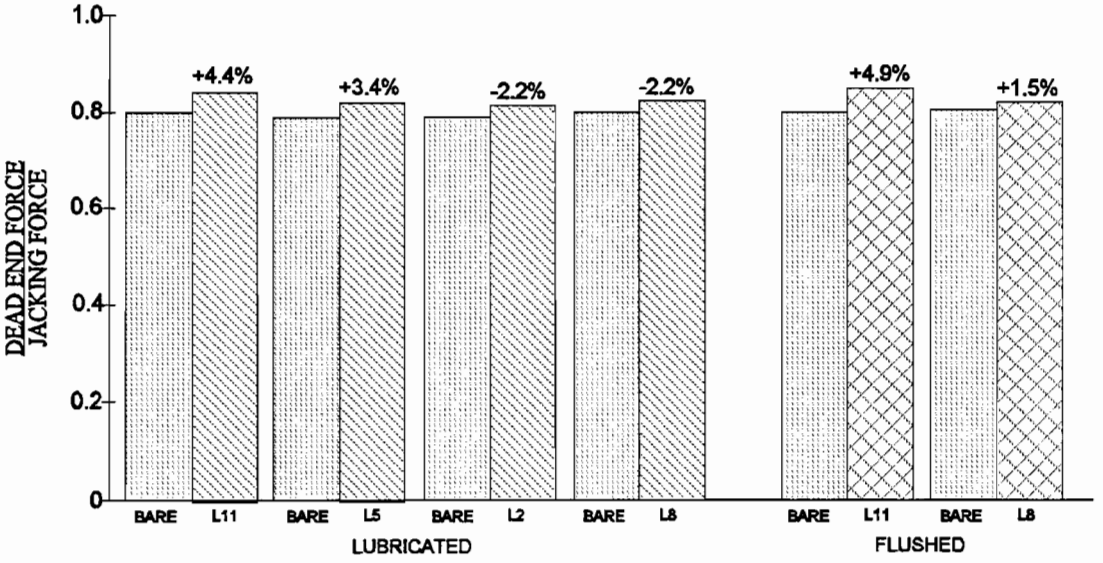

Figure 5.4 Lubricated monolithic friction test results - draped ducts

When effective lubricants are used, the curvature friction loss and wobble friction loss might be expected to drop proportionately. If both wobble and friction coefficients found by Dywidag [9] are assumed to drop in value proportionately for their lubricated tendon tests, the coefficients would change to $\mu = 0.10$ and k = 0.00023/ft. (0.00075/m) when L13 was used, and to $\mu = 0.11$ and k = 0.00026/ft. (0.00085/m) when L2 was used. Minimum curvature coefficients found in this study for lubricated tendons were $\mu = 0.125$ for L13, $\mu = 0.138$ for L2, $\mu = 0.106$ for L11, $\mu = 0.126$ for L8 and $\mu = 0.128$ for L5 as given in Table 5.2. These values are based on a wobble coefficient held constant at 0.00039/ft. (0.00128/m). Cleaning and pre-lubricating the duct surfaces were found in this program to be as effective in reducing friction as lubricating the tendon itself. This also would keep foreign material off the strand. Dead end forces for the flushed tests are also shown in Figure 5.4. The absolute minimum curvature friction coefficient found by Tran in any duct was $\mu = 0.105$ in Duct 8. This duct had been lubricated with L11 then flushed thoroughly.

Using the most effective water soluble lubricant, friction loss in the test specimen was reduced by 22%, which is substantially smaller than the reduction in friction loss seen by Dywidag (35% with L13 and 28% with L2). This 22% reduction in friction loss resulted in about a 10% increase in elongation with the one end jacking method used on the test specimen.

An average wobble coefficient of K = 0.00039/ft. (0.00128/m) and curvature coefficient of $\mu = 0.155$ will be assumed to characterize the friction loss behavior of the monolithic test girder tendons. Coefficients found from unlubricated tests in the segmental test girder will be directly comparable to these coefficients. Wobble friction coefficients for the segmental test girder would be expected to increase over those of the monolithic girder, while the curvature friction coefficient should remain about the same. Wobble friction coefficients measured in the straight ducts of both girders will certainly be confirmed if the curvature coefficients measured are similar.

The most effective lubricant (L11) used in the monolithic girder by Tran (10) was also tested in the segmental test girder. L11 reduced total friction loss in the monolithic test girder by 22%. Friction loss reductions in the segmental test girder ducts by lubrication might be expected to be equal to or less than 22% for L11.

5.3 Segmental Girder Results

5.3.1 Wobble Loss. Straight ducts were included in the large scale test specimens, monolithic and segmental, so that a direct comparison of wobble friction losses could be made for each construction technique. Friction loss associated with the segment joints is length-dependent and belongs in the wobble term. Analysis of the test results determined the relationship between duct offsets at segment joints and wobble loss.

5.3.1.1 Effect of Offsets. Mismatched ducts at the segment joints should increase wobble friction loss by introducing additional curvature change, and by providing a rough edge over which the tendon must ride during elongation. Figure 5.5 shows the normalized dead end force for the straight ducts tested, including the monolithic girder ducts. Friction loss increases as the offset becomes larger,

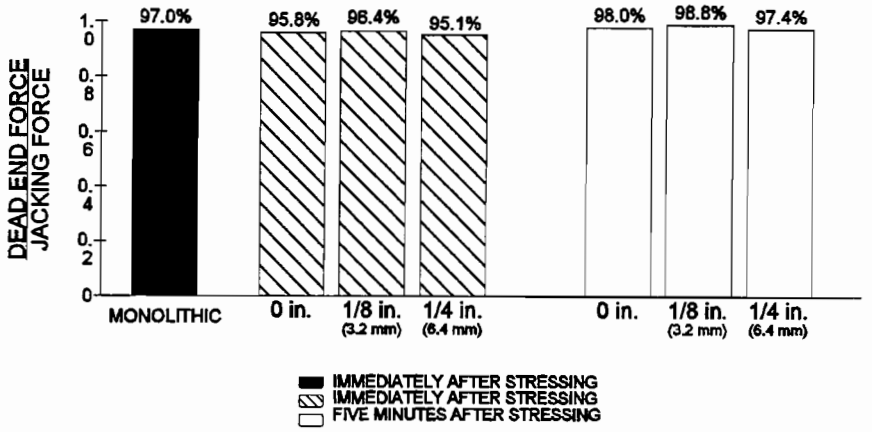

Figure 5.5 Bare strand segmental friction test results - straight ducts

although little significant difference is seen between the wobble friction loss in the ducts with 0-in. (0 mm) offsets and ducts with 1/8-in. (3.2 mm) offsets. In fact slightly less losses were noted in the 1/8" (3.2 mm) offset ducts.

Approximately the same dead end force increase over 5 minutes seen in the straight ducts was also seen in the draped ducts (2% of the jacking force) in the segmental specimen. Wobble loss measured in straight ducts may differ from wobble loss in a draped duct under the same construction conditions. Normal forces generated from side-to-side wobble of the duct will be small for straight and draped ducts with no horizontal curvature. Normal force from vertical wobble of the duct, including vertical mismatch at the segment joints, will be much larger in draped ducts. Friction loss has generally been found to increase with increased normal force. For this reason, wobble losses after tendon creep (long term) were not used to calculate wobble coefficients in Section 5.3.1.3. The 2% increase in dead end force after 5 minutes reduces the total friction loss in a draped duct, not just the friction loss caused by wobble.

5.3.1.2 Effect of Lubrication. Figure 5.6 shows that lubrication was ineffective in reducing wobble friction in the straight ducts. Duct scarring from the first test in each duct increased the wobble coefficient of the duct enough to cause a net increase in friction in the second test even with the lubricant.

5.3.1.3 Summary of Wobble Coefficients. Calculated wobble friction coefficients for each straight duct are shown in Table 5.3. Note that the wobble coefficient increases with the second test in a duct in most cases. A wobble coefficient of 5×10^{-4}/ft. (16×10^{-4}/m) adequately provides an estimate of the bare strand wobble loss in Ducts 5 and 11 where the duct offset at the segment joint is kept within tolerance of 1/8-in. (3.2 mm). A wobble coefficient of 6×10^{-4}/ft. (19.7×10^{-4}/m) better represents Duct 6 with the 1/4-in. (6.4 mm) offset. These are both higher than the 4×10^{-4}/ft. (13×10^{-4}/m) wobble coefficient found earlier for the monolithic girder.

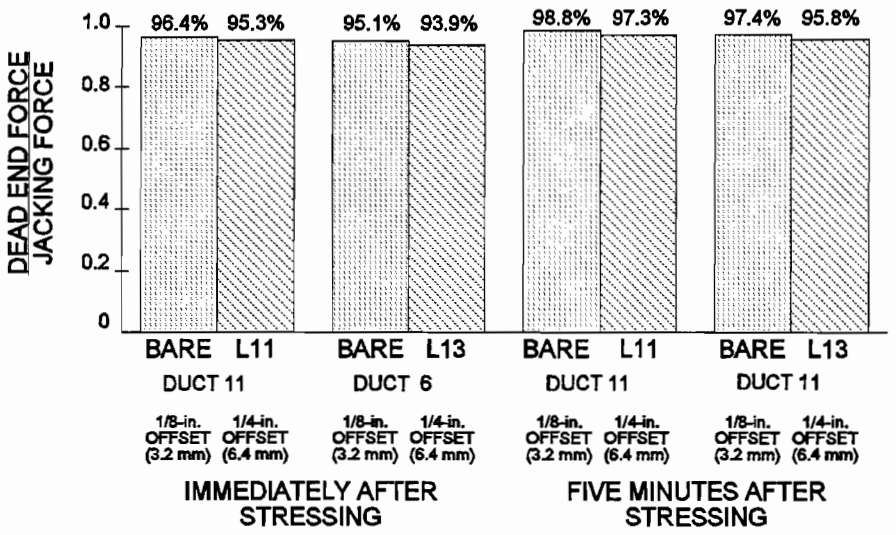

Figure 5.6 Lubricated strand segmental friction test results - straight ducts

Table 5.3 Segmental Wobble Friction Results - Straight Ducts

Duct	Offset in.	Offset (mm)	Test	Lubricant	$K_{initial}$ /ft	$K_{initial}$ (/m)	K_{final} /ft	K_{final} (/m)
5	0	(0)	1	Bare	5.58x10^{-4}	(18.3x10^{-4})	2.68x10^{-4}	(8.7x10^{-4})
5	0	(0)	2	Bare	4.76x10^{-4}	(15.6x10^{-4})	2.72x10^{-4}	(8.9x10^{-4})
11	1/8	(3.2)	1	Bare	4.75x10^{-4}	(15.6x10^{-4})	1.55x10^{-4}	(5.1x10^{-4})
11	1/8	(3.2)	2	L11	6.50x10^{-4}	(21.3x10^{-4})	3.45x10^{-4}	(11.3x10^{-4})
6	1/4	(6.4)	1	Bare	6.42x10^{-4}	(21.0x10^{-4})	3.30x10^{-4}	(10.8x10^{-4})
6	1/4	(6.4)	2	L13	8.36x10^{-4}	(27.4x10^{-4})	5.50x10^{-4}	(18.0x10^{-4})

These approximate wobble coefficients will be used to calculate the curvature friction coefficients in the draped ducts based on the test results. If the curvature coefficients are found to be relatively constant duct to duct, regardless of offset, then the wobble coefficients selected account for the correct amount of friction loss attributable to wobble friction.

5.3.2 Friction Losses in Draped Ducts. Draped ducts were also constructed in the segmental test specimen with intentional mismatch at the segment joints. The relatively small radii of curvature found in the draped ducts means that high normal forces were present across the mismatched duct joints. Lubricants were also tested in the draped ducts.

5.3.2.1 Effect of Offsets. Figure 5.7 shows that friction loss in the draped ducts was found to increase with an increase in the size of the duct offset. Once again, little difference was seen between the ducts with 0-in. (0 mm) offset and 1/8-in. (3.2 mm) offset at the segment joints. The increase in normal force on the offset did not substantially magnify the wobble friction loss seen in the straight ducts. Figure 5.7 shows the dead end force remaining after friction loss as a fraction of jacking force for the segmental and monolithic test specimens.

After five minutes of applied maximum jacking force, additional force had crept to the dead end. This behavior is characteristic of ducts with small radii of curvature, particularly in external tendons. For this reason when curvature coefficients were calculated from the test data, the tendon force before creep was used. Normal highway girders have larger minimum radii of duct curvature and may not be able to redistribute force along the tendon to the same degree. Burns, Helwig, and Tsujimoto [20] found no tendon creep after stressing medium radius of curvature (150-ft.) (46 m) greased and sheathed strands. The low friction loss per length did not provide the conditions needed for tendon creep. Table 5.4 shows a similar decline in time-dependent increases in dead end force when lubricants were used.

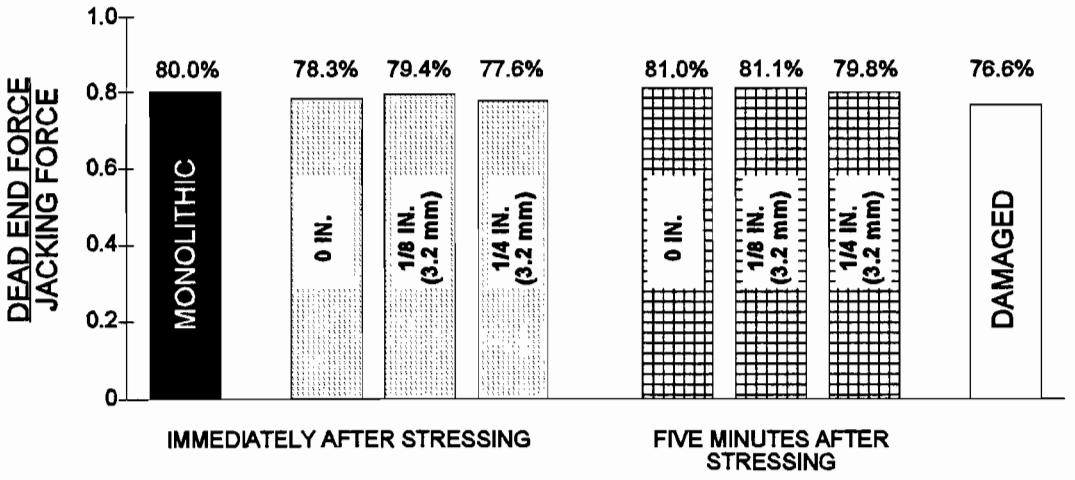

Figure 5.7 Bare strand segmental friction test results - draped ducts

Table 5.4 Summary of Wobble and Curvature Coefficients - Segmental Girder

Duct	Duct Type	Lubricant	P_{dead} Initial kips (kN)	P_{dead} Final kip (kN)	%	Mean %
5	Straight	None	192.23 (855)	196.64 (875)	2.22	2.1
5	Straight	None	192.95 (858)	196.09 (872)	1.57	
11	Straight	None	192.81 (858)	197.71 (879)	2.45	
6	Straight	None	191.17 (850)	195.88 (871)	2.34	
1	Draped	None	178.38 (793)	182.64 (812)	1.85	2.3
2	Draped	None	181.77 (808)	188.03 (836)	2.71	
2	Draped	None	177.55 (790)	184.93 (822)	3.20	
3	Draped	None	176.00 (783)	180.72 (804)	2.05	
3	Draped	None	167.99 (747)	175.70 (781)	3.35	
4	Draped	None	181.23 (806)	185.44 (825)	1.82	
4	Draped	None	178.95 (796)	183.42 (816)	1.92	
7	Draped	None	183.62 (817)	187.92 (836)	1.87	
8	Draped	None	179.47 (798)	185.29 (824)	2.53	
9	Draped	None	181.53 (807)	185.40 (825)	1.70	
10	Draped	None	178.77 (795)	185.17 (824)	2.78	
1	Draped	L13	180.54 (803)	188.47 (838)	3.45	1.8
3	Draped	L13	176.08 (783)	182.28 (811)	2.43	
4	Draped	L14	181.76 (808)	183.79 (817)	0.90	
7	Draped	L11	184.47 (820)	186.88 (831)	1.05	
8	Draped	L11	185.65 (826)	188.17 (837)	1.08	
9	Draped	L13	179.94 (800)	188.24 (837)	3.61	
10	Draped	L11	178.86 (795)	179.77 (800)	0.40	

Duct 3 was damaged with intrusion of epoxy past a gasket set at one of the segment joints. Friction loss across the blockage was substantial as shown in Figure 5.7.

5.3.2.2 EFFECT OF LUBRICATION. Lubricants L11, L13, and L14 were tested in the draped ducts. Normalized dead end force is plotted for the lubricated test and the previous dry test in each duct in Figure 5.8. The best lubricant was capable of increasing dead end force by 3% of the applied live end force. This corresponds to about a 15% decrease in overall friction loss. Performance of the lubricants in ducts draped at the radii of this test specimen are marginal at best. Slightly better friction reduction was obtained in the monolithic test girder (22%) with the use of a lubricant.

5.3.2.3 CALCULATING CURVATURE COEFFICIENTS. With the wobble coefficients assumed to be 5×10^{-4}/ft. (16.4×10^{-4}/m) for ducts with 0-in. (0 mm) and 1/8-in. (3.2 mm) duct offsets, and 6×10^{-4}/ft. (19.7×10^{-4}/m) with 1/4-in. (6.4 mm) offsets, curvature friction coefficients, μ, have been calculated and are shown in Table 5.5. These same wobble coefficients were also used to calculate curvature friction coefficients for the lubricated tests. For long girders where wobble loss is a considerable percentage of the total friction loss, use of a lubricant might warrant a reduction in both the curvature and wobble coefficients. Much of the wobble friction loss in a duct is attributable to side-to-side induced additional curvature, and can be reduced by a lubricant. The remaining wobble loss is generated by mechanical interlock across the segment joints and at other locations. The experiments indicated no decrease due to lubrication because of the scarring of the duct (see Figure 5.6). The magnitude of the wobble loss term in the test specimens is small compared to the curvature loss term, and therefore the wobble friction coefficient is assumed the same as measured unlubricated.

A friction coefficient of 0.16 is conservative for all first test in a duct results, except for the damaged Duct 3. This is the same magnitude of friction coefficient found in the monolithic test girder.

Given an exact plot of the elongation of a tendon along its full length and the properties of the tendon steel, friction and wobble coefficients could be chosen to generate an elongation curve fit to the exact curve using the least squares method. Elongation measurements were taken at several points along the tendon in four draped ducts and all the straight ducts to provide data to check the measured wobble coefficients.

Unfortunately, only the elongation data for Test 1 in Duct 10 was able to be modified correctly using the applicable terms, or fractions thereof, from the elongation equation. Elongation measurements needed to be taken at many load intervals, as was the movement of the ram body. Figures 5.9 through 5.12 show the adjusted measured elongations and the calculated elongation using $\mu = 0.16$ and $k = 5 \times 10^{-4}$/ft. (16.4×10^{-4}/m) or 6×10^{-4}/ft. (19.7×10^{-4}/m), depending on the duct offset. Apparent elongation associated with removing slack from the tendon was not linear along the length of the girder. Difficulties in measuring elongations in the field to match forces to even 10% accuracy are described by Freyermuth [21].

5.3.3 Indications. Table 5.5 gives test results for the draped tendons reduced to wobble and curvature friction coefficients.

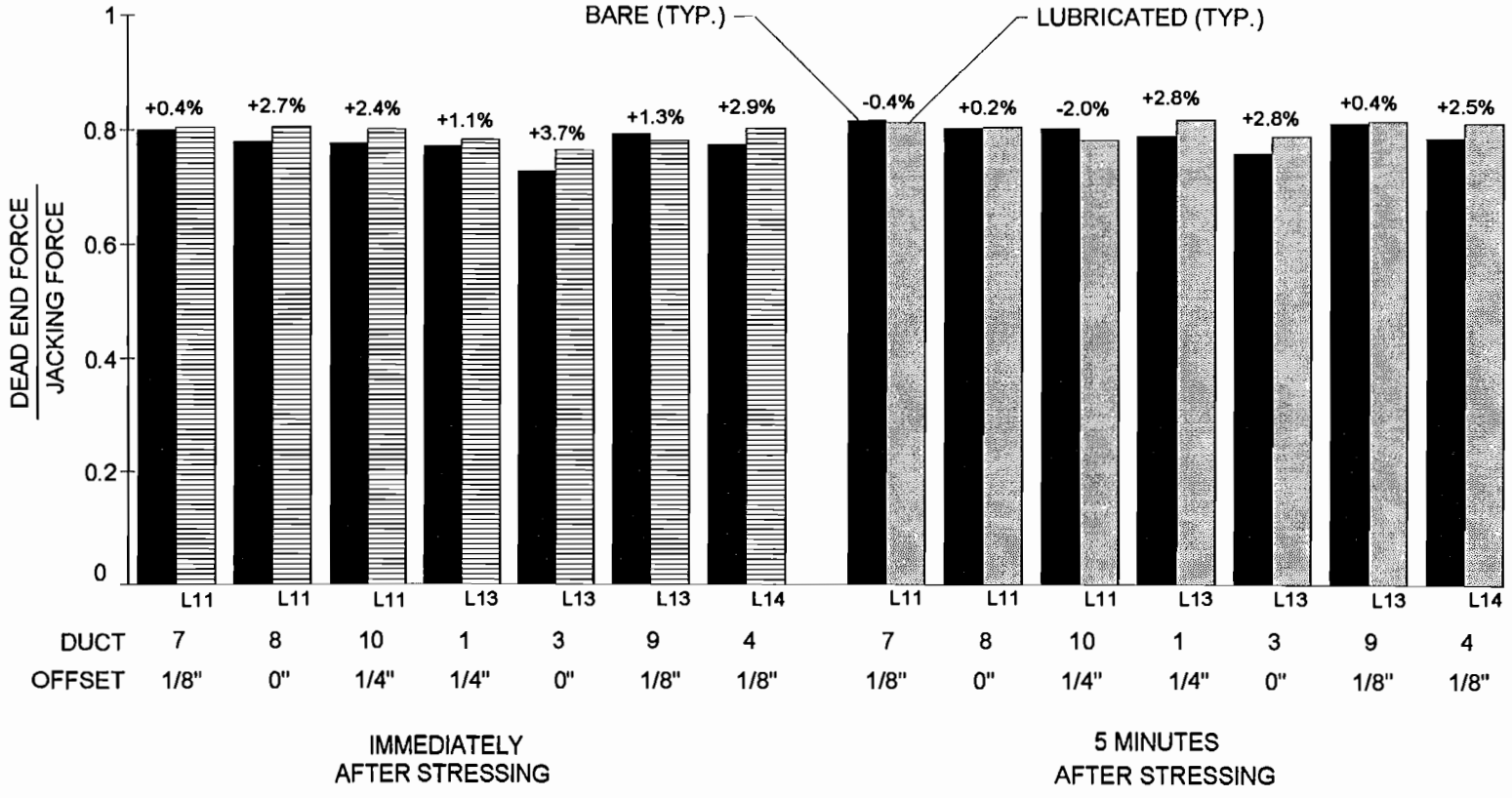

(1 inch = 25.4 mm)

Figure 5.8 Lubricated strand segmental friction test results - draped ducts

Table 5.5 Time-Dependent Increases in Dead End Force

Duct	Offset in. (mm)	Test	Lubr.	K /ft (/m)	$\mu_{initial}$	μ_{final}
1	1/4 (6.4)	1	Bare	6×10^{-4} (19.7×10^{-4})	0.160	0.142
		2	L13	6×10^{-4} (19.7×10^{-4})	0.149	0.116
2	0 (0)	1	Bare	5×10^{-4} (16.4×10^{-4})	0.153	0.127
		2	Bare	5×10^{-4} (16.4×10^{-4})	0.164	0.139
3	0 (0)	1	Bare	5×10^{-4} (16.4×10^{-4})	0.174	0.154
		2	Bare	5×10^{-4} (16.4×10^{-4})	0.210	0.177
		3	L13	5×10^{-4} (16.4×10^{-4})	0.173	0.149
4	1/8 (3.2)	1	Bare	5×10^{-4} (16.4×10^{-4})	0.154	0.137
		2	Bare	5×10^{-4} (16.4×10^{-4})	0.163	0.151
		3	L14	5×10^{-4} (16.4×10^{-4})	0.135	0.127
7	1/8 (3.2)	1	Bare	5×10^{-4} (16.4×10^{-4})	0.140	0.123
		2	L11	5×10^{-4} (16.4×10^{-4})	0.137	0.126
8	0 (0)	1	Bare	5×10^{-4} (16.4×10^{-4})	0.160	0.136
		2	L11	5×10^{-4} (16.4×10^{-4})	0.134	0.134
9	1/8 (3.2)	1	Bare	5×10^{-4} (16.4×10^{-4})	0.144	0.127
		2	L13	5×10^{-4} (16.4×10^{-4})	0.157	0.123
10	1/4 (6.4)	1	Bare	6×10^{-4} (19.7×10^{-4})	0.156	0.130
		2	L11	6×10^{-4} (19.7×10^{-4})	0.133	0.149

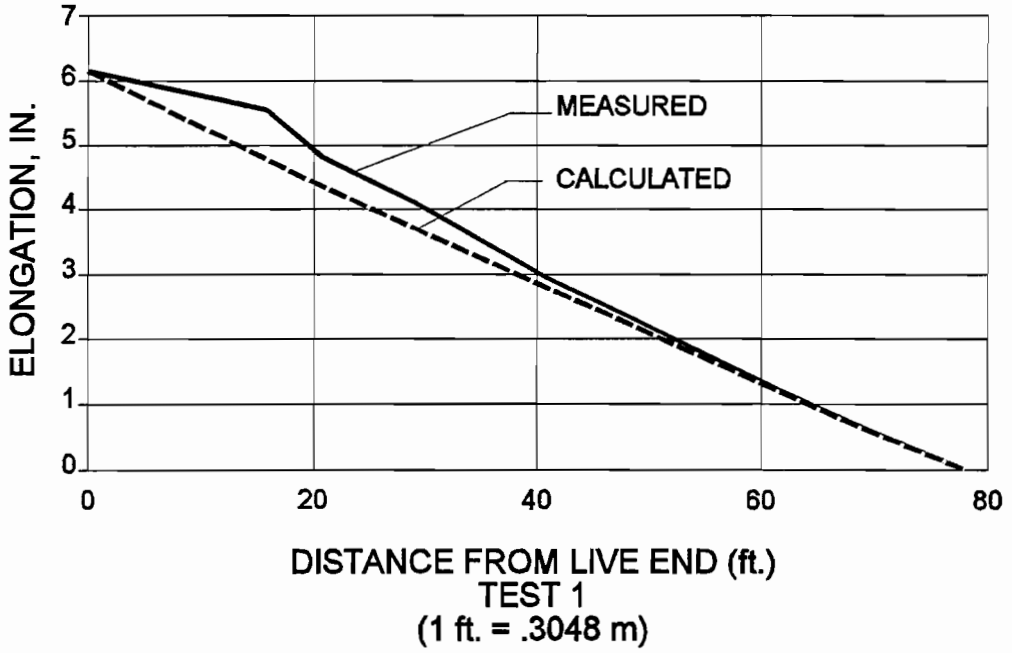

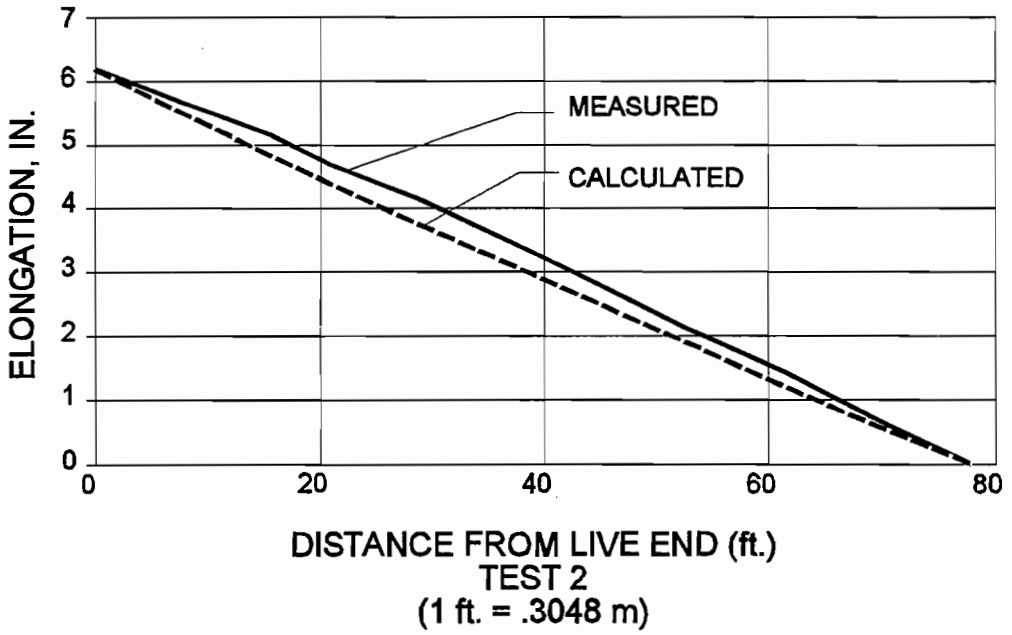

Figure 5.9 Elongation vs. Length in duct 2 - calculated vs. Measured

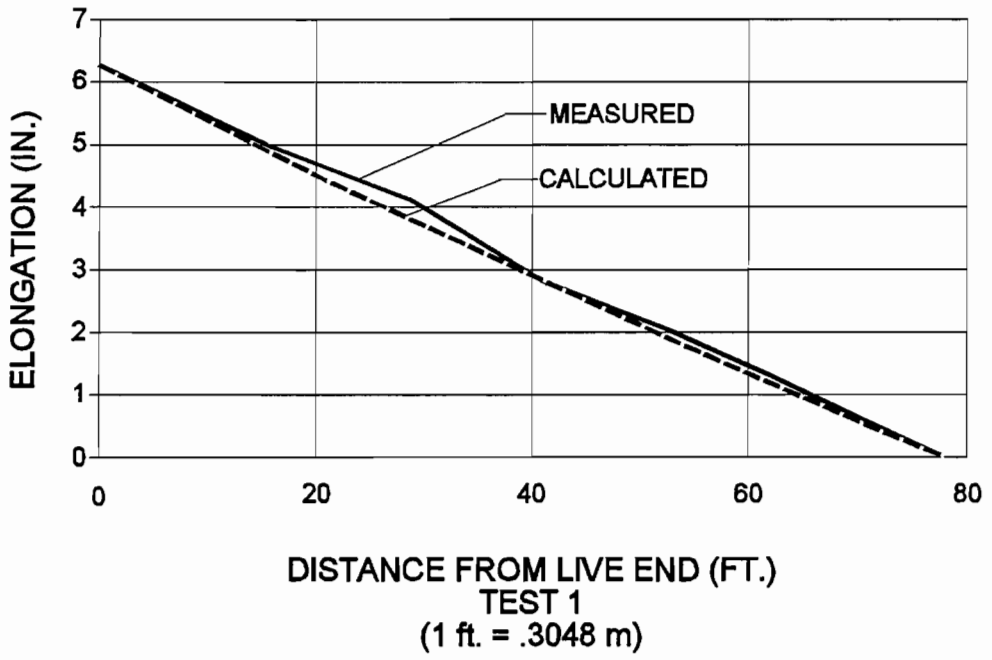

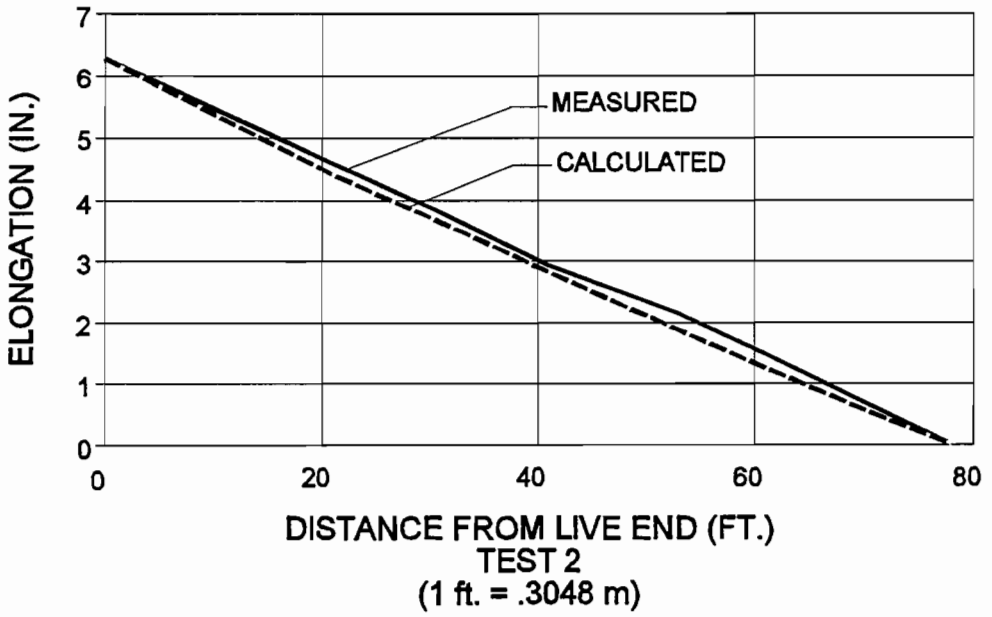

Figure 5.10 Elongation vs. length in duct 4 -- calculated vs. measured

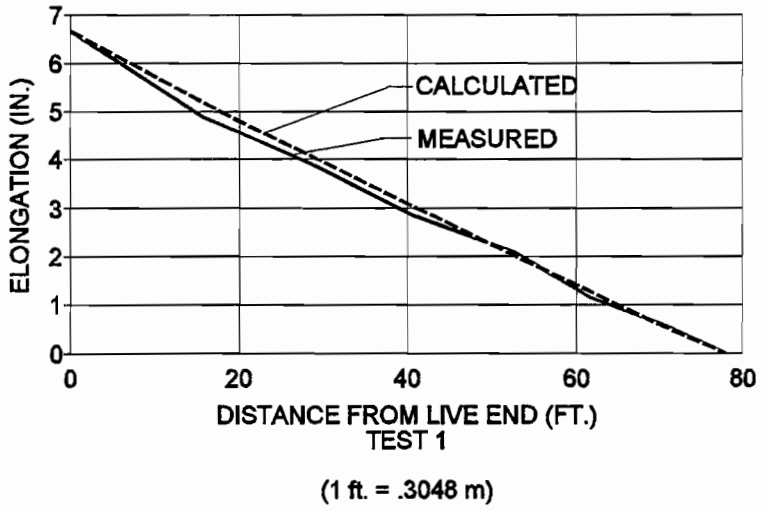

Figure 5.11 Elongation vs. length in duct 8 - calculated vs. measured

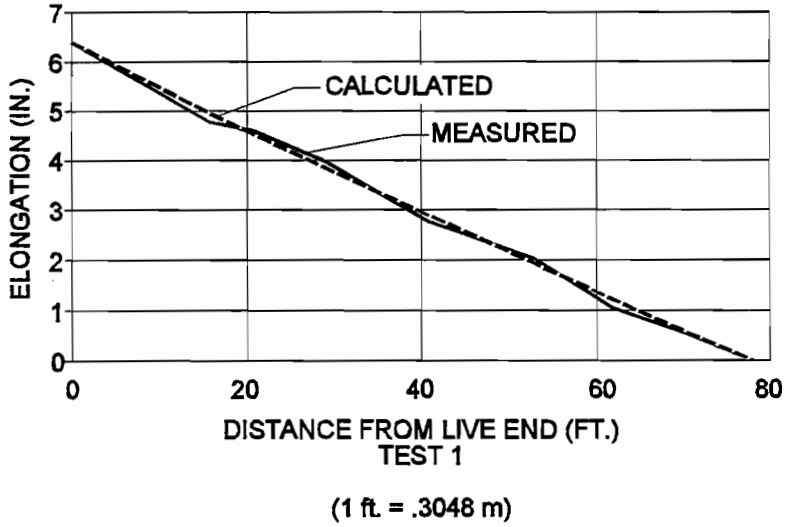

Figure 5.12 Elongation vs. length in duct 10 - calculated vs. measured

A curvature friction coefficient of μ=0.16 used with a wobble friction coefficient of K=0.0005/ft. (16.4 x 10^{-4}/m) for 0" (0 mm) and 1/8" (3.2 mm) offsets and K=0.0006/ft. (19.7 x 10^{-4}/m) for 1/4" (6.4 mm) offsets gives a conservative bound to the test results, except for the damaged duct. AASHTO [15] recommends using a wobble coefficient of 0.0002/ft. (0.00066/m) and then selecting a curvature friction coefficient. Using the AASHTO wobble value of 0.0002/ft. (0.00066/m), the test results would require that μ = 0.18, well below the recommended value of 0.25 for a seven-strand tendon in semi-rigid steel duct.

5.4 Design Examples Using Code Recommended Coefficients and Test Result Coefficients.

To show how the results of the test program compare to current code recommended practice, design examples with varying parameters have been calculated. The first example is the segmental test specimen itself. The other examples are moderately long segmental box girders with varying curvature to length ratios. These examples have potential for great friction loss and will show differences between loss calculations using different coefficients quite well.

The coefficients selected are middle of the range values from each of the codes. The coefficients used are as follows:

UT	μ = 0.16	K = 0.0005/ft.	(0.00164/m)
ACI-ASCE	μ = 0.25	K = 0.0015/ft.	(0.0049/m)
ACI-318-89	μ = 0.20	K = 0.00125/ft.	(0.0041/m)
PTI	μ = 0.18	K = 0.0005/ft.	(0.00164/m)
AASHTO	μ = 0.25	K = 0.0002/ft.	(0.00066/m)
Caltrans	μ = 0.20	K = 0	

UT coefficients are based on test results in the segmental test girder. The code coefficients are not specifically intended for the design of segmental girders.

5.4.1 Design Example 1 - Segmental Test Specimen. The segmental test specimen has a relatively high curvature to length ratio. The tendon was a 7-1/2-in. (12.7 mm) ϕ strand tendon in galvanized semi-rigid duct. The radii of curvature are smaller than those usually seen in a bridge girder. The segmental test specimen is shown in Figure 5.13 and friction loss is plotted in Figure 5.14.

The plot using UT coefficients shows the entire range of friction losses measured in the segmental test specimen. As expected, the coefficients derived from this study give excellent prediction. Plots using the PTI and Caltrans coefficients compare well to the plot of the test results. All other recommended combinations of coefficients plotted in Figure 5.14 are too conservative, including the AASHTO recommended coefficients.

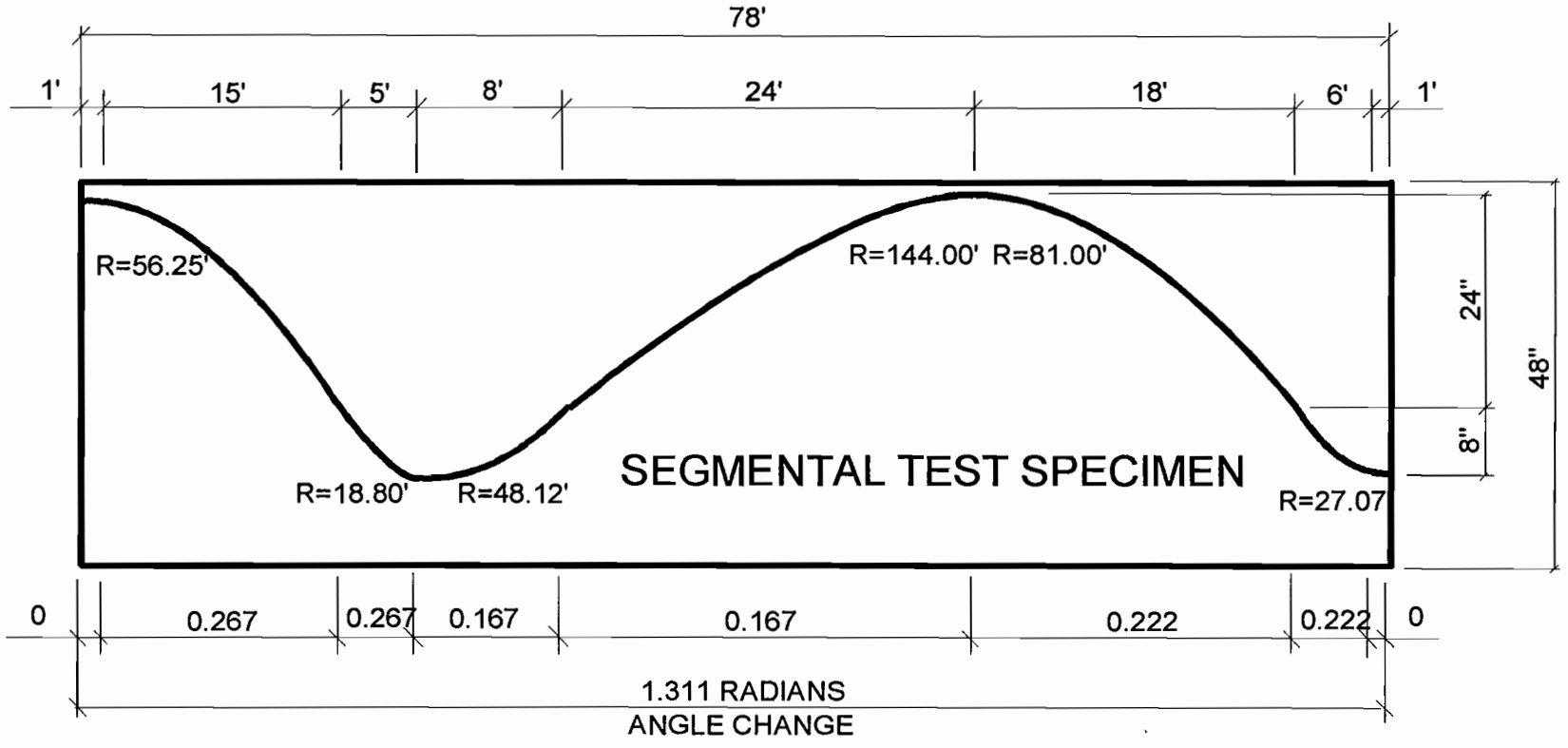

(1 ft. = .3048 m)

Figure 5.13 Design Example 1 - Elevation

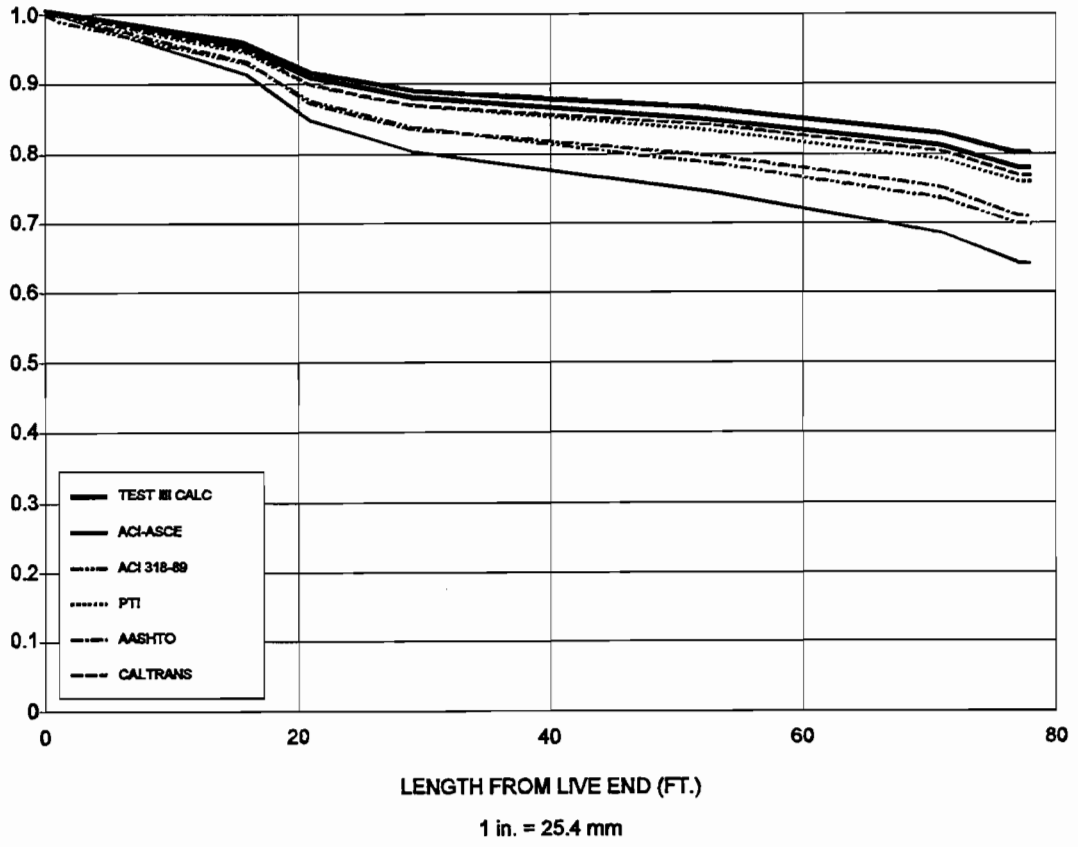

Figure 5.14 Design Example 1 - P_D / P_J vs. Length

5.4.2 Design Example 2 - Normal Curvature to Length Ratio. This example uses a segmental box girder with a normal span to depth ratio for an internally post-tensioned highway bridge girder. The tendon is assumed to be a 12-1/2-in. (12.7 mm) ϕ strand tendon in galvanized semi-rigid duct. Span to depth ratio of the girder is 22.5:1. The parabolic tendon profile is calculated to fit the girder. The girder is shown in Figure 5.15 and friction loss is plotted in Figure 5.16.

The percentage of total friction loss due to wobble friction in Example 2 is nearly 50%, as predicted by UT recommended coefficients. The Caltrans coefficient, with no wobble term, gives a friction loss prediction that is far less conservative than predicted by AASHTO, PTI, or UT-Davis coefficients.

5.4.3 Design Example 3 - High Curvature to Length Ratio. Example 3 is typical of a railroad segmental box girder or an incrementally launched girder. Span to depth ratio is 15:1 with the corresponding tendon profile. The tendon is assumed to be a 12-1/2-in. (12.7 mm) ϕ strand tendon in galvanized semi-rigid duct. The girder is shown in Figure 5.17 and friction loss is plotted in Figure 5.18.

The higher total curvature change to length ratio of Example 3 makes the friction losses predicted by the Caltrans and AASHTO coefficients more conservative than in Example 2. UT and PTI plots compare favorably.

5.4.4 Design Example 4 - Low Curvature to Length Ratio. This example represents a shallow segmental box girder used where clearance is a problem. The tendon profile is also similar to that of a continuous tendon in a haunched box girder. Span-to-depth ratio is 30:1. The tendon consists of 12-1/2-in. (12.7 mm) ϕ strands in galvanized semi-rigid duct. The girder is shown in Figure 5.19 and friction loss is plotted in Figure 5.20.

The girder chosen for Example 4 is more sensitive to the wobble coefficient than Example 2 girder. Friction loss predicted by the Caltrans coefficient is too unconservative. UT and PTI plots continue to compare well. The AASHTO plot gives a less conservative prediction of friction loss than in Example 2 or 3.

From the plots it can be seen that the recommended coefficients from ACI 318-89 and ACI-ASCE are probably too conservative for bridge construction. Caltrans coefficients apply to rigid conduit, and therefore unconservatively predict wobble loss in semi-rigid ducts. For the length of girder chosen in Examples 2, 3, and 4, the PTI and AASHTO coefficients compare well to the calculated losses based on the wobble and friction coefficients derived in this study from the measured test results. These design examples are discussed further in Section 6.1.3.1.

5.5 Other Factors

Many other variables were found to influence friction loss in the test specimen beyond the variables originally designed into the specimen. These factors may or may not be influential in a particular girder, but should be noted when trying to overcome consistently high friction losses.

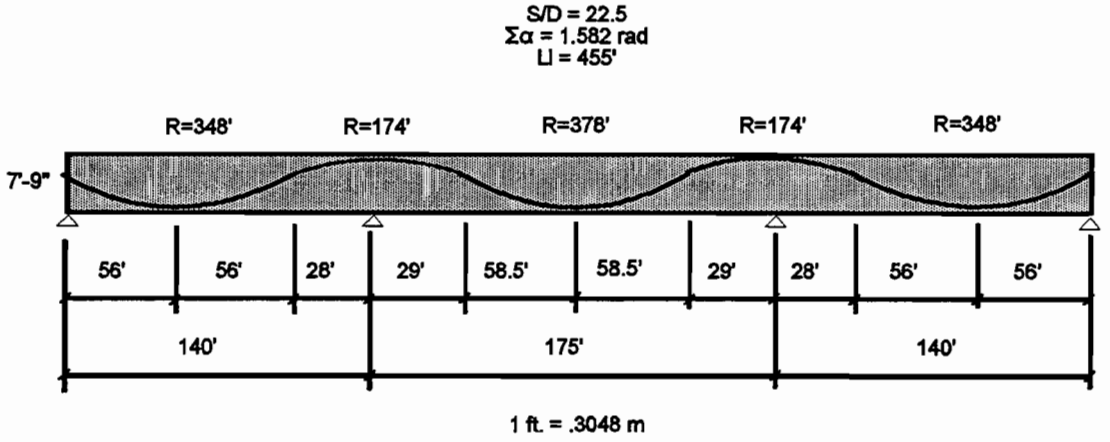

Figure 5.15 Design Example - Elevation

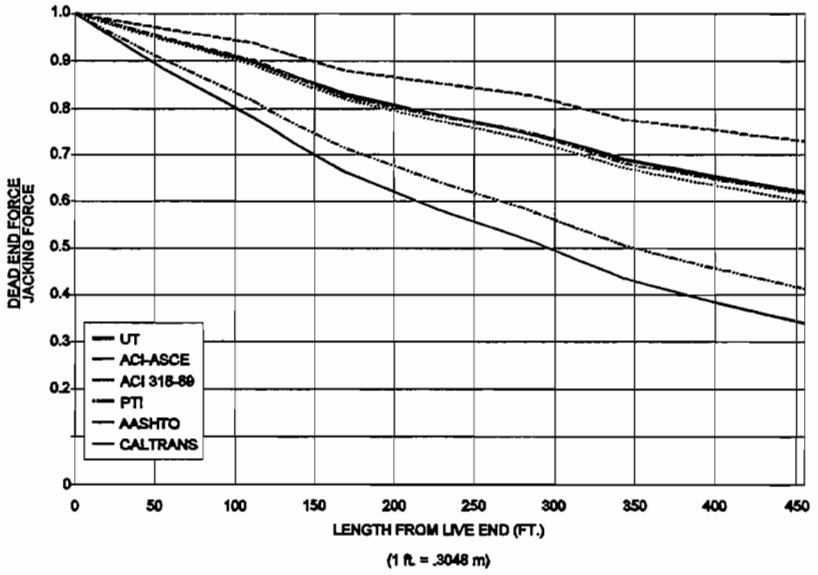

Figure 5.16 Design Example 2 - P_D / P_J vs. Length

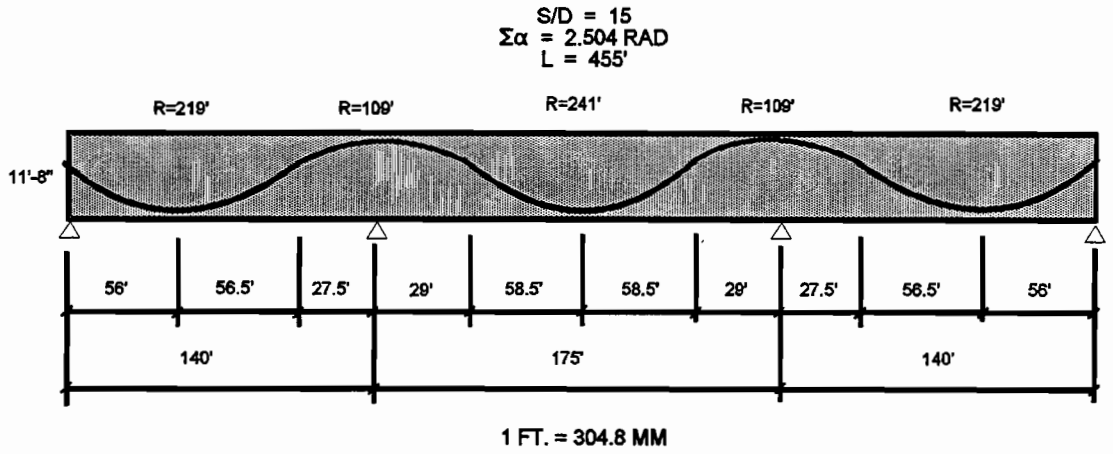

Figure 5.17 Design Example 3 - Elevation

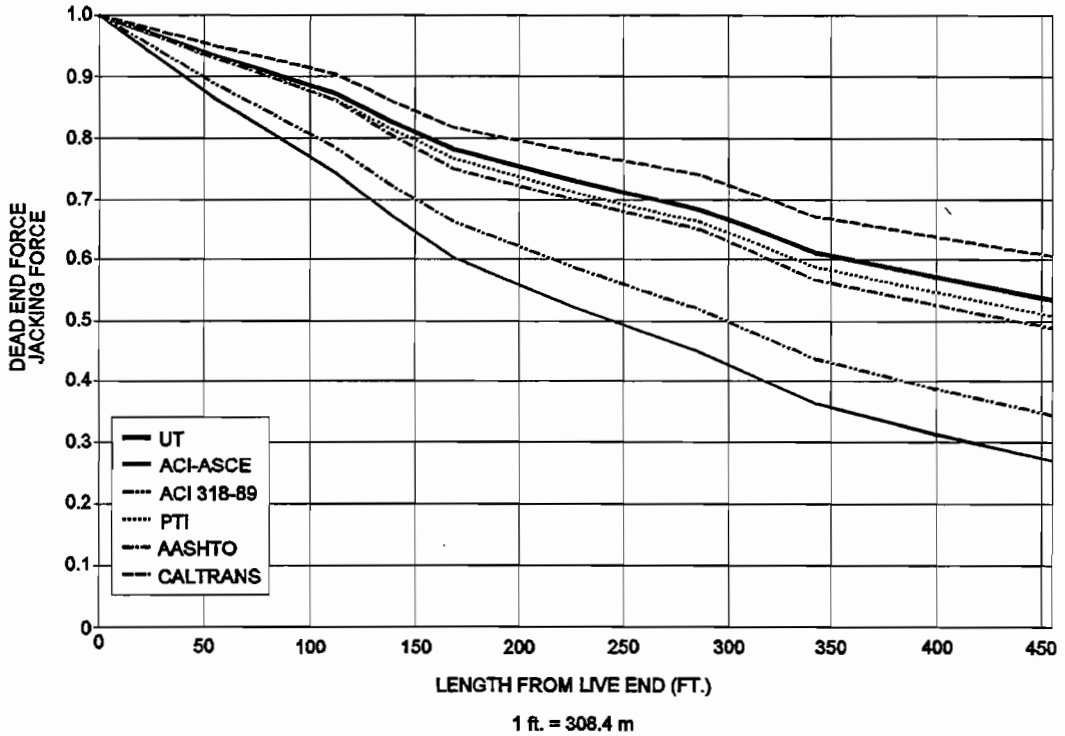

Figure 5.18 Design Example 3 - P_D / P_J vs. Length

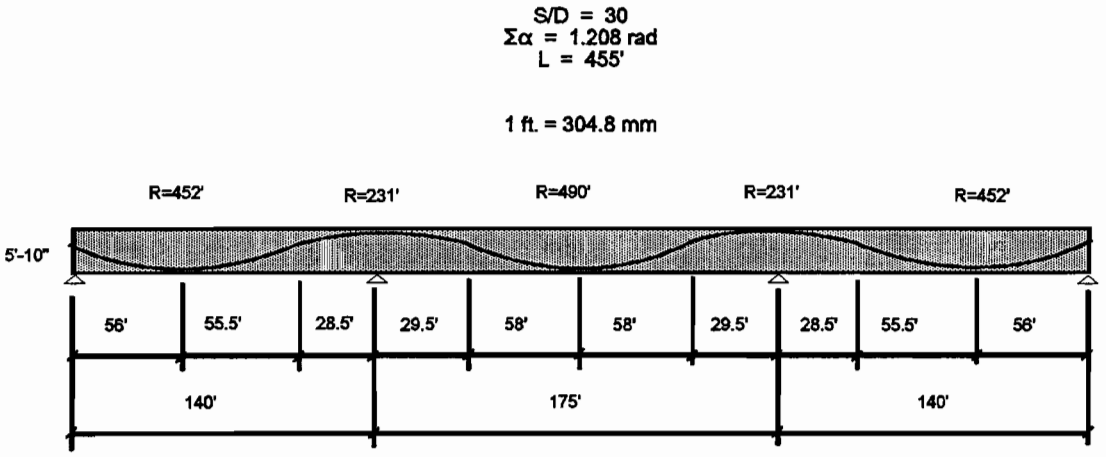

Figure 5.19 Design Example 4 - Elevation

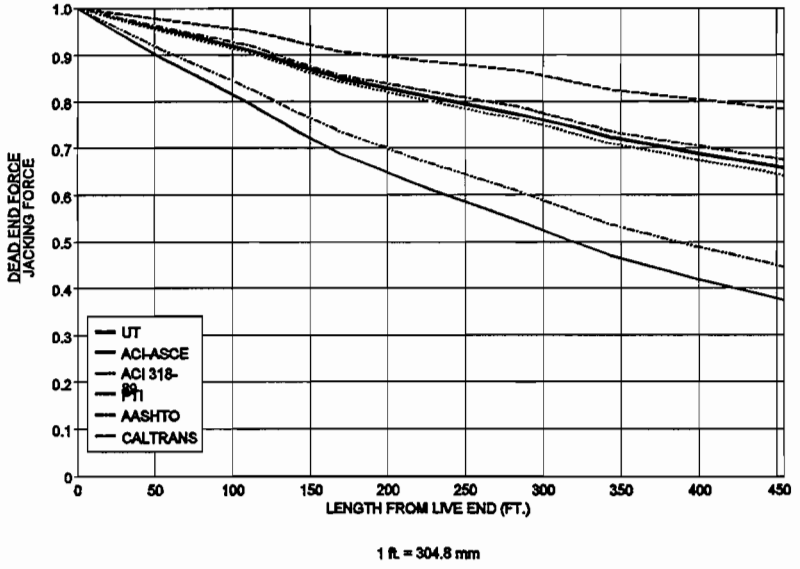

Figure 5.20 Design Example 4 - P_D / P_J vs. Length

5.5.1 Time-Dependent Increase in Dead End Force. The tendon in the segmental girder continued to move in the test specimen after final jacking force was reached. Force continued to increase on the dead end over a period of about five minutes. Force continued to increase at the dead end even if some of the load was taken off the ram at the live end, similar to an anchor set. The increase in force is tabulated in Table 5.4.

It might be expected that girders with lower curvature to length ratios or low friction losses in general might see less tendon creep. To characterize friction loss of a tendon during a field test, time should be allowed for static equilibrium to be reached along the entire length of the tendon.

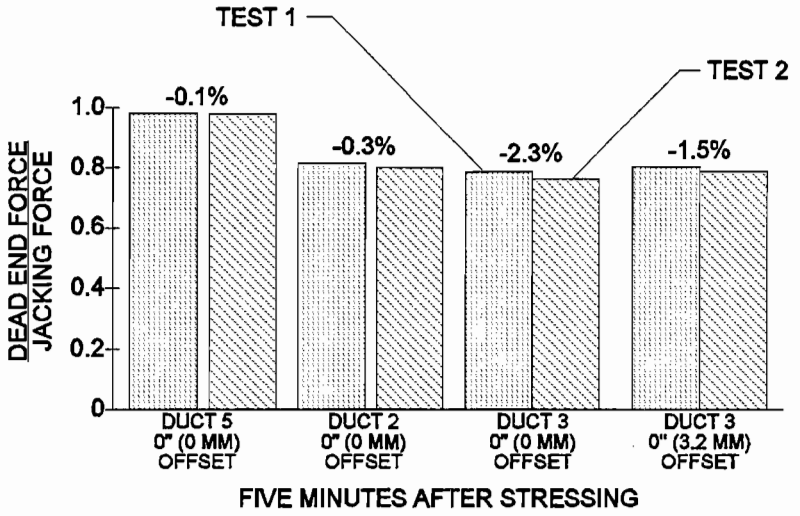

Figure 5.21 P_D / P_J vs Duct. Effect of repeated stressing

5.5.2 Repeated Stressing. As seen in the small-scale friction test specimens, repeated stressing results in an increase in friction loss. The effect of repeated stressing in ducts of the large scale segmental friction specimen is shown in Figure 5.21. Similar behavior was observed by Tran [10] in the large-scale monolithic friction specimen. A tendon should be lubricated before the first stressing if high friction loss is anticipated.

5.5.3 Friction Loss at the Anchorages. Friction loss in the anchorage zone at the live end may consume several percent of the total prestress force. Flaring of the strands to fit the anchor head induces a curvature change over a short distance that is substantial. Care should be taken to ensure anchorages are installed parallel and concentric to ducts. Figure 5.22 shows the discontinuity at an anchorage. Figure 5.23 depicts the angle change perceived by an individual strand as it is deflected through the anchor to meet the anchor head. Measurements taken by Roberts [4] during construction of the San Antonio Y project revealed live end anchorage zone losses of 2% to 3% of the total jacking force.

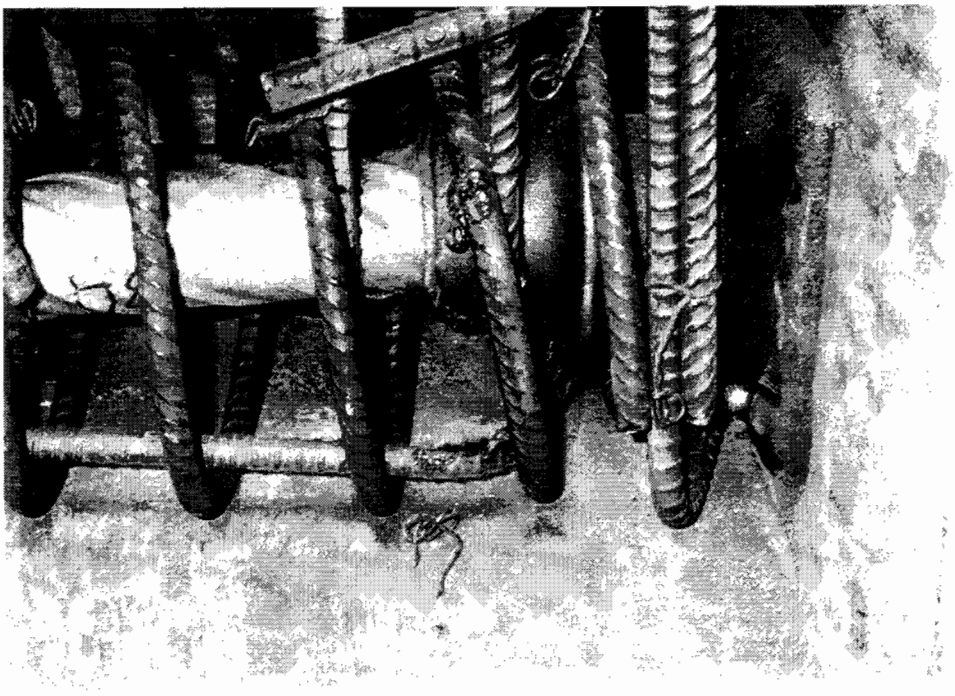

Figure 5.22 Duct at anchorage

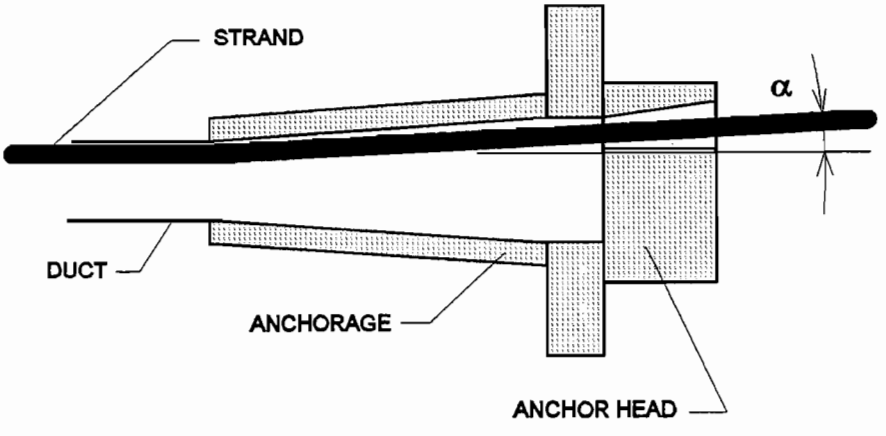

Figure 5.23 Tendon flare at anchorage

5.5.4 Lubricant Application Method. Lubricants were applied by several methods to the tendons tested in the segmental specimen. Strands were sprayed with lubricant one at a time and as a seven-strand group, while being pushed into the duct. The low point in one duct was filled with lubricant, causing that tendon to be completely immersed. Tendons were also run through a pan of lubricant as they were pushed into the specimen. Complete strand coverage was achieved in every case. No noticeable difference in friction reduction could be attributed to the varying methods of application.

5.5.5. Strand Installation Method. Strands were pulled through as a complete tendon, and pushed through the duct one at a time and several strands at a time. Tendons could be inspected through the elongation measurement blockouts. Strands lay parallel in the duct for every test regardless of installation method. Tangled multi-strand tendons are known to increase friction loss.

5.5.6 Strand Coatings. A thin gray film was present on the strand tested in the segmental friction test specimen. This film was a residual from the wire rolling process. Based on observations from preliminary friction tests where strand with no residual was tested, friction loss decreased with the gray coating.

5.5.7 Duct Type and Coatings. Galvanization on steel duct surfaces has been found in some cases to reduce friction. Repeated stressing in a duct removes the galvanizing and deepens scars in the duct surfaces which increases friction loss. Bezouska [22] found no decrease in friction with galvanized duct.

Polyethylene duct has a substantially lower coefficient of friction with strand tendons than does steel duct. Polyethylene duct is also considerably more expensive than steel duct. Tendon profiles with potential for high friction losses may warrant recommending polyethylene duct, based on friction coefficients recommended by the post-tensioning hardware supplier.

5.5.8 Damaged Ducts. One duct in each of the large scale friction specimens, monolithic and segmental, were damaged during construction. In the monolithic specimen, paste intruded into a duct apparently at a leaky seam. In the segmental specimen epoxy squeezed through one of the gasket assemblies at a segment joint during temporary stressing. In both cases, friction losses were substantially higher in these ducts than in the undamaged ducts.

5.5.9 Number of Strands. In general, friction loss tends to decrease as the number of strands in a tendon increases. One factor contributing to this trend is duct placement accuracy. Larger ducts generally lie on larger profiles with angle changes occurring over much larger lengths. Minor duct misalignment along the duct will have less influence on wobble friction losses than for smaller ducts. Also larger duct is stiffer and will hold its shape better than smaller diameter duct during concrete placement. AASHTO [15] recommends decreasing the curvature coefficient for semi-rigid steel duct after tendon size exceeds 12 strands.

5.5.10 Cleaned and Treated Ducts. Tests in ducts in the monolithic specimen (10) that had been apparently flushed clean of lubricant gave friction losses similar to those from the fully lubricated duct

tests. The decrease in friction was even greater in some cases than with the lubricated tendon and duct. These results were confirmed by the small-scale friction test .

During construction of the large-scale segmental friction test specimen, a substantial amount of dirt, grit and metal particles from the cold forming process was found on the inner duct surfaces. Removal of this material by flushing no doubt led to a substantial friction loss reduction during stressing. Also, the water soluble lubricants did not emulsify easily, and a lubricating film most likely remained on the duct surfaces.

CHAPTER SIX
RECOMMENDATIONS FOR DESIGN AND CONSTRUCTION

6.1 Friction Coefficients for Internal Tendons

Based on the test results from the large-scale monolithic and segmental friction test specimens as well as a review of other tests and field data, realistic friction coefficients have been selected. These coefficients are for seven-wire strand tendons in galvanized semi-rigid steel duct, and may vary with construction method, minimum radius of duct curvature, number of strands, and other factors.

6.1.1 Monolithic vs. Segmental Construction. A primary variable studied in this program was construction method. Friction loss was expected to increase when the segmental construction method for concrete box girders was used. The identical duct curvature in both the monolithic test specimen and the segmental test specimen allowed for a direct comparison of friction losses in each. Results showed a 25% increase in wobble friction loss in the segmental specimen, while curvature friction remained the same. Duct mismatch at the segment joints, although within tolerance, and the difficulty of accurately placing and securing short pieces of duct were to blame for the increase in wobble friction. Wobble loss seen in both specimens was at least twice as high as the wobble loss predicted using the AASHTO [15] recommended wobble coefficient.

6.1.2 Recommended Coefficients for Design. Friction coefficients have been found to increase with increasing normal force between tendon and duct, or with decreasing duct curvature. External tendons undergo large angle changes as they pass through deviators. Field experience has shown that the curvature friction coefficient with no assumed wobble generally never falls below 0.25 for external tendons. The small-scale friction tests, described in Chapter 2, also produced friction coefficients of 0.25 or greater, with no wobble loss. The normal force used in the small-scale friction test is typical of that produced by a tendon on a duct with a 30-ft (9 m) radius of curvature or smaller. Substantial duct scarring was noticed on the small-scale friction test specimens. This may be the cause for the increase in friction coefficient over those found in tendons with lower duct to tendon normal forces.

Draped ducts have constantly changing radii of curvature. Normal forces capable of duct scarring, producing an increase in friction coefficient, may exist only on short lengths along the duct. For this reason, the curvature friction coefficient selected for a draped duct must be an average. Both the monolithic and segmental large-scale friction test specimens from this study gave conservative curvature friction coefficients of 0.16, when wobble coefficients of 0.0004/ft. (0.0013/m) and 0.0005/ft. (0.0016/m) were assumed, respectively. The radius of curvature in these specimens was greater than 100 ft. (30 m) for over 70% of the length of the draped duct, with an absolute minimum radius of curvature of 19 ft. (5.8 m) at one location. These friction coefficients compared well with those found in other tests and in the field for tendons draped with a minimum radius of curvature greater than 100 ft. (30m). Figure 6.1 shows the relationship between friction coefficient and minimum radius of duct curvature for several laboratory and field tendons. A wobble coefficient of 0.0004/ft. (0.0013/m) was assumed for monolithic girders and 0.0005/ft. (0.0016/m) for segmental girders.

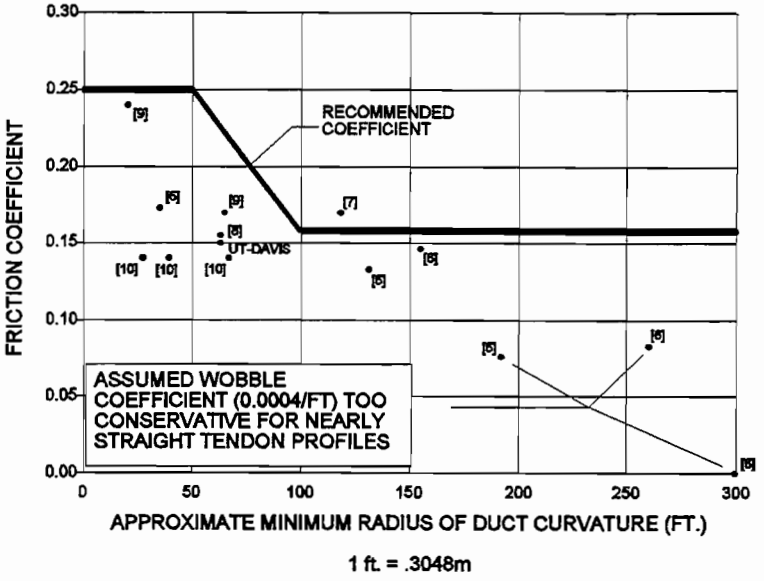

Figure 6.1 Minimum Radius of Duct Curvature vs. Curvature Coefficient

Tendons used in other tests or in the field with minimum radii of curvature less than 50 ft. (15 m) almost always gave a curvature friction coefficient approaching 0.25, when used with a wobble friction coefficient of 0.0004/ft. (0.0013/m) or greater.

Frequently ducts are chorded in segments to follow the horizontal curvature in that segment, particularly for bottom slab tendons. This forces the angle change to occur abruptly at the segment joint, even for large horizontal curvatures. Also, vertical curvature change in web ducts is frequently taken up within a single segment. This creates an internal tendon that behaves more like an external tendon for friction loss calculations. For both these cases, a curvature coefficient of 0.25 is a conservative choice when used with an appropriate wobble coefficient.

6.1.3 Comparison to Current Guide Specifications. Friction coefficients recommended by current guide specifications for strand tendons in galvanized semi-rigid duct, do not change with radius of duct curvature. Coefficients most commonly used by bridge designers come from the AASHTO Standard Specifications for Highway Bridges [15]. An allowance is made for decreasing the curvature coefficient from 0.25 to 0.15 as tendon size increases beyond 12 strands. The wobble coefficient stays fixed at 0.0002/ft. (0.00066/m). This wobble coefficient is suitable for calculating wobble friction losses in the rigid duct used by California contractors in monolithic box girder construction. A higher wobble loss coefficient should be used for semi-rigid steel duct in monolithic construction (0.0004/ft.) (0.0013/m), and increased further for segmental construction (0.0005/ft.) (0.0016/m). The wobble loss coefficient can be checked in the field with an in-place friction test. Tendon forces or size can be adjusted accordingly for the remainder of the project. Current practice is to change the assumed curvature friction coefficient, even though the same materials are

used bridge-to-bridge and contractor-to-contractor. Curvature coefficient should only change with normal force, addition of lubrication, and some other minor influencing factors, such as number of strands.

6.1.3.1 DESIGN EXAMPLES. Figures 5.13 through 5.20 show a direct comparison of friction loss calculations, using coefficients from several sources, for four design cases. Friction coefficients used are summarized in Section 5.4. The ACI-318-89 [13] and ACI-ASCE [6] coefficients give friction losses that are far more conservative than predicted using coefficients from other sources. These coefficients [13, 6] were intended more for building construction where tendons are generally smaller and more numerous, and wobble losses are higher. Caltran's coefficient, $\mu = 0.20$ was chosen based on their experience with friction losses in rigid duct used in monolithic girders. Using $\mu = 0.20$ with no wobble loss term may prove too unconservative for segmental construction with semi-rigid duct. The coefficients recommended by this study, AASHTO [15], and PTI [14] compared well in Examples 2, 3, 4. AASHTO's unconservative wobble coefficient and over-conservative curvature coefficient tended to balance out for the three lengthy girders in these examples. The AASHTO coefficients tended to penalize curvature too much in Example 1 (see Figure 5.14).

6.1.3.2 FIELD DATA. AASHTO [15] recommends using a wobble coefficient of 0.0002/ft. (0.0066/m) for seven-wire strand tendons in galvanized semi-rigid duct. The prestressing contractor generally holds the wobble coefficient constant at this value, and calculates the curvature coefficient based on the results of in-place friction tests. The curvature coefficient is also the apparent coefficient of friction between tendon and duct in a system with no wobble (see Section 1.2.2), and should be consistent bridge-to-bridge for duct profiles with similar radii of curvature. Curvature coefficients calculated with the wobble term held constant are sensitive to girder length and do not accurately reflect the true coefficient of friction.

For example, in field tests by Dywidag [9] in 560-ft. (171 m) galvanized semi-rigid four-inch (100 mm) ducts with total angle change of about 1.6 radians, and 29- or 31-strand tendons, curvature friction losses were calculated and measured using an assumed wobble coefficient of 0.0002/ft. (0.00066/m). The average curvature friction factor found for four unlubricated ducts was 0.241, based on the dead end forces found by lift-off tests. The average curvature coefficient found by calculation using elongation measurements was 0.289. Even though estimated elongations could have easily be in error by seven percent (see Freyermuth [21]), these coefficients both approached or exceeded the coefficient of friction found between strand and duct at very small curvatures.

Using the wobble coefficient recommended by Tran [10] for monolithic construction (K = 0.0004/ft. (0.0013/m)), the curvature coefficients in the Dywidag tests became 0.169 based on the lift-off tests, and 0.217 based on elongation measurements. $\mu = 0.169$ would be a good estimate of the friction coefficient for the large radius duct profiles used in the Dywidag tests. The AASHTO recommended wobble coefficient of 0.0002/ft. (0.00066/m) was too unconservative for this case. The wobble coefficient should have been assumed higher, and then checked by the in-place friction tests, holding the curvature coefficient constant.

6.2 Use of Lubricants

Lubricants have been occasionally used in post-tensioning ducts to decrease friction loss, provide corrosion protection, or both. The lubricants tested in this study, shown in Table 2.1, varied greatly in their ability to reduce friction, prevent corrosion, and also in their ability to be flushed from the duct and tendon surfaces.

6.2.1 Friction Reduction Capability. Tests by Bezouska [7] and Dywidag [9] using tendons lubricated with water-soluble oils and soap gave reductions in overall friction loss greater than 30% of the bare strand duct losses. This was somewhat higher than even the best lubricants in the monolithic girder in this study, shown in Figure 5.4, which gave overall reductions in friction loss measured at the dead end of 22%. Results of tests from this phase in the segmental test specimen, shown in Figure 5.8, gave reductions in friction loss no greater than 15% for the best lubricant tested versus the bare tendon friction loss. Apparently the smaller radii of curvature found in the segmental and monolithic friction test specimens made the lubricant less effective than when used in the large radius ducts by Dywidag [9]. Dywidag tested lubricants L2 and L13 (see Table 2.1).

Ducts tested by Tran [10] that had been previously lubricated then flushed with generous amounts of water, showed reductions in friction loss over bare duct similar to the reduction seen in the fully lubricated duct and tendon tests (see Figure 5.4). Tests using small-scale friction test specimens gave similar reductions in friction when lubricated then flushed (see Figure 2.7). A pre-lubricated duct may eliminate the need for contaminating the tendon with oil or other lubricant, unless corrosion protection is required.

6.2.2 Change in Friction Coefficients. The performance of most lubricants tested in this study was marginal at best. When lubricants L5, L11, L13 or L14 are used, overall friction could be expected to decrease by 20% in large radius ducts (greater than 100 ft. (30 m) minimum radius). Lubricants applied in ducts with smaller minimum radii of curvature may be less effective. Wobble friction and curvature friction can be assumed to be reduced proportionately when lubricants are used.

6.2.3 Other Effects. Lubricants are often used for corrosion protection, or sometimes have anti-corrosion agents added to them. These lubricants, whether used for friction reduction or corrosion protection, may have an extremely adverse effect on strand to grout bond. This is especially important in girders designed to have bonded tendons at ultimate strength. Tests by Kittleman [17] reveal the effectiveness of the lubricants in this study for preventing corrosion, as well as the ability of each lubricant to be flushed clean of the tendon.

6.2.3.1 CORROSION PROTECTION CAPABILITY. Corrosion tests by Kittleman [16] were designed to simulate two accelerated corrosive environments that tendons may experience. These tests were performed using the apparatus shown in Figure 6.2. The two corrosive environments were deionized water and NaCl solution. The results of these tests for lubricants L1 through L11 are shown in Figures 6.3 and 6.4. Voltage charges between the test wire and the reference electrode gave an indication of the corrosion that was taking place on the test wire. Test wires were immersed in the lubricants, installed in the apparatus, and tested for three days.

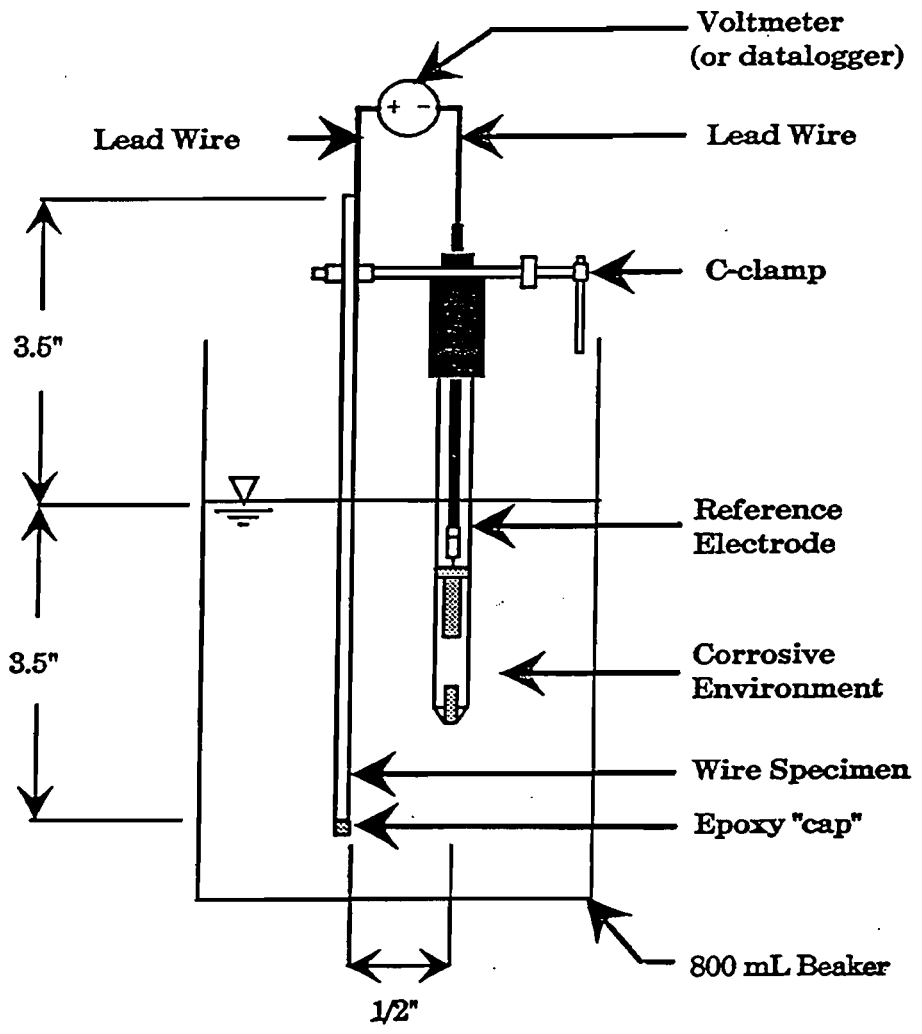

(1 inch = 25.4 mm)

Figure 6.2 Corrosion test apparatus [16].

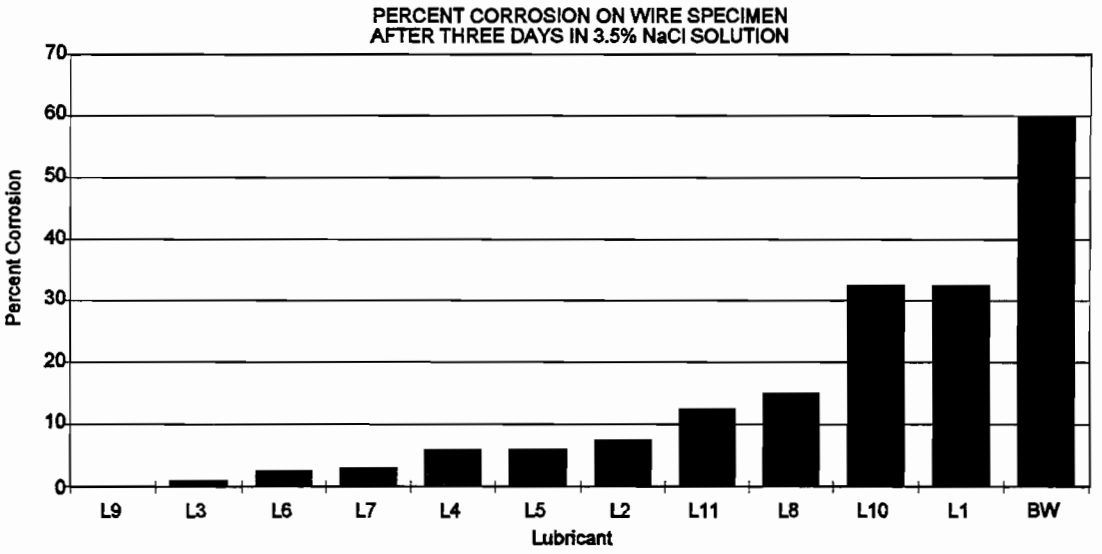

Figure 6.3 Percent corrosion after three days in 3.5% nacl solution [16]

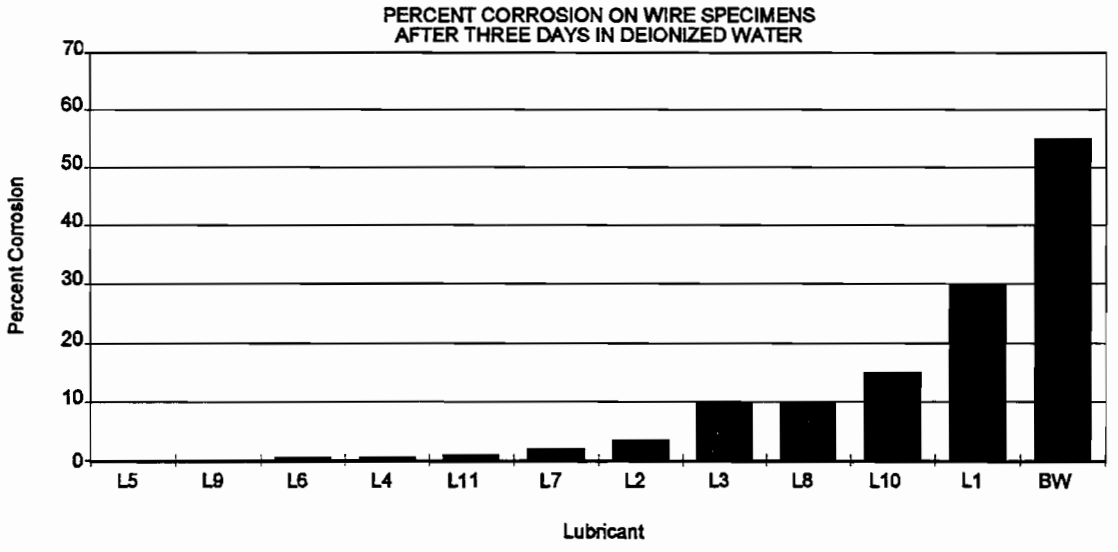

Figure 6.4 Percent corrosion after three days in deionized water [16]

Kittleman also performed tests in ambient conditions. Single wires as well as entire strands were immersed in oil, then subjected to a daily wetting/drying cycle for 46 days. Refer to Kittleman's thesis [16 for a complete description of all corrosion tests. Lubricants L13 and L14 were not expected to provide any corrosion protection, and were not tested.

6.2.3.2 STRAND TO GROUT ADHESION. Extensive pullout tests, described in Chapter 2, were performed by Kittleman [16], Tran [10] and Davis [18] to evaluate each lubricant's impact on strand to grout adhesion or bond. Even after thorough flushing with water, only two lubricants, L13 and L14, and one corrosion inhibitor, L10, did not significantly effect strand to grout bond. All the water soluble oils, synthetic or natural, should be assumed to destroy bond for consideration in designs.

6.3 Duct Placement Tolerance.

The impact of the current AASHTO [19] segmental girder duct placement tolerance of 1/8-in. (3.2 mm) at segment joints on friction loss was studied. The monolithic friction test specimen had draped tendon profiles exactly like those in the segmental test specimen. The monolithic specimen wobble loss results did not include any loss associated with duct mis-match, and could be directly compared to those ducts tested in the segmental specimen with intentional offsets of 0-in. (0 mm), 1/8-in. (3.2 mm) and 1/4-in. (6.4 mm) at the segment joints (see Figure 3.6).

6.3.1 Friction Increase with Duct Offset. The wobble friction coefficient for monolithic girder found by Tran [10] was 0.0004/ft. (0.0013/m). The wobble loss coefficient found by Davis [18] in the segmental friction test specimen in ducts with 0-in. offsets at segment joints was 0.0005/ft. (0.0016/m). The increase of 0.0001/ft. (0.0003/m) was due to construction method alone. Ducts in the segmental specimen were more difficult to place accurately and secure because of their short length.

Wobble friction coefficients for ducts in the segmental specimen set at 1/8 in. (3.2 mm) offset, the current tolerance, were also 0.0005/ft. (0.0016/m). The 1/4-in. (6.4 mm) offset ducts gave a wobble loss of 0.0006/ft. (0.0020/m) or higher.

6.3.2 Recommendations for Construction. Wobble friction coefficients found in both the monolithic girder and in the segmental girder were significantly higher than that recommended by AASHTO [15]. The difference in wobble loss between the two girders was small (0.0001/ft.) (0.0003/m) for ducts constructed within tolerance in the segmental specimen. The current AASHTO [19] tolerance for duct placement at the segment joints of 1/8-in. (3.2 mm) is adequate. Friction losses significantly increased when ducts were constructed at a 1/4-in. (6.4 mm) intentional offset in the segmental girder.

6.4 Suggested AASHTO Changes

Analysis of experimental data, field data, and the results from this research project indicates the need for several modifications to the current AASHTO Guide Specifications [15, 19]. The current duct placement tolerance at segment joints of 1/8-inch (3.2 mm) is adequate for all sizes of galvanized semi-rigid duct.

6.4.1 Friction Coefficients. The AASHTO [15] recommended wobble friction coefficient of 0.0002/ft. (0.00066/m) for galvanized semi-rigid duct is too low. A wobble coefficient of 0.0004/ft. (0.0013/m) is recommended for monolithic construction by Tran [10], and a coefficient of 0.0005/ft. (0.0016/m) is recommended for segmental construction using segments 8-ft. (2.4 m) long or longer by Davis [18].

Curvature friction coefficients for galvanized semi-rigid duct with strand tendons change with increasing normal force, or decreasing radius of curvature. Since larger tendons are mostly used with larger radius tendon profiles, the effect of number of strands per tendon is viewed secondary to minimum radius of duct curvature for changing friction loss. For tendon profiles with a minimum radius of curvature of 100 feet (30 m) or greater, which includes most internal longitudinal bridge tendons, a curvature coefficient of 0.16 is suggested. For tendon profiles with minimum radius of curvature of 50-ft. (15 m) or less, including chorded ducts, a curvature coefficient of 0.25 is recommended. Coefficients for tendon profiles with minimum radii between 50-ft. (15 m) and 100 ft. (30 m) can be interpolated at the discretion of the design engineer. Table 10-2 in Division I of the 1989 AASHTO Guide Specifications for Design and Construction of Segmental Concrete Bridges should be modified as follows:

	Friction Coefficient μ	Wobble Coefficient K /ft (/m)
1. For strand in draped galvanized semi-rigid steel duct	0.16 - 0.25*	0.0005 (0.0016)
* A friction coefficient of 0.16 is appropriate for draped tendons with minimum radius of curvature of 100 ft. (30m). 0.25 is appropriate for draped tendons with minimum radius of curvature of 50 ft. (15 m) or smaller.		

The friction coefficient table in Section 9.16.1 of the 1989 AASHTO Standard Specifications for Highway Bridges should be modified to include:

Type of Steel	Type of Duct	Wobble Coefficient K /ft (/m)	Friction Coefficient μ
Strand	Draped galvanized semi-rigid steel	0.0004 (0.0013)	0.16 - 0.25*

*A friction coefficient of 0.16 is appropriate for draped tendons with minimum radius of curvature of 100 ft. 0.25 (30m) is appropriate for draped tendons with minimum radius of curvature of 50 ft. (15 m) or smaller.

The average curvature friction coefficient found by Tran [10] in undamaged ducts in the monolithic test specimen was $\mu = 0.155$, using K = 0.0004/ft. (0.0013/m). The average curvature coefficient found by

Davis [18] in the segmental test specimen in undamaged ducts placed within tolerance at the segment joints was $\mu = 0.150$, using K = 0.0005/ft. (0.0016/m). Average minimum radius of curvature for these draped ducts was 63 ft. (19.2m). Friction losses predicted by these recommended coefficients were conservative in all undamaged ducts tested in both the monolithic and segmental test specimens.

6.4.2 Use of Lubricants. Reductions in overall friction loss by lubrication of greater than 22% were not seen in this study. Results from field tests by Dywidag [9] and others showed reductions in total friction loss of 30%, and as high as 50%, were obtainable. The effectiveness of a lubricant in a particular duct profile must be determined by in-place friction tests. The effectiveness of most lubricants tested in this study for reducing friction loss was marginal to poor.

For girders designed to have bonded tendons at ultimate moment, the water soluble oils are not recommended for use on the tendons. Lubricants L13 and L14 were the only lubricants tested that did not adversely effect strand to grout bond after flushing. L14 (powdered graphite) was the superior lubricant and is recommended overall. If oils must be used as corrosion inhibitors, ultimate moment capacities should be checked using an assumed unbonded tendon in regions of high tendon stress gradient.

Friction reduction realized in lubricated then flushed ducts was considerable. Pre-lubrication of the duct surfaces keeps lubricant off of the tendon surfaces as well.

The results of this study concerning the use of lubricants suggest that the following changes should be made to the 1989 AASHTO Guide Specifications for Design and Construction of Segmental Concrete Bridges, Division II, Section 5.8, paragraph 2. The first sentence should read:

"When friction must be reduced on post-tensioning tendons, graphite may be used subject to the approval of the Engineer. Graphite shall be flushed from the duct by use of water under pressure..."

CHAPTER SEVEN
CONCLUSIONS AND CLOSING REMARKS

7.1 Summary

Two large-scale friction test specimens were constructed and tested for this study. A monolithic specimen was constructed with two straight duct profiles and eight draped profiles. A segmental specimen was constructed with three straight duct profiles and eight draped profiles, identical to those in the monolithic girder. Friction tests revealed the differences in friction losses between monolithic and segmental construction. Lubricated tendon tests, using water soluble oils and other lubricants, were performed in both specimens.

Small-scale tests were also performed to rank lubricants selected for this study by their friction reduction capability, and for their impact on strand to grout bond. Results from all tests were used to (1) determine more accurate friction and wobble coefficients for strand tendons in internally draped galvanized semi-rigid ducts, (2) recommend lubricants for friction loss reduction, and (3) check the current AASHTO [15] recommendations for duct placement tolerance at segment joints.

7.2 Friction Coefficients

Friction coefficients were found to increase when strand to duct normal forces were increased. Friction coefficients were recommended for ducts with different radii of curvature based on the test results from this study, other studies, and field data. The wobble coefficient was also found to increase for segmental construction over monolithic construction.

7.2.1 Monolithic vs. Segmental Construction. Tests in the straight duct profiles of the monolithic test specimen gave a wobble loss coefficient of 0.0004/ft. (0.0013/m), twice that recommended by AASHTO [15]. Straight duct profiles in the segmental test specimen had intentional duct offsets at the segment joints of 0-in. (0 mm), 1/8-in. (3.2 mm) and 1/4-in. (6.4 mm) in each of the three ducts, respectively. The wobble friction coefficient measured increased to 0.0005/ft. (0.0016/m) for 0-in. (0 mm) and 1/8-in. (3.2 mm) offset ducts, and 0.0006/ft. (0.0020/m) or greater for the 1/4-in. (6.4 mm) offset duct. The current duct placement tolerance in the AASHTO Specification [19] is 1/8-in. (3.2 mm). Curvature friction coefficients for all draped ducts, using the wobble coefficients found from the straight ducts, were fairly constant and could conservatively be taken as 0.16 for both the monolithic and segmental specimens.

7.2.2 Use of Lubricants. Lubricants have been used in the field with varying success for reducing friction losses during post-tensioning. Reductions in friction loss as high as 50% have been seen by Bezouska [7] in California. The greatest reduction in total friction loss seen in the large-scale monolithic friction test specimen was 22%. Lubricants applied to tendons in the large scale segmental friction test specimen were only able to decrease total friction loss by a maximum of 15%. Most lubricants tested in the small-scale friction tests of this study gave poor to marginal reductions in friction. Side-by-side friction tests in similarly draped ducts need to be performed in the field to determine the effectiveness of a lubricant for reducing friction in

those ducts. The water soluble oils and soaps apparently are more effective when tendon profiles producing low normal forces are used.

Most of the lubricant tests, except L13 and L14, were found to destroy strand to grout bond, even after a thorough flushing with water. Since L13 is of questionable reactivity with steel (soap-based), L14 (Graphite) is recommended for friction reduction. When water soluble oils are used for corrosion protection, ultimate moment calculations should not reflect bonded tendon stresses. While corrosion inhibitor L10 did not destroy bond, it greatly increased friction loss, and is therefore also not recommended.

7.2.3 Recommended Values. The AASHTO [15] recommended wobble coefficient for strand tendons in galvanized semi-rigid duct was found to be too small, especially for segmental construction. AASHTO recommended curvature friction coefficients are too conservative, except for tendons on small radii of curvature. Friction coefficients recommended by this study are given in Table 7.1

Table 7.1 Recommended Friction Coefficient Ranges

	Minimum Radius of Curvature	μ	Construction Method	K /ft	K (/m)
For 7-wire strand tendons in galvanized semi-rigid steel duct	R > 100 ft. (30m)	0.16	Monolithic	0.0004	(0.0013)
	100 ft. (30m) > R > 50 ft. (15m)	0.16 - 0.25	Segmental**	0.0005	(0.0016)
	R < 50 ft. (15m)	0.25			

** Wobble coefficient may be larger for segments shorter than 8 feet (2.4m).

7.3 Duct Placement Tolerance

Since little difference was seen between friction losses in the straight or draped ducts with 0-in. (0 mm) and 1/8-in. (3.2 mm) offsets in the segmental test specimen, the current AASHTO [19] tolerance of 1/8-in. (3.2 mm) appears to be adequate. Two-inch (50 mm) diameter galvanized semi-rigid ducts were tested. The tolerance should have even less impact on ducts of larger diameter. Wobble friction loss increased substantially in ducts with offsets of 1/4-in. (6.4 mm).

7.4 Current Design and Construction Practices

Currently, design codes do not differentiate between friction coefficients for segmental girders and those of monolithic girders. The wobble coefficient is assumed to be 0.0002/ft. (0.00066/m), if AASHTO [15] is used, and the curvature coefficient is selected, and later modified in the field as necessary. Differences in construction procedures should effect the wobble term only.

Also, when curvature coefficients are checked in the field, using lift-off tests at the dead end anchorage or elongation measurements, and the coefficient is greater than 0.25, the wobble loss term is probably not high enough. Similarly, when lubricants are used, both the curvature coefficient and the wobble coefficient must be modified. After stressing a lubricated tendon, if curvature coefficients are found to be below about 0.09 or above 0.25, the wobble loss coefficient selected is most likely incorrect.

Lubricants are sometimes used in the field when elongations fail to meet tolerance. The field engineer should be aware of the consequences of using water soluble oils to reduce friction. A few percent increase in prestress force may cost the bridge a large decrease in ultimate strength because of the unbonded tendons. For this reason alone, L14 (Graphite) is a good choice for a lubricant.

7.5 Future Research Needs

Side-by-side friction tests need to be performed to study the effect of duct radius on friction increase for a variety of duct materials. The use of polyethylene duct is becoming more popular as a way to reduce high friction losses substantially without using lubricants. Polyethylene duct is substantially more expensive than corrugated steel duct. Research should be performed to determine when polyethylene duct becomes economical. A well-developed relationship between duct radius and curvature friction coefficient is required for any economical analysis to be valid. Wobble losses could then be easily calculated bridge-to-bridge and contractor-to-contractor.

REFERENCES

1. Post Tensioning Manual, Fifth Edition, Post-Tensioning Institute, Phoenix, Arizona, 1990.

2. Kashima, S. and Breen, J.E., "Construction and Load Tests of Segmental Precast Box Girder Bridge Model," Research Report 121-5, Center for Transportation Research, The University of Texas at Austin, February 1975.

3. American Segmental Bridge Institute, Segmental Concrete Bridges: Types, Applications and Advantages, Phoenix, Arizona, 1992.

4. Roberts, Carin L., "Measurement Based Revisions for Segmental Bridge Design and Construction Criteria," Ph.D. Dissertation, The University of Texas at Austin, December 1993.

5. Chang, W.R., Etsion, I., Bogy, D.B., "Static Friction Coefficient Model for Metallic Rough Surfaces," Journal of Tribology, Transactions of the American Society of Mechanical Engineers, Vol. 110, January 1988.

6. ACI-ASCE Committee 323, "Tentative Recommendations for Prestressed Concrete," Journal of the American Concrete Institute, Proceedings V. 54, January 1958.

7. Bezouska, T.J., "Friction Loss in Post-Tensioned Prestressing Steel Units," Report SSR-3-66, Division of Highways, Department of Public Works, California, September 1966.

8. Bezouska, T.J., "Friction Losses in Rigid Post-Tensioning Ducts," Division of Highways, California Department of Public Works, California, February 1971.

9. Dywidag Systems International, USA, Inc., "Methods for Reducing Friction in Post-Tensioning Tendons," Dywidag Report, Lincoln Park, New Jersey, February 1988.

10. Tran, T.T., "Reducing Friction Loss for Post-Tensioning Tendons in Monolithic Girders," Master's Thesis, The University of Texas at Austin, December 1992.

11. Harstead, G.A., Kummerle, E.R., Archer, J.C., Porat, M.M., "Testing Large Curved Prestressing Tendons," Journal of the Power Division, Proceedings of the American Society of Civil Engineers, March 1971.

12. Yasuno, H., Kondo, S., Tadano, N., Mogami, T., Sotomura, K., "Friction Problems with Multi-strand Tendons," Proceedings of the 9th Congress of the Federation Internationale de la Precontrainte, Volume 2, Wexham Springs, England, June 1982.

13. Building Code Requirements for Reinforced Concrete (ACI 318-89) and Commentary - ACI 318R-89, American Concrete Institute, Detroit, 1989.

14. Post-Tensioning Manual, Fifth Edition, Post-Tensioning Institute, Phoenix, Arizona, 1990.

15. Standard Specifications for Highway Bridges, Fourteenth Edition, American Association of State Highway and Transportation Officials, Washington, D.C., 1989.

16. Kittleman, W., "Evaluation of Water-Soluble Oils for Use in Friction Reduction and Temporary Corrosion Protection for 7-Wire Strands," Master's Thesis, The University of Texas at Austin, December 1992.

17. Kittleman, W.M., Davis, R.T., Hamilton, H.R., Frank, K.H., and Breen, J.E., "Evaluation of Agents for Lubrication and Temporary Corrosion Protection of Post-Tension Tendons," Research Report 1264-1, Center for Transportation Research, The University of Texas at Austin, September 1993.

18. Davis, R.T., "Friction Losses in Segmental bridge Tendons," Masters Thesis, The University of Texas at Austin, December 1993.

19. Guide Specifications for Design and Construction of Segmental Concrete Bridges, American Association of State Highway and Transportation Officials, Washington, D.C., 1989.

20. Burns, N.H., Helwig, T., Tsujimoto, T., "Effective Prestress Force in Continuous Post-Tensioned Beams with Unbonded Tendons," ACI Structural Journal, January-February 1991.

21. Freyermuth, C.L., "Rational Application of the Elongation Tolerance for Post-Tensioning Tendons," American Segmental bridge Institute, Phoenix, Arizona, August 1990.

22. Bezouska, T.J., "Friction Losses in Ungalvanized Post-Tensioning Ducts," California Department of Transportation, Division of Project Development, Sacramento, California, December 1977.

23. Yates, D.L., "A Study of Fretting Fatigue in Post-Tensioned Concrete Beams," Master's Thesis, The University of Texas at Austin, December 1987.

24. Freyermuth, C.L., "Comparative Advantages of Segmental Concrete Bridges," American Segmental Bridge Institute, Phoenix, Arizona, November 1991.